CHALMERS
UNIVERSITY OF TECHNOLOGY

The effect of soil-structure interaction on the behaviour of onshore wind turbines with a gravity-based foundation

Master's thesis in Structural Engineering and Building Technology
Master's thesis in Sound and Vibration

JONATAN ISAKSSON
DAVID TENENBAUM

Department of Architecture and Civil Engineering
Division of Geology and Geotechnics
Engineering Geology and Geotechnics
CHALMERS UNIVERSITY OF TECHNOLOGY
Gothenburg, Sweden 2018
Master's thesis ACEX30-18-48

MASTER'S THESIS ACEX30-18-48

The effect of soil-structure interaction on the behaviour of onshore wind turbines with a gravity-based foundation

Master's thesis in Structural Engineering and Building Technology
Master's thesis in Sound and Vibration

JONATAN ISAKSSON
DAVID TENENBAUM

Department of Architecture and Civil Engineering

Division of Geology and Geotechnics

Engineering Geology and Geotechnics

CHALMERS UNIVERSITY OF TECHNOLOGY

Gothenburg, Sweden 2018

The effect of soil-structure interaction on the behaviour of onshore wind turbines with a gravity-based foundation

JONATAN ISAKSSON
DAVID TENENBAUM

Master's thesis ACEX30-18-48
Department of Architecture and Civil Engineering
Division of Geology and Geotechnics
Engineering Geology and Geotechnics
Chalmers University of Technology
SE-412 96 Gothenburg
Sweden
Telephone: +46 (0)31-772 1000

Cover:
Wind turbines at the Swedish countryside, Photographer: Rikard Edman, Saleby Sweden.

Chalmers Reproservice
Gothenburg, Sweden 2018

The effect of soil-structure interaction on the behaviour of onshore wind turbines with a gravity-based foundation

Master's thesis in Structural Engineering and Building Technology
Master's thesis in Sound and Vibration
JONATAN ISAKSSON
DAVID TENENBAUM
Department of Architecture and Civil Engineering
Division of Geology and Geotechnics
Engineering Geology and Geotechnics
Chalmers University of Technology

Abstract

The demand in the world for renewable energy sources leads to an increase in the number of large wind turbines, with a power output exceeding 1.5 MW. Onshore wind turbines are often supported by a gravity foundation on soil. The effect of soil-structure interaction (SSI), on the behaviour of an onshore wind turbine with a gravity-based foundation, is investigated to see whether SSI should be considered in the design. The effect of SSI is modelled with 6 degrees of freedom (DOF) and is implemented via boundary conditions in the open source wind turbine simulation software FAST. The 6 DOF model is representing the foundation-soil system with linear stiffness and damping properties. A comparison of the wind turbine behaviour is conducted for clamped, undamped-spring and damped-spring boundary conditions. The results indicate that the inclusion of SSI in the analyses of a wind turbine is: lowering the natural frequencies of the system; not affecting the maximum moment in the base of the wind turbine tower; increasing the displacement in the top of the tower. The moment time signal is also affected by the implementation of SSI. A fatigue analysis on the bolts in the connection between tower and foundation is performed for a number of different turbulent wind scenarios. The analyses show that SSI is influencing the sustained damage on the detail, however, no final conclusion can be drawn if the effect of SSI is beneficial or detrimental.

Keywords: Soil-structure interaction (SSI), Onshore wind turbines, FAST, Soil dynamics

CONTENTS

List of Figures

List of Tables

PREFACE

We would like to thank our supervisor Alexandre Mathern for his availability and support, our examiner Jelke Dijkstra for his support but mostly for his passion during meetings, our unofficial supervisor Lars Hall, our friends at Chalmers, Viktor Sandahl for the coffee and finally the fika-breaks with our new found friends at NCC.

If anybody would have told us 7 months ago that we would write this thesis together, it would seem unlikely, but it is in the unlikelihood where creativity thrives. The project was a real challenge for us since it covered a wide topic, but it was fun to have this final challenge before graduation. The musical theme throughout the thesis have been Avicii and ironically, Soilwork.

1 Introduction

The seventh of the sustainable development goals, stated by the UN Department of Economic and Social Affairs (2015), is to "Ensure access to affordable, reliable, sustainable and modern energy for all". A part of this is to substantially increase the share of renewable energy in the global energy production. Among energy sources considered to be renewable is wind energy. According to the World Energy Council (2016) global energy output from wind power will more than double until 2030. Electrical power generated from wind turbines in Sweden has increased by a factor of ten between 2006 and 2016. During 2016 wind turbines accounted for nine percent of the total electricity produced in Sweden (Swedish Energy Agency, 2016). The mean power capacity of the constructed turbines year 2015 was 3.2 MW. Furthermore, the majority of the added effect of wind turbines in Sweden are from onshore turbines.

Wind turbines produce electricity by converting wind energy into electricity through an induction generator (DNV/Risø, 2002). An important part of the wind turbine is the foundation which serves the purpose of providing stability and a safe connection between the ground and the superstructure. The foundations of onshore wind turbines are typically designed as gravity based reinforced concrete structures (Perry et al., 2017). In current design, the superstructure and the foundation are usually analysed separately. Design loads used for the foundation and the tower are usually based on the assumption that the wind turbine tower has a clamped connection. The foundation and tower is then designed based on these loads and current soil conditions. The design loads obtained based on a fixed-end tower are considered to be conservative. A more realistic approach would be to take soil-structure interaction into account, adding the soils stiffness and damping properties to the calculation of design loads on the wind turbine tower and foundation.

Wind turbines are tall and slender structures. To increase the energy output it is required to enlarge the rotor size. By this enlargement, it is necessary to increase the tower height which in turn has an impact on the foundation design. In current design standards DNV/Risø (2002) it is proposed that the static stiffness may be used for foundation stiffness design with a discrepancy for a reduced natural frequency of the system. The stiffness used in the standard is derived by Gazetas (1983) who studied the dynamic response of foundations. Furthermore Dobry and Gazetas (1986) proposed coefficients to vary the properties of the soil as a function of frequency.

The influence of soil-structure interaction (SSI) on the behaviour of wind turbines under dynamic loading is a topic studied for both onshore and offshore structures with varying foundation types. The SSI for offshore structures founded on monopiles have been studied regarding the response of the tower, where it is shown that the influence from the SSI is considerable (Aasen, Page, Skau, & Nygaard, 2017), (Jung, Kim, Patil, & Hung, 2015). In onshore design the gravity based foundations have been investigated considering SSI, where a considerable influence is shown regarding the top displacement of the structure, especially for softer soils (Harte, Basu, & Nielsen, 2012). Further studies indicate that a layered soil beneath an onshore foundation could amplify the tower response due to SSI (Taddei, Butenweg, & Klinkel, 2015).

1.1 Aim and objectives

The aim of this study is to investigate how to implement soil-structure interaction (SSI) and the impact of including it in the analysis of an onshore wind turbine, supported on a gravity based concrete foundation. The specified research questions for this project are:

- What properties need to be considered in the supporting soil underneath a vibrating foundation?
- How can SSI for an onshore wind turbine with a gravity foundation be implemented in the software FAST?
- How is the structural behaviour of a wind turbine influenced by including the effect of SSI in the analysis?
- Will the inclusion of SSI in analysis have an impact on the design of a wind turbine foundation?

1.2 Method

The initial task of this Thesis was to understand the wind turbine system, focused towards the structural dynamic aspects of the system. The properties of soil under dynamic loading was then treated to provide knowledge to be able to understand the dynamic response of a foundation on soil. The wind turbine simulation software FAST was then investigated with focus on the possibilities to implement the effect of SSI. The implementation of the SSI into FAST was verified against results from finite element (FE) calculations in CALFEM. Furthermore, a comparison in the behaviour of a wind turbine modelled with and without considering SSI were conducted. Finally, the estimated fatigue life of a bolt in the tower-base connection was investigated and compared between a fixed tower and a tower with boundary conditions considering SSI.

1.3 Limitations

A number of limitations have been set for this project.

- The only wind turbine foundation considered is an onshore gravity concrete foundation, other types of foundations used for wind turbines is not discussed.
- The foundation used in the study is based on a wind turbine with similar design loads, a foundation design is not performed.
- The studied soil is isotropic linear elastic without considering pore water.
- Water pressure and buoyancy effects are not included in the analysis.

- The numerous scenarios that need to be simulated to get the final design loads for a wind turbine is not performed. The results in this study are only showing how SSI influences the wind turbine for specific conditions.

- The influence of the mass of the foundation and mobilised soil is not included in the analysis.

2 Design considerations of onshore wind turbines

2.1 Wind turbines

Wind turbines are power plants converting wind power into electricity. Most wind turbines are small scale units producing 10 kW or less, whilst most of the wind energy output in the world is produced from larger wind turbines, in the range from 1.5 to 5 MW (Manwell, McGowan, & Rogers, 2010) which are in focus in the Thesis. The most common wind turbine today is the horizontal axis wind turbine (HAWT). HAWTs design can operate in upwind or downwind depending on the rotor orientation (Manwell et al., 2010). The upwind turbines need a yawing system to control the direction of the rotors to face the wind. The downwind turbines have the rotors on the lee side of the tower, which removes the system but reduces their capacity due to the shadow effect from the tower (Warren-Codrington, 2013). A typical onshore HAWT can according to Manwell et al. (2010) be described as 6 subsystems, see Figure 2.1.

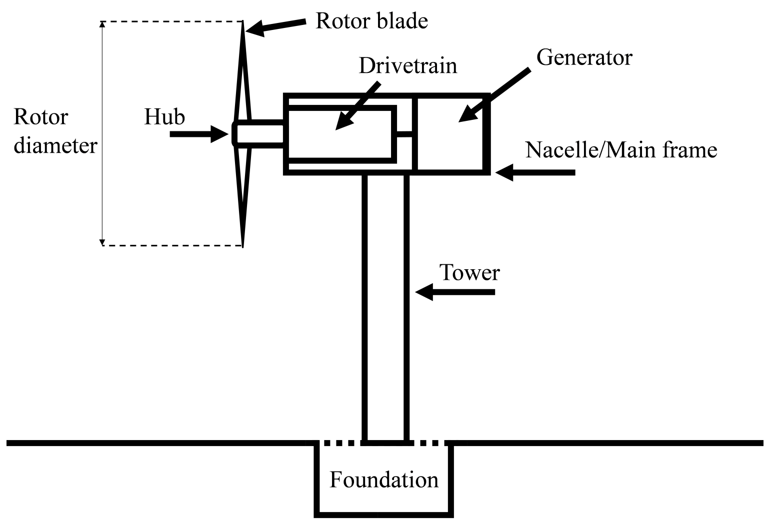

Figure 2.1: Overview of a wind turbine.

The hub and blades form the rotor of a wind turbine which is the part that transfers the wind pressure to kinetic energy. The blades are flexible and constructed in light-weight composite materials such as carbon/glass-fibre reinforced polymer (Manwell et al., 2010). The blades are mounted to the hub. The hub-blade connection can be able to control the angle of the blades, making it possible to control the amount of kinetic energy harnessed by the blades. The hub is in turn mounted to the nacelle. The nacelle contains parts such as gearbox, generator, brakes and control systems. The gearbox converts the low speed rotation from the rotor into high speed rotation, more suitable to be converted to electrical power in the generator. The connection between the wind turbine tower and nacelle is designed with the ability to rotate. For an upwind configured wind turbine the nacelle is kept in place by a yaw drive system. A free standing tower is often designed as a steel or concrete tube but can also be a lattice structure. The height of the wind turbine tower vary and typical relations between the rotor diameter height of the tower and power output can be seen in Table 2.1 (Manwell et al., 2010).

Table 2.1: Rated power output with corresponding geometry for various wind turbines

Capacity [kW]	Rotor diameter [m]	Tower height [m]
25	10	18
250	24.4	30
660	47	50
1800	80	60
3600	104	74
5000	126	87
6000	126	138

2.2 Wind as a structural load

The wind pressure on a wind turbine is of importance both as an energy source as well as a structural load. This Section is describing the basics on how wind can be treated as a load. Wind is created due to uneven heating of the earth surface. This heating creates atmospheric pressure gradients, which in a flow model would mean that air rises at the equator and sinks at the poles (Manwell et al., 2010). Apart from gradients the wind is also influenced by the rotation of the earth, turbulence caused by friction at the earth surface, inertia of the air and from gravitational forces. These properties can be used to describe different wind phenomenons at different levels such as the local, regional and global-level (Ackermann, 2005).

Wind turbines operate close to the ground in the local wind field. At the local level the wind field is acting turbulent due to rough ground disturbing the wind flow. Turbulence is lasting in the range of a minute, referred to as the turbulent peak. The turbulence peak is a quick varying phenomenon which may be analysed using stochastic models. Apart from the turbulent peak the diurnal and synoptic peak exist. The diurnal peak is created from daily variations in the wind, for instance the sea-land breeze. The synoptic peak consists of the daily, weekly to seasonal changes in the weather (Ackermann, 2005).

The amount of power P [W] in a wind that flows through an area, A [m^2], can be described with the mass of air ρ_{air} [kg/m^3] and the velocity v_{air} [m/s] according to Equation 2.1:

$$P = \frac{1}{2}\rho_{air} v_{air}^3 A \tag{2.1}$$

John Smeaton discovered these properties of the wind in the 18th century (Manwell et al., 2010). Smeaton also discovered that the torque in a wind turbine is proportional to the square of the wind velocity. The density of air is a function of temperature and height but is in general set as a constant for wind turbine analysis. The power that the blades of a wind turbine can extract from the wind depends on the area of the blade facing the wind, which corresponds to A in Equation 2.1. This power is not physically possible to extract since all air mass would lose all velocity in the area. The theoretical solution to compensate for this phenomena is to reduce the velocity. Ackermann (2005) states that this was discovered by Albert Betz in 1926 who proposed that the potential power in the wind is a reduced form of Equation 2.1 defined as:

$$P_{betz} = \frac{1}{2}\rho_{air}v_{air}^{3}A * 0.59 \tag{2.2}$$

2.3 Design of tower and gravity foundation

The loads acting on a wind turbine are composed of static and dynamic loads. The static loads are caused by the self weight of the superstructure. The dynamic loads are caused by the wind front. There are mainly three dynamic load components on an onshore wind turbine. The lateral load at the hub height caused by the turbulent wind speeds acting upon the wind turbine, Figure 2.2 indicates that the dominating power of the turbulent wind (Kaimal spectrum) is found at low frequencies. The hubs rotation frequency is commonly referred to as 1P. This rotation generates a dynamic load at the hub height with varying frequency from the variable speed of the machine (Bhattacharya, 2014). The rotation of each blade causes an additional load from the shadowing effect of the tower. This dynamic load has a frequency corresponding to the number of blades multiplied with the rotation frequency of the hub, in this case 3P. The full wind turbine-foundation system must be designed to not coincide with the 1P and 3P load frequencies. The design can be achieved with three different concepts: the soft-soft, soft-stiff or stiff-stiff. In the soft-soft design the natural frequency is placed below 1P, in soft-stiff it is designed between 1P and 3P and in the stiff-stiff case it is designed to be above 3P, see Figure 2.2 (Bhattacharya, 2014).

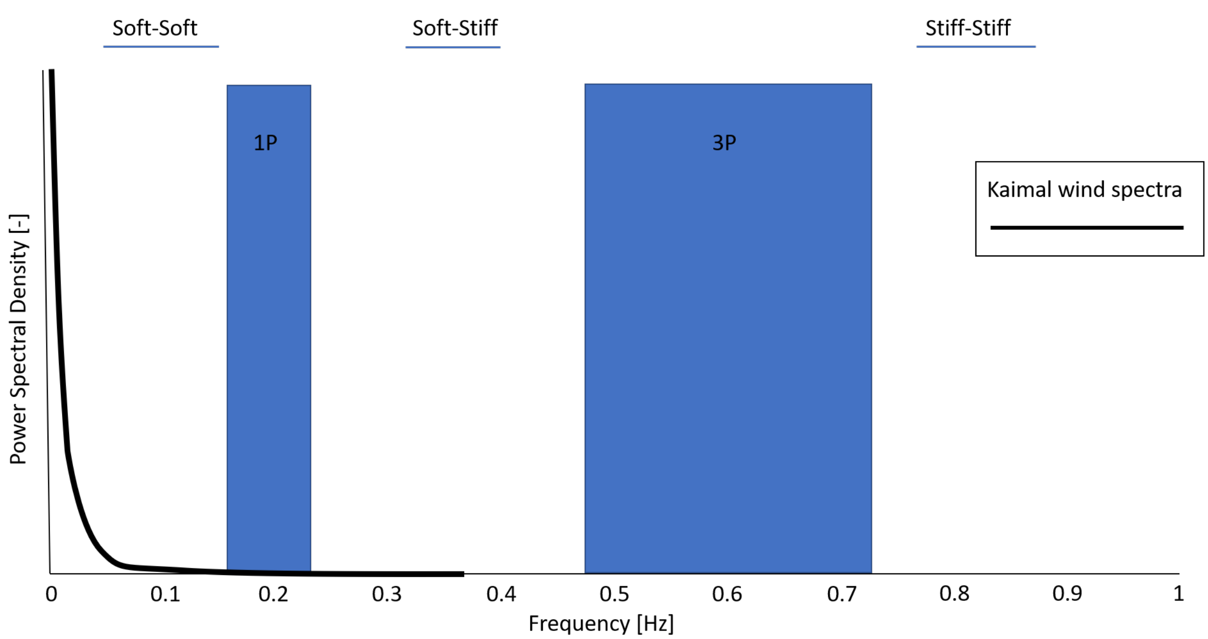

Figure 2.2: Power spectral density for loads at various frequencies subjected to a wind turbine. Obtained from Bhattacharya, Nikitas, and Jalbi (2018).

When designing a wind turbine and the wind turbine foundation, the ultimate and fatigue strength of the turbine and its structural elements must be verified. The standard IEC-61400 (2014) describes the design load cases that need to be evaluated to cover all load scenarios that the wind turbine might experience. The 8 design situations are;

- Power production
- Power production plus occurrence of fault
- Start up
- Normal shutdown
- Emergency shutdown
- Parked
- Parked and fault conditions
- Transport, assembly, maintenance and repair

These design situations are classified as normal, abnormal or transport and erection, this determines which partial safety factors to use in the design (IEC-61400, 2014). The different design situations are classified as either a fatigue load scenario, an ultimate load scenario or both. Extreme events need to be considered for the ultimate load and normal operational scenarios for the fatigue load. The design situations including the corresponding classifications result in a minimum of 22 design load cases. The dynamic simulations should be simulated with at least six 10-min stochastic simulations or a continuous 60 min simulation, this should be done for each mean wind speed. Some extreme events require at least 12 simulations to give statistical reliability of the characteristic loads. When considering turbulent winds, the first 5 seconds, or more if necessary, should be disregarded due to the influence of the initial loads (IEC-61400, 2014).

Gravity foundations for onshore wind turbines can be used when the top soil layer is competent enough to support the superstructure (DNV/Risø, 2002). The gravity foundation, is a spread out solid concrete slab that due to a large diameter is able to resist the high overturning moments from the wind turbine (Warren-Codrington, 2013). The gravity foundation is often circular and is functioning as a cantilever from the centre of the foundation. This gives the possibility to reduce the height of the foundation towards the edge Figure 2.3. The connection detail can be designed in different ways and should be able to transfer the loads from the tower to the foundation. A commonly used connection is a bolt cage. The bolt cage is designed with a cast in steel ring given the same dimension as the tower bottom flange. The cast in steel ring is then connected to the tower flange by prestressed bolts Figure 2.3.

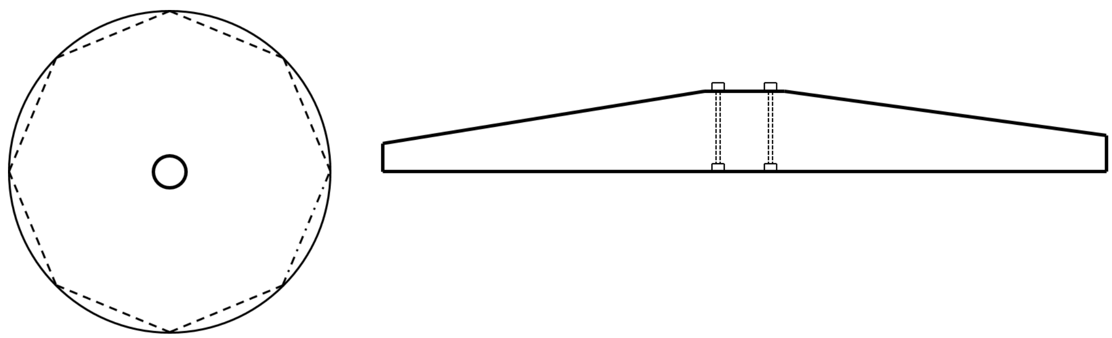

Figure 2.3: a) Illustration of gravity foundation with circular or octagonal shape. b) Illustration of a bolt cage connection commonly used to connect wind turbine tower to a gravity foundation.

The foundation of a wind turbine should provide necessary support during the design life time of the structure. Important conditions that need to be fulfilled are the bearing resistance of the soil (ULS), the sliding resistance (ULS), the overall stability (ULS) and settlements/displacements (SLS) In accordance with EN1997 (2005) the following limit states should be checked when designing earthworks:

- Loss of equilibrium of the structure or the ground, considered as a rigid body, in which the strengths of structural materials and the ground are insignificant in providing resistance (EQU);
- Failure or excessive deformation of the ground, in which the strength of soil or rock is significant in providing resistance (GEO);
- Loss of equilibrium of the structure or the ground due to uplift by water pressure (buoyancy) or other vertical actions (UPL);
- Hydraulic heave, internal erosion and piping in the ground caused by hydraulic gradients (HYD).

2.4 Fatigue design

Fatigue is the process of crack initiation and propagation in a material due to variations in load effect. The stress level needed to create a so called fatigue crack is well below the ultimate stress of the material. After a number of load cycles the fatigue cracks will propagate and might lead to failure of the detail. The resistance of a detail against fatigue failure is commonly evaluated by testing. A number of tests need to be performed on identical specimen to investigate the number of load cycles with a certain stress range that will lead to failure in the specimen. The tests are performed with different stress levels and the test results give the so called Wöhler curve for the detail, see Figure 2.4. Different details show the same linear logarithmic relation between applied stress and number of cycles to failure and can therefore be easily differentiated only by the classification of detail category. The detail category is defined as the stress range that will lead to failure after 2 million cycles. The constant amplitude fatigue limit (CAFL) is the stress amplitude where a certain detail will not be subjected to fatigue damage when subjected to a constant amplitude loading. The cut off limit is the stress amplitude that will not cause any damage to the detail no matter the number of cycles. If a detail is subjected to variable amplitude loading and there exist stress amplitudes higher than the CAFL stresses between the CAFL and the cut off limit will still induce damage.

The damage subjected to a detail by a number of cycles with different stress amplitude can be evaluated using the Palmgren-Miner accumulative damage rule. The rule defines damage caused to a detail as the ratio between the number of applied cycles (n_i) within a stress range and the number of cycles leading to failure (N_i) for that stress range. The damage caused by a cycle of a certain stress range can be evaluated independently of previous cycles. The damage caused by variable loading can therefore be accumulated and failure occurs when the sum of the total damage is equal to 1, see Equation 2.3.

$$D_{PM} = \sum \frac{n_i}{N_i} \leq 1 \tag{2.3}$$

To evaluate the fatigue damage in a structural detail the stress history over time is needed. The stress history was evaluated using rainflow counting which identifies stress cycles in the stress history and gives the information of the mean stress for the stress cycle and the stress range of the cycle. The variable load effect was discretised as a number of cycles of different stress ranges and the damage caused by the load was then evaluated by using the Wöhler curve, Figure 2.4.

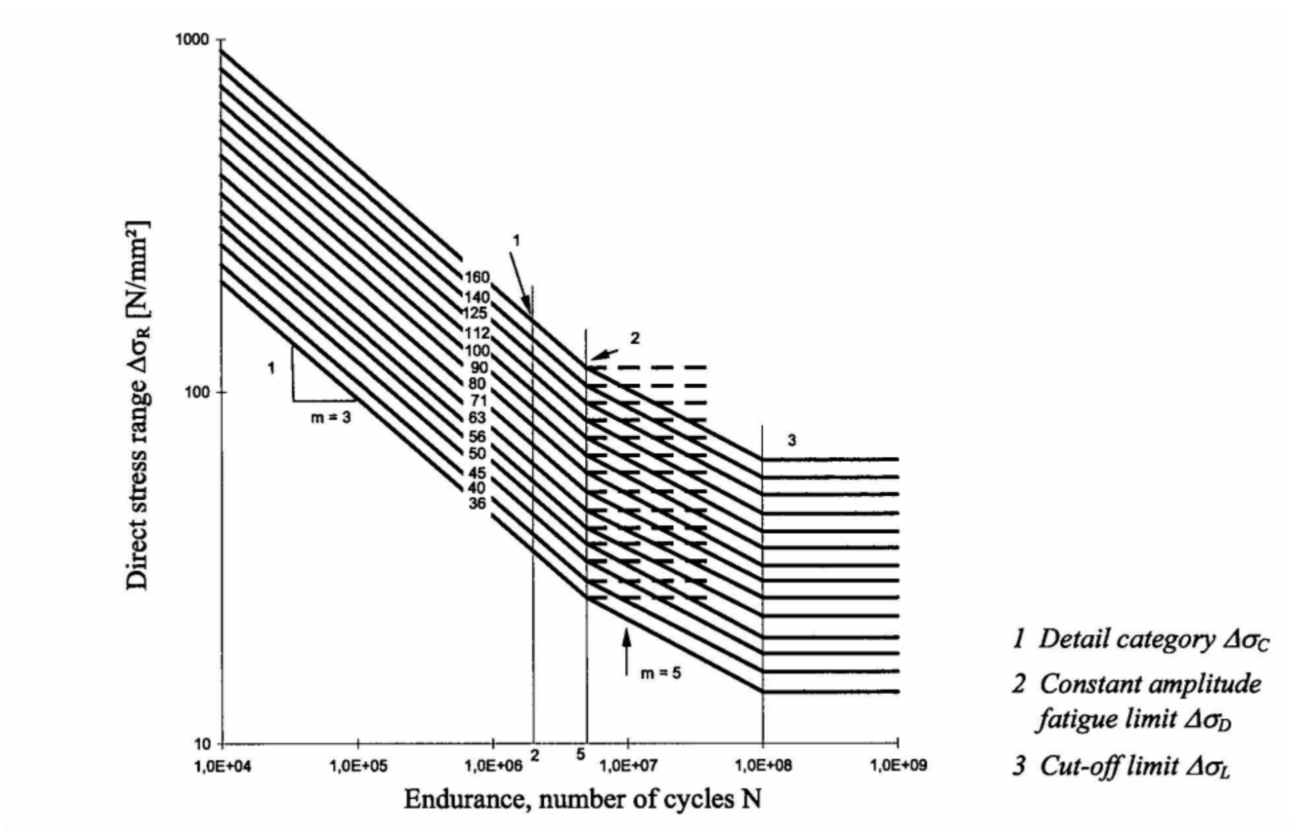

Figure 2.4: Wöhler curve for the 14 different detail categories considered in Eurocode 3, obtained from EN1993-1-9 (2005).

3 Soil subjected to dynamic loading

The soil below a wind turbine foundation will be subjected to both static and dynamic loads. These loads will induce deformations and movement in the soil (GCR12-917-21, 2012). The movement in the foundation will influence the wind turbine structure by an increase in flexibility and the introduction of damping. The inclusion of the soil-structure interaction (SSI) in analysis provides more realistic structural models and should better reflect the collective response of the structure-soil system. To make it possible to implement SSI in the analysis of a wind turbine the properties of soil, focused towards stiffness and damping, under dynamic excitation need to be known.

Soil as a material is built up by single soil particles of different sizes and shapes in contact with each other (Knappet & Craig, 2012). The particles are affecting each other by forces from inter particle contact and in some cases by electrostatic forces from surface attraction. The behaviour of a soil will be governed by the chemical composition and shape of the soil particles as well as the size distribution of the particles. Other factors, among many, affecting the behaviour of a specific soil is the geological history of the site where the soil is found, loading history and confining pressure on the soil.

3.1 A basic dynamic system

The behaviour of a dynamic system is investigated using a basic conceptual model. The dynamic model consists of a mass (m) [kg], a linear spring (K) [N/m], a viscous damper (C) [Ns/m] and a displacement z [m]. The system is excited by an external arbitrary force and the spring and damper are assumed to be rigidly connected to the ground, see Figure 3.1.

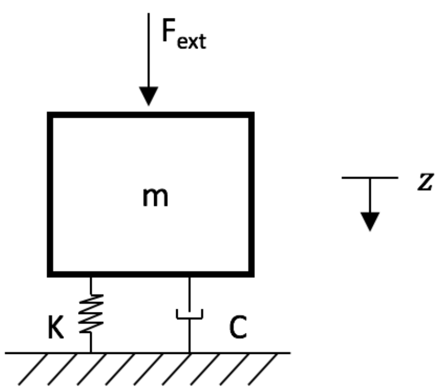

(a) Mass-spring-damper model

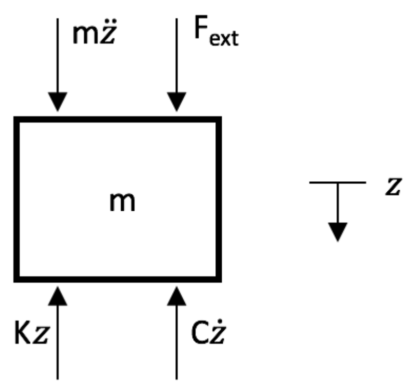

(b) Free body diagram of the model

Figure 3.1: Mass-spring-damper model and free body diagram

The system is then studied by applying Newton's second law of motion, Equation 3.1, where the forces on the body are equal to the body's mass times acceleration

$$\sum F_i = ma \tag{3.1}$$

The equilibrium equation for the free body can be set up by defining the spring force according to Hooke´s law, the viscous damper force acting in the opposite direction of the body's movement, the inertia of the body and the external force, see the free body diagram in Figure 3.1.

Thus the equation of motion for the system is written as a linear differential equation (Verruijt, 2010):

$$F_{ext} = m\frac{\partial^2 z}{\partial t^2} + C\frac{\partial z}{\partial t} + Kz \tag{3.2}$$

Some basic characteristics of Equation 3.2 can be observed by excluding the external force and the damper. A trivial solutions is when z=0, which is the static case. The other solution for the system, when not at rest, can be found by assuming a harmonic response of the system. The solution is:

$$\omega_0 = \pm\sqrt{\frac{K}{m}} \tag{3.3}$$

where ω [rad/s] is the angular frequency defined as $\omega = 2\pi f$. Equation 3.3 is referred to as the eigenfrequency or natural frequency (Kropp, 2015). The eigenfrequency is the frequency where the magnitude of the spring force and the inertia are equal and compensate each other. Exciting the system with an arbitrary periodic small force of this frequency will cause large displacements. The natural frequency of a system can be interpreted by hitting a teacup with a spoon, the sound that can be heard corresponds to the natural frequencies of the cup (Kropp, 2015). This thought experiment is a easy way to practically interpret the natural frequency. To further study the system the damper may be included. There are different ways to define the damping properties of a system. One way to model the damper is with viscosity properties. A convenient substitution can be done defining the damping ratio ζ as a measure describing the damping in the system. The magnitude of ζ will give the system different behaviour which is often referred to as small, strong or critically damped (Verruijt, 2010). The small damped system has an oscillating response towards equilibrium in contrast to the critical and strongly damped cases that show a none oscillating behaviour. The small damped system has a damping ratio lower than 1, the critically damped system is equal to 1 and the strong damped system is larger than 1.

Soils can be modelled with a hysteretic damping that represents the damping caused by dry friction in the material (Verruijt, 2010). The hysteretic damper can also be modelled with a modified damping ratio substitution ζ_h.

The variation between the damping ratios are shown Equation 3.4 as:

$$2\zeta = \frac{C\omega_0}{K} \qquad ; \qquad 2\zeta_h = \frac{C\omega}{K} \tag{3.4}$$

To study the complete system a periodic harmonic force is added. The behaviour of the viscous and hysteretic damping ratios are shown in Figure 3.2 where the displacement amplitudes of Equation 3.2 are plotted.

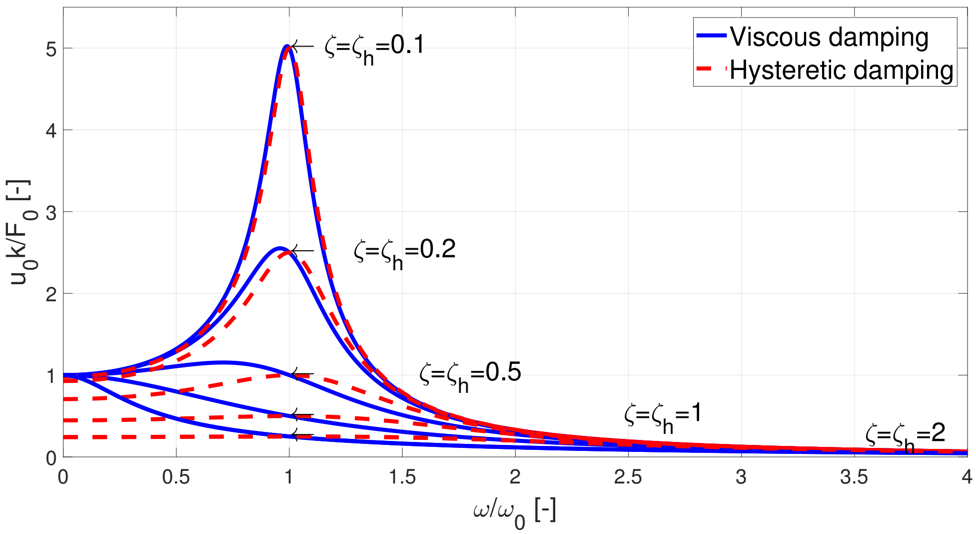

Figure 3.2: Normalised displacement amplitude (z [m] of a mass spring damping system, with a viscous and hysteretic damper. With input parameters $K = 10000$ [N/m], $m = 1$ [kg], $C = 4\pi^2$ [Ns/m] and $F_0 = 1$ [N]

.

Both systems show that a small damping ratio yields a clear peak in the displacement which corresponds to an undamped system. When the damping ratio is increased the displacement decreases. The hysteretic damper indicates smaller displacement amplitudes at lower frequencies which is analogue with the definition of this damping. The influence of the spring stiffness is visualised in Figure 3.3 by plotting five different springs.

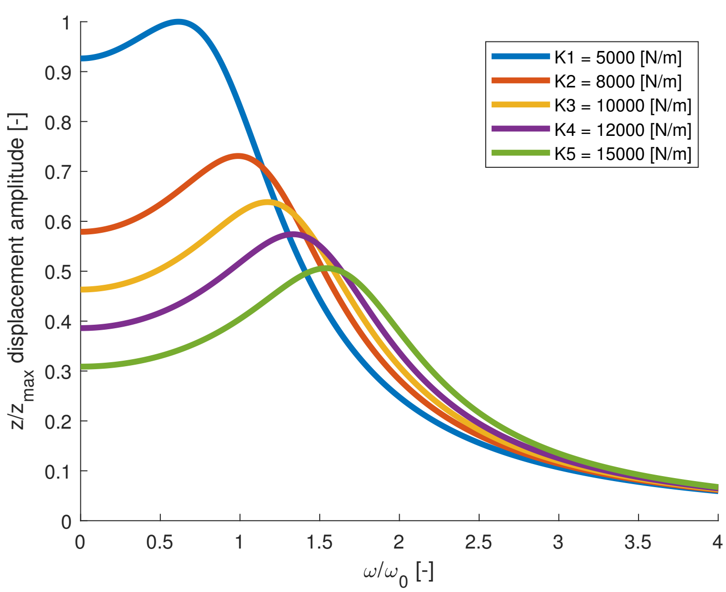

Figure 3.3: Normalised displacement amplitude (z [m]) of a mass-spring-damping system, with varying stiffness parameters and constant viscous damping. With input parameters, $m = 1$ [kg], $c = 4\pi^2$ [Ns/m] and $F_0 = 1$ [N]

It is clearly shown that a reduction of stiffness reduces the eigenfrequency of the system and increases the displacement amplitude. The increase of the displacement amplitude is derived from the displacement expression which is divided by the stiffness, see (Verruijt, 2010) for the derivation.

3.2 Soil stiffness

The stiffness in soil can be described with the shear modulus G [Pa], defined as the relation between shear stress τ [Pa] and shear strain γ [-] according to Equation 3.5:

$$G = \frac{\tau}{\gamma} \tag{3.5}$$

Most soils show a non-linear stress-strain behaviour when subjected to load. During a cycle with increasing and decreasing strain, the soil changes in stiffness due the history dependent non-linear shear modulus. The shear modulus G is decreasing with an increased strain. The maximum shear modulus G_{max} is obtained at a very low strain. The general behaviour of a soil under shear stress from cyclic loading can according to Darendeli (2001) be described with an linear-elastic region for strains up to the elastic threshold strain γ_t^e, defined as the strain where $G(\gamma)$ is 98% of G_{max}. The soil will for higher strains show a non-linear elastic stress-strain behaviour until the plastic threshold strain is reached. The plastic threshold strain, γ_t^p, is reached when soil show permanent irreversible deformations when unloaded. To account for softening due to the strain in the soil, Darendeli (2001) suggests the following relation between the shear modulus at a specific strain γ and the maximum shear modulus Equation 3.6. Typical behaviour of shear modulus as a function of strain can be seen in Figure 3.4.

$$G = G_{max} \frac{1}{1 + (\frac{\gamma}{\gamma_r})^a} \tag{3.6}$$

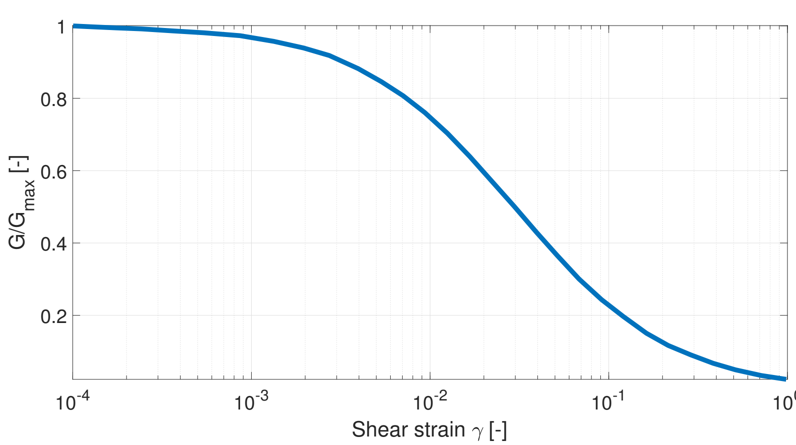

Figure 3.4: Degradation of shear modulus as a function of strain. Obtained from Darendeli (2001).

where a is a curvature coefficient, see Table 3.1, and the reference shear strain γ_r, defined as the strain where $G/G_{max} = 0.5$, that can be obtained from testing. The reference shear strain can also be calculated according to Darendeli (2001) as a function of a soils over consolidation ratio (OCR), plasticity index (PI) and mean confining pressure σ'_0 according to Equation 3.7 using constants presented in Table 3.1.

$$\gamma_r = (\phi_1 + \phi_2 PI * OCR^{\phi_3})\sigma'_0{}^{\phi_4} \tag{3.7}$$

Table 3.1: Coefficients used in Equations 3.6 and 3.7

Coefficient	[-]
ϕ_1	0.0352
ϕ_2	0.010
ϕ_3	0.3246
ϕ_4	0.3483
a	0.9190

3.3 Damping in soil

The soil supporting the wind turbine will induce damping to the structure. (Gazetas, 1991). The damping results partly from waves in the soil emitted by the vibrating foundation (radiation damping) and partly by the energy dissipating in the soil material under a loading cycle (hysteretic damping).

The vibrating foundation will give rise to waves in the supporting soil (Verruijt, 2010). These waves will propagate through the soil and spread out over an increasing area when moving away from the source. This spreading of wave energy may lead to damping in the system, this form of damping is called radiation damping. The radiation damping is related to the speed of the waves propagating away from the foundation. Four different wave types are generated in the soil (Richart, Hall, & Woods, 1970) all four waves are propagating with different speeds which gives different magnitude of radiation damping.

The pressure wave (P-wave) is propagating when soil particles are moving and pushing other particles in the direction of the wave. The movement of a shear wave (S-wave) is due to the fact that soil particles are moving perpendicular to the direction of the wave. P and S waves are referred to as body waves. The Rayleigh waves (R-wave) are propagating in a spiral-like movement. Characteristic for the R-wave is that it is propagating along the surface and rapidly decreasing in amplitude towards the depth, noticeable is also the fact that the R-wave is attenuating slower than the P-wave and S-wave (Richart et al., 1970). Apart from these three waves the Love waves exists, which are more uncommon than the P, S and R-waves, since they demand special site conditions. The various direction of movement in the vibrating foundation will give rise to somewhat different types of waves in the soil.

The hysteretic damping can partly be explained by two different phenomena in the soil (Darendeli, 2001). The first is due to energy losses in system arising from friction in between soil particles. The second phenomena is energy loss due to plastic work during loading. Darendeli (2001) suggests that these two phenomena are evaluated independently from each other since the frictional losses are constant with strain level and the plasticity losses are strain dependent. The damping related to frictional losses is defined as D_{min} and the damping due to plasticity is defined as D_{pl}. Darendeli (2001) states that the damping due to friction is a function of Plasticity Index (PI), oveconsolidation ratio (OCR) and the effective overburden pressure (σ'_0) according to:

$$D_{min} = (\phi_6 + \phi_7 PI * OCR^{\phi_8})\sigma'_0{}^{\phi_9}[1 + \phi_{10} ln(frq)] \tag{3.8}$$

Table 3.2: Coefficients used in Equation 3.8 and Equation 3.10

Coefficient	[-]
ϕ_6	0.8005
ϕ_7	0.0129
ϕ_8	-0.0129
ϕ_9	-0.2889
ϕ_{10}	0.2919
ϕ_{11}	0.6329
ϕ_{12}	-0.0057

As discussed in Section 3.2 the plasticity of soils is increasing with strain level which gives an increase in the damping due to plasticity of the soil D_{pl}. Darendeli (2001) propose an equation, based on adjustments to a model proposed by Masing published in 1926, to predict the damping due to plasticity as:

$$D_{pl} = b\left(\frac{G}{G_{max}}\right)^{0.1} D_{Masing} \tag{3.9}$$

The factor b is a scaling factor considering number of loading cycles (N):

$$b = \phi_{11} + \phi_{12} ln(N) \tag{3.10}$$

With coefficients according to Table 3.2. The ratio between G and G_{max} is correcting the curve based on current strain amplitude. The damping formulated by Masing (D_{Masing}) is based on energy dissipated from a system during a loading/unloading cycle. The Masing damping is varying with strain level γ_r, Equation 3.7, and the curvature coefficient a, see Table 3.1, and is defined as:

$$D_{Masing} = \frac{4}{\pi} * \frac{\int \left(\frac{\gamma}{1+(\frac{\gamma}{\gamma_r})^a}\right) d\gamma - \frac{1}{2}\frac{\gamma^2}{1+(\frac{\gamma}{\gamma_r})^a}}{\frac{\gamma^2}{1+\frac{\gamma}{\gamma_r}^a}} \tag{3.11}$$

The total damping D_{soil} can then be described as the combination of frictional and plastic damping as Equation 3.12 and is also shown in Figure 3.5.

$$D_{soil} = D_{pl} + D_{min} \tag{3.12}$$

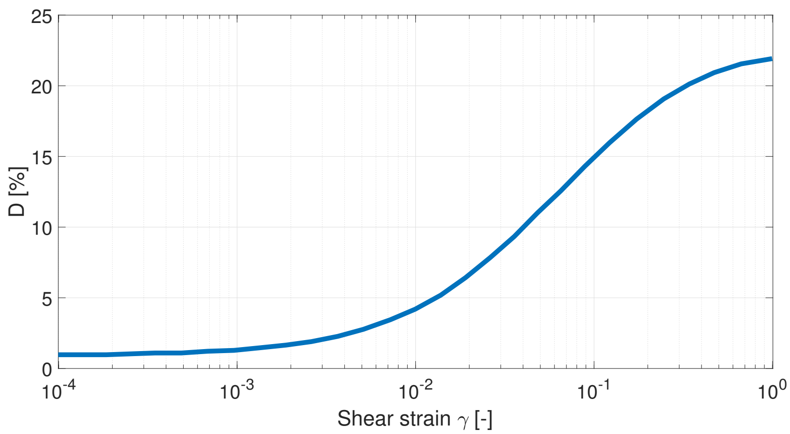

Figure 3.5: Behaviour of damping ratio as a function of strain. Obtained from Darendeli (2001).

3.4 Soil subjected to cyclic loading

The soil underneath a vibrating foundation will be loaded and unloaded numerous times during the lifetime of the structure. Soil has been shown to accumulate deformations when subjected to cyclic loading. Wichtmann (2005) has performed experiments on various sands that show that strains in the soil are increasing with the number of load cycles applied on the soil. However, the experiments show little or no change in the stiffness of the soil under repetitive loading. This indicates that the accumulated strain in sand due to number of load cycles will not affect the maximum shear modulus of the soil. The shear modulus of sand can therefore be treated only as a function of the shearing strain within a load cycle as discussed in Section 3.2.

3.5 Dynamic response of circular foundations

The behaviour of vibrating foundations supported on soil has been investigated by Gazetas and co-workers in several publications. Gazetas proposes formulations for stiffness and damping induced on a foundation arising from the soil as a function of the foundation shape and properties of the supporting soil. This Section presents expressions and models based on these works.

3.5.1 The foundation as a dynamic system with six degrees of freedom

Dobry and Gazetas (1986) presents the basic dynamic model for the soil-foundation system as a rigid disk and circular shape resting on a elastic homogeneous half-space. The system is excited by six dynamic forces and moments with corresponding degrees of freedom, see Figure 3.6. This definition will be continuously used in this Thesis.

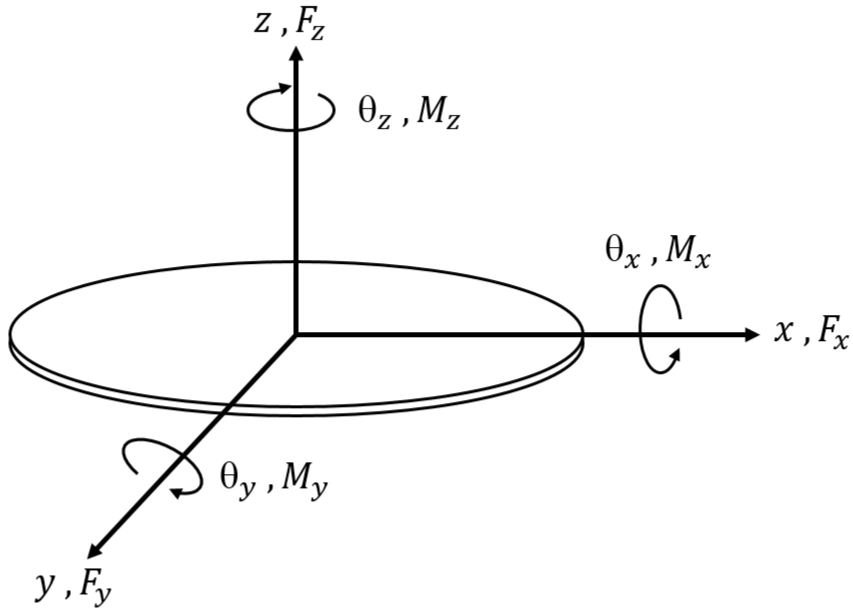

Figure 3.6: Definition of coordinate system for the soil and foundation system with directions of movement, rotations and corresponding forces and moments.

The vertical force F_z, the horizontal forces F_x and F_y the rocking moments M_x and M_y and the torsional moment M_z can be written in the form $F_x = F_{x,0}e^{i\omega t}$. u_z is the vertical complex displacement and ω which is the loading frequency. The dynamic spring $\hat{K}$ and the dashpot coefficient C can be defined for each of these modes of vibration as:

$$[(\hat{K}_z - m\omega^2) + i\omega C_z]u_z = F_z \tag{3.13}$$

In the same manner as in Equation 3.13 formulations for the other degrees of freedom can be formulated and is presented in Table 3.3.

Table 3.3: Equation of motions for the six degrees of freedom formulating the SSI response.

Direction of motion	Equation of motion
Vertical (z)	$[(\hat{K}_z - m\omega^2) + i\omega C_z]u_z = F_z$
Horizontal (x)	$[(\hat{K}_x - m\omega^2) + i\omega C_x]u_x = F_x$
Horizontal (y)	$[(\hat{K}_y - m\omega^2) + i\omega C_y]u_y = F_y$
Rocking (x)	$[(\hat{K}_{\theta x} - (I_x\rho)\omega^2) + i\omega C_{\theta x}]\theta_x = M_x$
Rocking (y)	$[(\hat{K}_{\theta y} - (I_y\rho)\omega^2) + i\omega C_{\theta y}]\theta_y = M_y$
Torsion (z)	$[(\hat{K}_{\theta z} - (I_z\rho)\omega^2) + i\omega C_{\theta z}]\theta_z = M_z$

3.5.2 Stiffness and damping for rigid circular foundations

The basic formulation of stiffness K is dependent on the area of the foundation as well as the soils shear modulus and Poisson's ratio, described in Section 3.2. The basic formulation of radiation dashpot C is dependent on the velocity of wave propagation and the density of the soil.

A reasonable choice of wave speed for the different direction of movement is important when modelling radiation damping since the speed of the wave is relevant for the radiation damping. Dobry and Gazetas (1986) is discussing this matter and claims that the shear wave velocity is representative for wave propagation from horizontal and torsional vibrations.

Equation 3.14 is an appropriate selection of wave speed for the two horizontal and the torsional modes of vibration:

$$V_s = \sqrt{\frac{G}{\rho}} \tag{3.14}$$

Further on, it is suggested that Lysmer's analog wave velocity, Equation 3.15, is a good choice of wave speed for the vertical and rocking modes of vibration.

$$V_{La} = \frac{3.4}{\pi(1-\nu)} V_s \tag{3.15}$$

Table 3.4: Stiffness (K) and damping (C) formulations for circular foundations on a homogeneous elastic halfspace.

Direction	Static stiffness	Radiation dashpot (high frequency approximation)
Vertical (z)	$K_z = \frac{4GR}{1-\nu}$	$C_z = \rho V_{La} A$
Horizontal (x)	$K_x = \frac{8GR}{2-\nu}$	$C_y = \rho V_s A$
Horizontal (y)	$K_y = \frac{8GR}{2-\nu}$	$C_y = \rho V_s A$
Rocking (θ_x)	$K_{\theta x} = \frac{8GR^3}{3(1-\nu)}$	$C_{\theta x} = \rho V_{La} I_x$
Rocking (θ_y)	$K_{\theta y} = \frac{8GR^3}{3(1-\nu)}$	$C_{\theta x} = \rho V_{La} I_y$
Torsion (θ_z)	$K_{\theta z} = \frac{16GR^3}{3}$	$C_{\theta z} = \rho V_s I_z$
$I_x = \frac{1}{4}\pi R^4$, $I_y = I_x$, $I_z = \frac{1}{2}\pi R^4$		

The stiffness formulations in Table 3.4 are based on the assumption of an infinitely deep soil layer. Different assumptions of the geometry of the soil will give different spring stiffness. Gazetas (1983) gives solutions for the spring stiffness for a soil layer with a depth (H) overlaying bedrock, Figure 3.7, and where there is a change in stiffness properties of the soil at depth (H), see Figure 3.7 c.

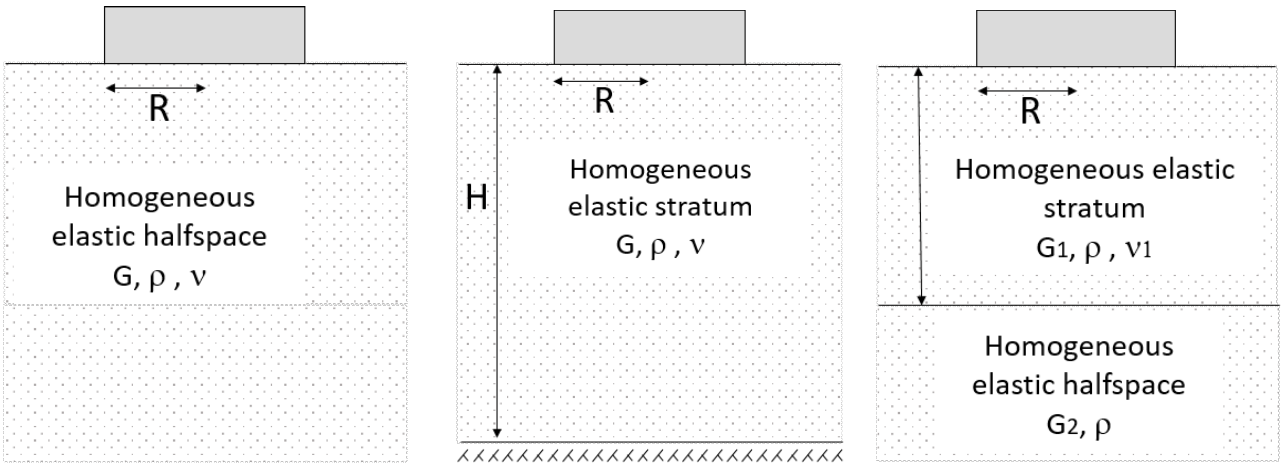

(a) Homogeneous elastic halfspace. **(b)** Homogeneous elastic stratum on bed rock. **(c)** Homogeneous elastic stratum on stiffer homogeneous elastic halfspace.

Figure 3.7: Parameters used to formulate the soil stiffness and damping for a rigid foundation on top of different soil profiles.

A spring stiffness for each mode of motion is presented in table Table 3.5 for each of the two cases. For the case with a change of stiffness it is demanded that the stiffness is increasing at depth H for the expressions to be valid.

Table 3.5: Stiffness (K) formulation for circular foundations on a homogeneous elastic stratum over bedrock or over a stiffer homogeneous elastic halfspace.

Shallow layer on bedrock	Valid	Stiffness increase	Valid
$K_z = \frac{4GR}{1-\nu}(1 + 1.28\frac{R}{H})$	$\frac{H}{R} > 2$	$K_z = \frac{4GR}{1-\nu_1}\frac{1+1.28\frac{H}{R}}{1+1.28\frac{R}{H}\frac{G_1}{G_2}}$	$1 < \frac{H}{R} < 5$
$K_x = \frac{8GR}{2-\nu}(1 + \frac{R}{2H})$	$\frac{H}{R} > 1$	$K_x = \frac{8GR}{2-\nu_1}\frac{1+\frac{R}{2H}}{1+\frac{R}{2H}\frac{G_1}{G_2}}$	$1 < \frac{H}{R} < 4$
$K_y = K_x$	$\frac{H}{R} > 1$	$K_y = K_x$	$1 < \frac{H}{R} < 4$
$K_{\theta x} = \frac{8GR^3}{3(1-\nu)}(1 + \frac{1R}{6H})$	$1 < \frac{H}{R} < 4$	$K_{\theta x} = \frac{8GR^3}{3(1-\nu_1)}\frac{1+\frac{R}{6H}}{1+\frac{RG_1}{HG_2}}$	$0.75 < \frac{H}{R} < 2$
$K_{\theta y} = K_{\theta x}$	$1 < \frac{H}{R} < 4$	$K_{\theta y} = K_{\theta x}$	$0.75 < \frac{H}{R} < 2$
$K_{\theta z} = \frac{16}{3}GR^3$	$\frac{H}{R} < 1.25$	Not presented	-

Dobry and Gazetas (1986) present the stiffness and damping properties for an elastic soil. The relation between the dynamic stiffness $\hat{K}$ and the static stiffness K are dependent on the loading frequency and defined as $\hat{K} = Kk$. It is possible to obtain k graphically by using a dimensionless variable a_0 which is defined as:

$$a_0 = \frac{\omega R}{V_s} \tag{3.16}$$

a_0 is also used to obtain the variable c ,accounting for radiation damping C as $\hat{C} = Cc$. The graphs are included in Dobry and Gazetas (1986) for various foundation types and directions of excitation. As discussed in Section 3.3 soils can be modelled with a hysteretic damping which is defined as β. The hysteric damping is considered by changing the stiffness according to:

$$\hat{K}(\beta) \simeq \hat{K} - \omega C \beta \tag{3.17}$$

and increasing the dashpot coefficient to:

$$\hat{C}(\beta) \simeq C + \frac{2\hat{K}}{\omega}\beta \tag{3.18}$$

Furthermore, the radiation damping is depending on the loading frequency where an increased frequency yields an increased damping. The loading frequency of a wind turbine is well below 1 Hz, as discussed in Section 2.3, which leads to a dynamic stiffness equal to the static stiffness. In addition, the low loading frequency leads to no radiation damping $C = 0$. Thus, the only damping induced is due to the hysteretic damping in the soil.

3.5.3 Coupled spring model

The forces from the wind turbine are acting in the shear centre of the foundation, see Figure 3.8. The support from the soil is mobilised at the bottom of the foundation. The distance e_x is defined as the vertical distance between the shear centre of the foundation and the soil-foundation interface. This eccentricity has to be considered by a coupling between the horizontal and rocking displacements.

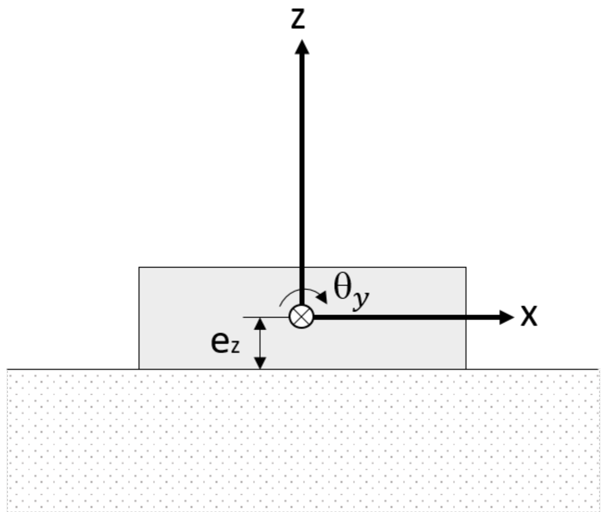

Figure 3.8: Definition of coordinate system for the soil and foundation system with directions of movement, rotations and corresponding forces and moments.

The compatibility combined with the equilibrium gives us the following equations:

$$F_x = K_x u_x - K_x \theta_y e_z \tag{3.19}$$

$$M_y = K_{ry} \theta_y + F_x e_z \tag{3.20}$$

Inserting Equation 3.19 into Equation 3.20 gives:

$$M_y = K_{ry} \theta_y + K_x u_x e_z - K_x e_z^2 \theta_y \tag{3.21}$$

The coupled stiffness matrix for the movement in x direction and the rocking around the y axis can then be described in matrix format as:

$$\begin{bmatrix} K_x & -K_x e_z \\ -K_x e_z & K_{ry} + K_x e_z^2 \end{bmatrix} \begin{bmatrix} u_x \\ \theta_y \end{bmatrix} = \begin{bmatrix} H_x \\ M_y \end{bmatrix} \tag{3.22}$$

The coupling between H_y and M_x is performed in the same manner and the six equations of motion are formulated as:

$$\begin{bmatrix} K_x & 0 & 0 & 0 & -K_x e_z & 0 \\ 0 & K_y & 0 & -K_y e_z & 0 & 0 \\ 0 & 0 & K_z & 0 & 0 & 0 \\ 0 & K_y e_z & 0 & K_{rx} + K_y e_z^2 & 0 & 0 \\ -K_x e_z & 0 & 0 & 0 & K_{ry} + K_x e_z^2 & 0 \\ 0 & 0 & 0 & 0 & 0 & K_{rz} \end{bmatrix} \begin{bmatrix} u_x \\ u_y \\ u_z \\ \theta_x \\ \theta_y \\ \theta_z \end{bmatrix} = \begin{bmatrix} F_x \\ F_y \\ F_z \\ M_x \\ M_y \\ M_z \end{bmatrix} \tag{3.23}$$

The influence of the eccentricity between the shear centre of the foundation and the soil interface will also affect the damping matrix in a similar way.

4 Wind turbine simulation and implementation of SSI in FAST

The National Renewable Energy Laboratory (NREL) is a federal American laboratory researching and promoting renewable energy in the US. NREL has developed a number of computer-aided engineering tools to support the development of renewable energy sources. This report uses three open source NREL software's: FAST, BModes and Turbsim. The following will give the reader an basic overview of the software's provided by NREL and establish a very basic understanding on how to implement SSI into FAST.

4.1 Functionality of FAST

FAST (Fatigue, Aerodynamics, Structures and Turbulence) is the primary CAE tool for simulating coupled dynamic response of a wind turbine provided by NREL. FAST couples the nonlinear aero-hydro-servo-elastic simulations in the time domain by coupling aero-, hydro-, control/electrical- and structural-dynamics (J. Jonkman, 2018). FAST offers the ability to simulate different wind turbines and scenarios by controlling different modules. The modules used in this report are shown in Figure 4.1.

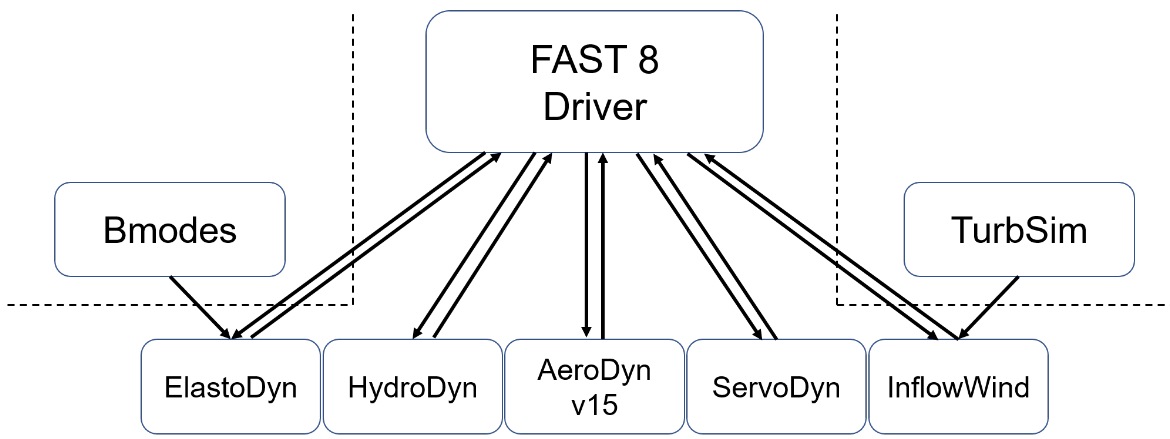

Figure 4.1: Schematic overview of utilised NREL software's connected to FAST 8.

The modules are part of the FAST v8 archives available from NREL's website. In this archive it is possible to conduct certification cases to verify that the software is functioning properly. A simulation in FAST is done by controlling the main driver file to call for the modules where detailed properties are specified. The modules are enabled under the "feature and switches and flags" section in the main file with corresponding input files for the modules, see Appendix C. The input files for FAST and the modules are text files with switches that are controlled by changing the content in the files. Each input file has, apart from the switches and properties, an output section where the outputs from the simulation are determined. The outputs from the modules can be compiled automatically from the main file at the end of a simulation as a text file or a binary file.

In the InflowWind module it is possible to read inflow wind data. The module may also be used to simulate steady wind conditions by defining, a wind speed at a given height and a power law exponent. Other software may be used to create more advanced wind fields which is used as input in the InflowWind module. TurbSim is a stochastic wind simulator that simulates turbulent winds using a statistical model (B. Jonkman & Kilcher, 2012). A pseudorandom number generator is included in TurbSim to be able to reproduce different wind fields. This generator is used by assigning a number in the input file in TurbSim. The wind field that TurbSim generate is a two-dimensional vertical grid with three-component windspeed vectors (B. Jonkman & Kilcher, 2012). The grid size and number of grid points are user defined. Furthermore, it is possible to assign the turbulence conditions in accordance with the IEC-61400 (2014) standard. An example of a TurbSim input file is shown in Appendix F.

The following modules, ServoDyn and AeroDyn, are included in FAST but are not user defined in this research. ServoDyn represents the control and electrical-drive of the wind turbine. In this module it is possible to regulate and control the generator torque and brakes. Furthermore, it enables the simulation of extreme cases such as an emergency shutdown. AeroDyn is the module that computes the aerodynamic loads on the tower and blades.

The module ElastoDyn computes the structural dynamics of the tower and the blades. In the input file of ElastoDyn the degrees of freedom, initial conditions and turbine properties are specified, see Appendix D. The structural elements are modelled as flexible beam elements using linear modal representation (J. Jonkman & Buhl, 2005). These elements depend on the mode shapes of the structural member which is specified in the tower input file as normalised sixth-order polynomials, where two modes in the fore-aft and side-side direction are required as inputs. When the boundary conditions of the structural member is changed so is the mode shape polynomial for that member.

BModes is a software that computes mode shapes using a finite element method (FEM) formulation followed by an eigenmode analysis (Bir, 2007). The inputs for a computation are the distributed structural properties of the member, including inertia, density and stiffness, for an isotropic material. Furthermore, it is possible to account for tip attachment by including a rigid mass with a described offset as well as the rotational inertia of the attachment. (Bir, 2007). After a calculation the mode shapes need to be fitted onto a normalised sixth-order polynomial to fit the FAST input. Note that FAST needs the first and second fore-aft and side-side mode shapes. BModes computes the coupled modes which include the flexural, axial and torsional motion, therefore it is crucial to properly identify the corresponding modes that required by FAST.

HydroDyn is a module to calculate the hydrodynamic loads on the wind turbine. (J. Jonkman, Robertson, & Hayman, 2014). When performing a simulation in FAST the main driver gives the position, velocity, orientation and acceleration of the substructure to HydroDyn which computes the hydrodynamic-load and returns the loads to ElastoDyn. ElastoDyn assumes that the substructure is a six DOF rigid body (J. Jonkman et al., 2014).

4.2 Modelling SSI in FAST

The software FAST does not provide any specific inputs to consider SSI. However NREL supports a forum related to FAST. In the forum, the creator of FAST Jason Jonkman, suggests ways to mimic the impact of SSI for both onshore gravity based foundations and offshore monopile foundations (J. Jonkman, 2015). Jonkman suggests that the boundary conditions arising from the soil supporting a gravity based concrete foundation, see Figure 4.2 can be implemented in the HydroDyn module, see Appendix E. The boundary conditions can be formulated as 6x6 stiffness damping and mass matrices implemented at bottom platform of the tower. The matrices are specified under the header "Platform additional stiffness and damping" in the HydroDyn input file. The deactivation of all hydrodynamic properties in the module, such as waves, currents and potential flow together with the defined stiffness, damping and mass matrix, should provide the desired boundary conditions for the tower. Without recompiling the source code of FAST8 it is only possible to model linear stiffness and damping in the six DOF at the tower base. A non linear stiffness can be implemented in FAST but requires user change in the FAST code. Krathe (2015) implemented a non linear spring for an offshore wind turbine supported by a monopile but the same procedure can be used for a gravity based onshore concrete foundation.

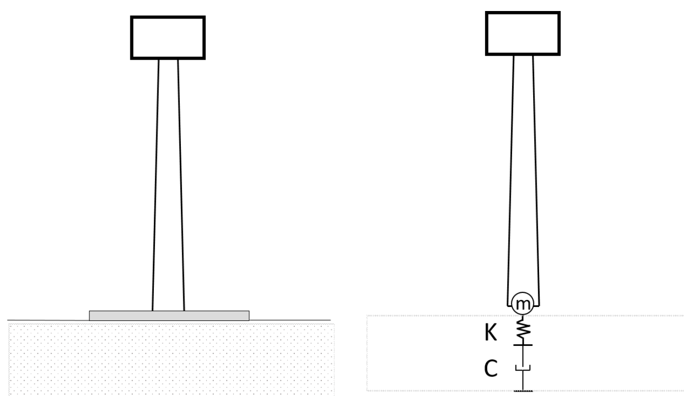

(a) Soil-structure system. **(b)** Model of soil-structure interaction.

Figure 4.2: The influence of soil on the wind turbine are modelled in FAST using 6x6 stiffness- (K), damping- (C) and mass-matrices (m).

4.3 SSI verification - NREL 5 MW reference wind turbine

To verify the implementation of SSI in FAST a comparison of results from FAST and CALFEM was conducted. A 5MW wind turbine defined by NREL (J. Jonkman, Butterfield, Musial, & Scott, 2009) was used in this Thesis. This 5 MW turbine is widely used by researchers and developers as a reference turbine. The 5 MW wind turbine should be representative of a utility scale wind turbine as it is a composite of prototype turbines and conceptual models. The 5MW turbine has a hub height of 90 m, 3 blades and an upwind rotor configuration. All details of the 5MW turbine can be found in (J. Jonkman et al., 2009). The most important structural parameters can be seen in Figure 4.3. The tower has a circular hollow cross-section. The outer diameter of the tower base is 6 m and it decreases to 3.87 m at the tower top. The steel thickness at the bottom is 27 mm and decreases to 19 mm at the tower top. The decrease in thickness and radius of the tower is changed linearly from bottom to top. The density of the tower is 8500 kg/m^3 and in addition to the self weight of the structural steel including details such as bolts, welds, flanges and paint. The steel is defined with a Young's modulus of 210 GPa and a shear modulus of 80.8 GPa.

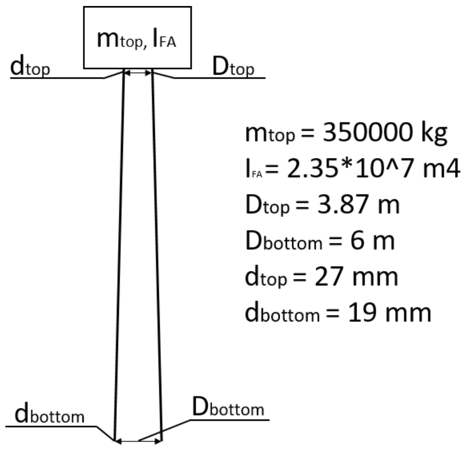

Figure 4.3: Model of the 5MW NREL reference wind turbine

The influence of SSI on the 5MW wind turbine was investigated by the implementation of supporting springs in the tower base. The springs were formulated in accordance with Gazetas theory presented in Section 3.5. Based on the assumption of a rigid concrete foundation resting on top of a deep homogeneous soil strata the spring supports in the bottom of the tower were formulated with the foundation radius R, the Poisson's ratio and the shear modulus of the soil. The tower base was allowed to move and the spring stiffness and damping from the foundation were implemented in the Hydrodyn module of FAST. Due to numerical stability of the FAST analysis the torsional and vertical degrees of freedom in the base of the tower was prevented from moving. These simplifications were not considerably affecting the results and were implemented for all analysis where SSI was taken into consideration. In the verification of FAST no damping was implemented in the bottom of the wind turbine. Damping was introduced after the FAST verification including the stiffness had been conducted.

The radiation damping and soil stiffness are dependent on the loading frequency as discussed in Subsection 3.5.2. The operational rotor speed of the wind turbine is approximately 12 RPM, which corresponds to a loading frequency of 0.2 Hz. This loading frequency gives no radiation damping, ($C = 0$) and a dynamic stiffness equal to the static stiffness. The damping in the soil is, due to no radiation damping, only a function of the stiffness and the soil damping ratio.

4.3.1 Case 1 - Clamped wind turbine

To verify the implementation of SSI into FAST the behaviour of a clamped 5 MW wind turbine was used as reference, defined as Case 1. The clamped wind turbine support was modelled by preventing movement for all six degrees of freedom in the tower base.

4.3.2 Case 2 - Wind turbine supported on soil

For Case 2 the foundation was assumed to have a radius of 12.5 m. The assumption was based on a foundation designed for a wind turbine with similar load effect. The supporting soil was given the Poisson's ratio 0.3 and the shear modulus of 50 MPa, see Figure 4.4. The stiffness was calculated with the expressions in Table 3.4. This shear modulus corresponds to a soft soil compared with the shear wave velocities in Knappet and Craig (2012), calculating the modulus with Equation 3.14 and assuming a dry density of 1650 kg/m^3.

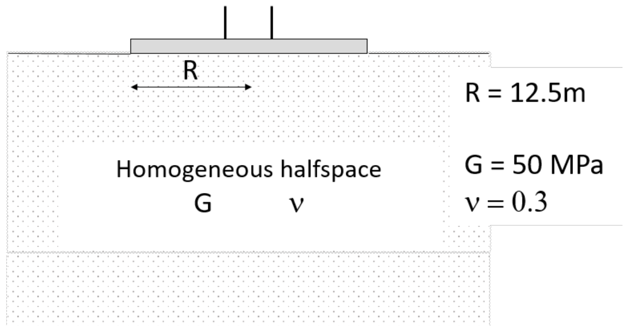

Figure 4.4: Soil properties and foundation geometry for Case 2

4.3.3 Case 3 - Wind turbine supported on soft soil

To further investigate whether SSI was correctly implemented in FAST, Case 3 was defined. Case 3 was given a reduced shear modulus of 5 MPa compared to Case 2. This reduction was based on the assumption of a relatively high shearing strain of approximately 0.2 %, see Figure 3.4. The same properties for the foundation radius and Poisson's ratio were used as in Case 2, see Figure 4.5. The shear modulus corresponds to a very soft soil compared with the shear wave velocities in Knappet and Craig (2012), calculating the modulus with Equation 3.14 and assuming a dry density of 1650 kg/m^3.

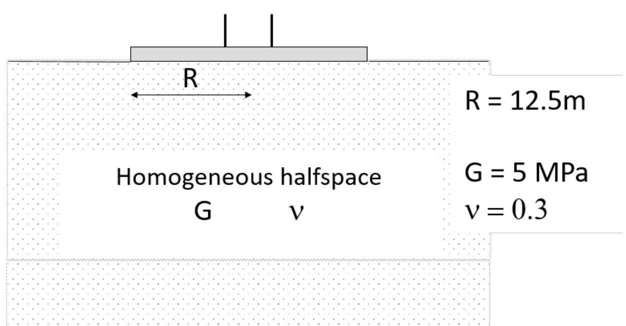

Figure 4.5: Soil properties and foundation geometry for Case 3

4.4 Wind turbine modelled in CALFEM

To verify the structural response in FAST a FEM formulation of the wind turbine based on the open source function package Computer Aided Learning of the Finite Element Method (CALFEM) developed at Lund University, was implemented using MATLAB. The CALFEM model is defined according to Euler-Bernoulli beam theory, see Equation 4.1 with the elastic modulus E the second moment of inertia I and the deflection w along the length of the element x

$$M(x) = -E(x)I(x)\frac{d^2w}{d^2x} \tag{4.1}$$

The model consists of a finite number of nodes connected with stiffness ($EI(x)$) from the Euler Bernoulli theory and the distributed mass ($m(x)$) of the tower was lumped in these nodes. The tower top mass (m_{top}) and inertia (I_{FA}) was assigned to the end node of the cantilevered wind turbine tower. The boundary conditions for the three cases are formulated in Table 4.1. The displacements in the bottom of the wind turbine was set to zero in Case 1. In Case 2 and Case 3 the boundary conditions are applied as forces ($f_{x,1}, f_{z,1}, M_{y,1}$) depending on the displacement ($u_{x,1}, u_{z,1}, \theta_{x,1}$) and spring stiffness ($k_x, k_y, k_{\theta y}$).

Table 4.1: Boundary conditions for the wind turbine model for Case 1 (clamped tower), Case 2 (spring supported tower) and Case 3 (soft spring supported tower).

BC: Case 1	BC: Case 2	BC: Case 3
$u_{x,1} = 0$	$f_{x,1} = k_x(G, R)u_{x,1}$	$f_{x,1} = k_x(\frac{G}{10}, R)u_{x,1}$
$u_{z,1} = 0$	$f_{z,1} = k_z(G, R)u_{z,1}$	$f_{z,1} = k_z(\frac{G}{10}, R)u_{z,1}$
$\theta_{y,1} = 0$	$M_{y,1} = k_{\theta y}(G, R)\theta_{y,1}$	$M_{y,1} = k_{\theta y,1}(\frac{G}{10}, R)\theta_{y,1}$

4.4.1 Static analysis of wind turbine in CALFEM

The basic behaviour of the wind turbine was investigated with the MATLAB script Windturbine.m using CALFEM and can be seen in Appendix G. By applying a horizontal point load ($f_{x,top}$) in the top of the wind turbine the change in displacements and rotation when implementing spring boundary conditions could be verified. This was done for the three different cases described in Section 4.3 The horizontal displacement of the tower top ($u_{x,top}$) along with the rotation in the bottom om the wind turbine ($\theta_{y,1}$) are presented in Table 4.2.

Table 4.2: CALFEM results for the displacement in top of tower $u_{x,top}$ and base rotation $\theta_{y,1}$ due to a force $f_{x,top}$ applied in the top of wind turbine.

		Case 1	Case 2	Case 3
$f_{x,top}$	[kN]	635	635	635
$u_{x,top}$	[m]	0.349	0.382	0.674
$\theta_{y,1}$	[rad]	0	0.00037	0.0037

4.4.2 Natural frequencies and mode shapes wind turbine modelled in CALFEM

The natural frequencies of the wind turbine and the corresponding mode shapes of a dynamic system, as discussed in Section 3.1, are important parameters in describing the behaviour of a dynamic system. The stiffness matrix (K) and mass matrix (M) from the static analysis has been used to solve the natural frequencies and corresponding mode shape X of the system according to:

$$[K - \omega^2 M]X = 0 \tag{4.2}$$

The natural frequency is calculated as:

$$f_n = \frac{\omega}{2\pi} \tag{4.3}$$

The first three natural frequencies and corresponding mode shapes were computed in Windturbine.m, see Appendix G, according to Equation 4.2 for the three different cases. The frequencies are presented in Table 4.3 and the mode shapes in Figure 4.6.

Table 4.3: First three natural frequencies for the three cases calculated in CALFEM

		Case 1	Case 2	Case 3
$f_{n,1}$	[Hz]	0.332	0.317	0.236
$f_{n,2}$	[Hz]	2.278	2.187	1.851
$f_{n,3}$	[Hz]	5.055	4.813	4.247

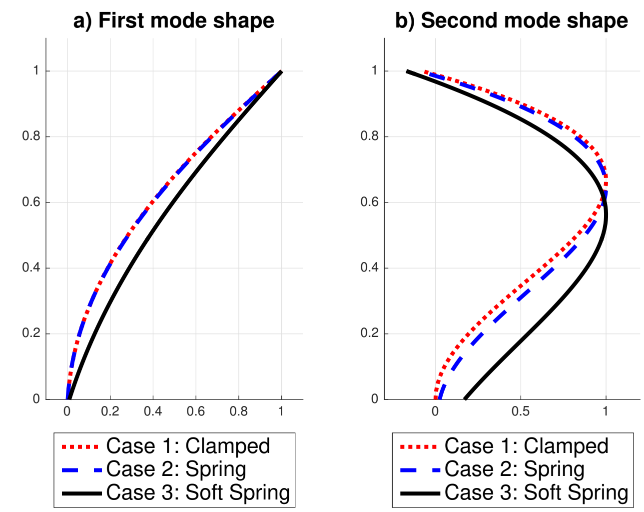

Figure 4.6: Comparison of the first mode shape and second mode shape for Case 2: Soft spring BC from CALFEM and FAST

4.4.3 Free vibration of wind turbine modelled in CALFEM

To further validate the implementation of SSI into FAST, a FEM-formulation describing the behaviour of the wind turbine in the time domain has been implemented in the MATLAB script Dynamicbeammodel.m using CALFEM, see Appendix J. At time $t = 0$ a displacement of 0.5 m was prescribed in the top of the tower and the tower was then released and allowed to vibrate freely. The displacement over time is presented in Figure 4.7 where the wind turbine shows a cyclic displacement the amplitude is at all times within the prescribed displacement amplitude. The system does not show any attenuation of displacements, which is expected since the system was modelled without damping.

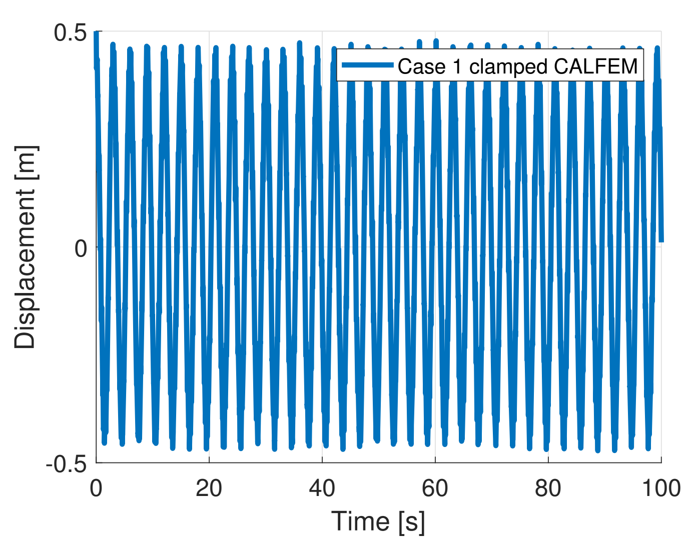

Figure 4.7: Fore-aft displacement, $u_{x,top}$ of the tower top after being released from a prescribed displacement of 0.5 m for Case 1 simulated in CALFEM.

To simplify the comparison of the different cases, the displacement over time signal was transformed into the frequency domain using a fast Fourier transformation, see Appendix I. The results are presented in Figure 4.8, the first and second amplitude peaks are found at the highest frequency for Case 1 and the lowest frequency for Case 3. Notice that the amplitude peaks are found at the natural frequencies calculated in Subsection 4.4.2.

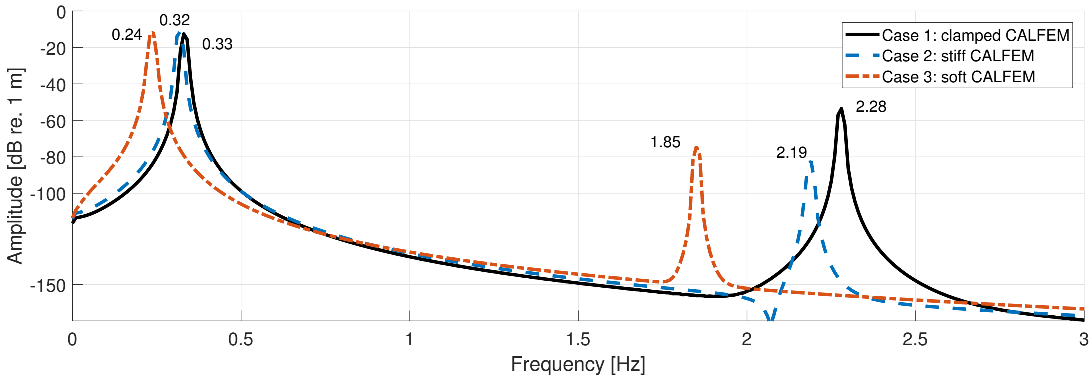

Figure 4.8: Fore-aft displacement amplitudes for case 1, 2 and 3 in CALFEM. The highlighted values are the peak frequencies for each case.

4.5 Wind turbine modelled in FAST

The software FAST was used to simulate the behaviour of the wind turbine under similar conditions as used in Section 4.3 for the CALFEM model. A constant wind analysis of the wind turbine was followed by an investigation of the mode shapes and natural frequency calculated in BModes. Finally a FAST simulation of a free vibrating wind turbine are presented.

4.5.1 Convergence study on number of nodes and time steps used in FAST

To determine the number of tower nodes and time steps to be used in FAST simulations a convergence study were conducted. The number of nodes used in the tower was studied to find convergence of FAST using a time step in the main file of 0.002 s. This time step is used since a larger step aborts the simulation due to numerical errors. The results of the study is shown in Table 4.4.

Table 4.4: Tower nodes convergence study of the normalised fore-aft displacement. Simulated using a total simulation time of 630 s and a uniform wind of 12 m/s

Nodes	FA min [-]	FA max [-]
10	1	1
20	1.0005	1.0005
30	1.0008	1.0008

With the previously described nodes the sensitivity of time steps was studied to find convergence. 20 nodes were used and three different time steps. The results of the time step convergence is shown in Table 4.5

Table 4.5: Time-step convergence study of the normalised fore-aft displacement. Simulated using a total simulation time of 630 s and a uniform wind of 12 m/s

Time step [s]	FA min [-]	FA max [-]
0.002	1	1
0.001	1	1
0.0005	1	1

No variation can be seen when changing the time steps except for when the code crashes due to overly large time steps. To have reliable results from FAST it is therefore recommended to use at least 10 number of nodes and a time step of 0.002 s. In the following FAST simulations, a time step of 0.002 s and 20 tower nodes have been implemented.

4.5.2 Constant wind analysis of wind turbine in FAST

To resemble a static load a FAST model of the wind turbine loaded by a constant wind field of 12 m/s was implemented. The results presented in Table 4.6 are representative values and show, for a similar load, the lowest displacements in Case 1 and highest in Case 3.

Table 4.6: FAST results for the displacement in top of tower $u_{x,top}$ and base rotation $\theta_{y,1}$ due to a uniform wind field of 12 m/s.

		Case 1	Case 2	Case 3
$u_{x,top}$	[m]	0.370	0.405	0.731
$\theta_{y,1}$	[rad]	0	0.00039	0.00400

4.5.3 Natural frequencies and mode shapes for wind turbine modelled in FAST

The natural frequencies of the wind turbine were calculated using the software BModes. The structural properties used as inputs in BModes is defined in Appendix B. Case 1 uses a cantilevered connection, in case 2 and 3 the wind turbine are constrained against torsional and axial displacement. The soil stiffness was implemented in the tower support subsystem as a hydrodynamic 6x6 stiffness matrix. The natural frequencies for the wind turbine are calculated with BModes and the three first natural frequencies in the fore-aft direction are presented in Table 4.7.

Table 4.7: First three natural frequencies for the three cases calculated in BModes.

		Case 1	Case 2	Case 3
$f_{n,1}$	[Hz]	0.322	0.307	0.228
$f_{n,2}$	[Hz]	2.241	2.129	1.705
$f_{n,3}$	[Hz]	5.198	4.844	3.879

The two first mode shapes computed by BModes in the fore-aft direction are presented in Figure 4.9. The two cases supported by springs show both a base rotation and a base displacement whereas the clamped case has zero rotation and displacement at the base. The softer spring in Case 3 gives rise to larger rotation and displacement in the base than Case 2.

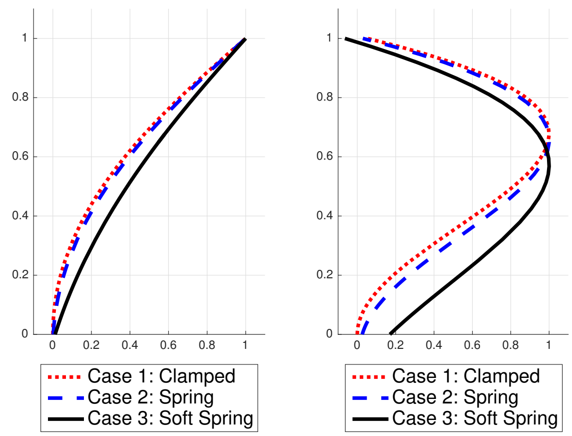

Figure 4.9: Normalised mode shapes from BModes in the fore-aft direction

4.5.4 Free vibration of wind turbine modelled in FAST

The wind turbine was given a prescribed displacement of 0.5 m in the top of the tower and was then released and allowed to vibrate freely. The resulting time signal for Case 1 is shown in Figure 4.10.

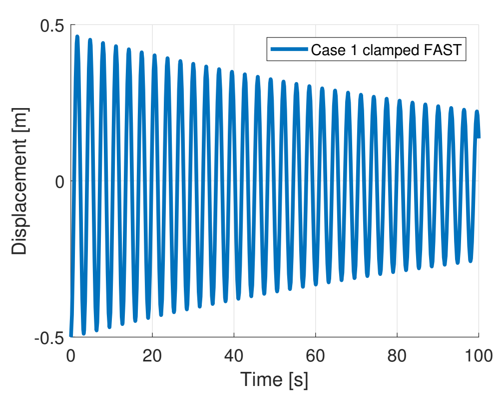

Figure 4.10: Fore-aft displacement, $u_{x,top}$ of the tower top after being released from a prescribed displacement of 0.5 m for Case 1 simulated in FAST.

The amplitude is starting at 0.5 m and decreasing due to the damping in the structure. A fast Fourier transformation, see Appendix I, was applied to analyse the displacement in the frequency domain for Cases 1-3, see Figure 4.11. The amplitude of the first mode is large compared to the second mode.

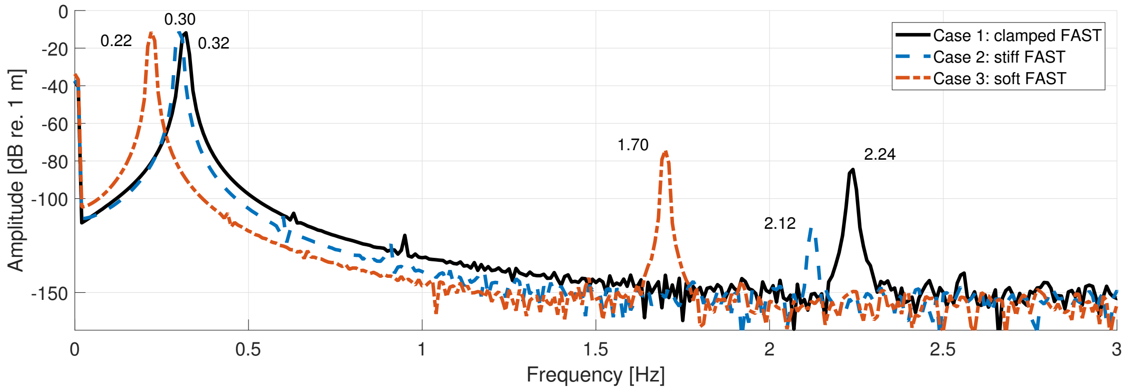

Figure 4.11: Fore-aft displacement amplitudes for case 1, 2 and 3 in FAST. The highlighted values are the peak frequencies for each case.

The natural frequencies calculated in BModes are similar to the frequencies where the amplitude peaks are found for the vibrating system of FAST. The trend of lower natural frequencies with a softer system are also found in the analysis.

4.6 Verification of the implemented SSI in FAST

To verify the implementation of SSI into FAST this Section initially compares the results from CALFEM and FAST. Finally a discussion is conducted followed by a statement about if the implementation of SSI into FAST has been successful or not. Comparison of results from analysis of the wind turbine response due to a constant force in top of tower in CALFEM and a constant wind speed in FAST for Case 1,2 and 3 are presented in Table 4.8. The results are presented both with absolute values and the normalised values. The value of the horizontal displacement $u_{x,top}$ are generally lower from CALFEM than from FAST. When looking at the normalised values of the horizontal displacements the two analyses show a similar magnitude change when changing the support conditions. The base rotation $\theta_{y,1}$ are zero for the clamped case and are similar in value and magnitude for the cases with springs as boundary condition. The natural frequencies computed in CALFEM are together with the natural frequencies from BModes presented in Table 4.9. The results are presented both with values and normalised against the natural frequency for Case 1. The values of the natural frequencies for the two analysis are similar to each other. The small differences could be explained by a slightly different geometry between the models.

Table 4.8: Analysis of the response due to a constant force at top of the tower in CALFEM and a constant wind speed in FAST for Case 1-3. The results are presented followed by a normalisation against Case 1.

		Case 1	Case 2	Case 3
CALFEM $f_{x,top}$	[kN]	635	635	635
FAST $f_{x,top}$	[kN]	630	635	650
CALFEM $u_{x,top}$	[m]	0.349	0.382	0.674
FAST $u_{x,top}$	[m]	0.37	0.405	0.731
CALFEM $\theta_{y,1}$	[rad]	0	0.00037	0.0037
FAST $\theta_{y,1}$	[rad]	0	0.00039	0.0040
CALFEM $(f_{x,top}/f_{x,top,Case1})$	[-]	1	1	1
FAST $(f_{x,top}/f_{x,top,Case1})$	[-]	1	1.008	1.032
CALFEM $(u_{x,top}/u_{x,top,Case1})$	[-]	1	1.095	1.931
FAST $(u_{x,top}/u_{x,top,Case1})$	[-]	1	1.095	1.976
CALFEM $(\theta_{y,1}/\theta_{y,1,Case2})$	[-]	-	1	10
FAST $(\theta_{y,1}/\theta_{y,1,Case2})$	[-]	-	1	10.25

Table 4.9: Natural frequencies for the wind turbine from CALFEM and FAST for Case 1-3. Results are presented with the value followed by a normalisation of the results with Case 1

		Case 1	Case 2	Case 3
CALFEM $f_{n,1}$	[Hz]	0.332	0.317	0.236
FAST $f_{n,1}$	[Hz]	0.322	0.307	0.228
CALFEM $f_{n,2}$	[Hz]	2.278	2.187	1.851
FAST $f_{n,2}$	[Hz]	2.241	2.129	1.705
CALFEM $f_{n,3}$	[Hz]	5.055	4.813	4.247
FAST $f_{n,3}$	[Hz]	5.198	4.844	3.879
CALFEM $(f_{n,1}/f_{n,1,Case1})$	[-]	1	0.984	0.733
FAST $(f_{n,1}/f_{n,1,Case1})$	[-]	1	0.953	0.708
CALFEM $(f_{n,2}/f_{n,2,Case1})$	[-]	1	0.960	0.812
FAST $(f_{n,2}/f_{n,2,Case1})$	[-]	1	0.950	0.761
CALFEM $(f_{n,3}/f_{n,3,Case1})$	[-]	1	0.952	0.840
FAST $(f_{n,3}/f_{n,3,Case1})$	[-]	1	0.932	0.746

The mode shapes from CALFEM are compared to the mode shapes from BModes see Figure 4.12. In common for all three cases is that the first mode is very close in shape between CALFEM and FAST. In the second mode shape a small difference in shape can be detected, this difference is increasing towards the tower top and are about the same for the different cases.

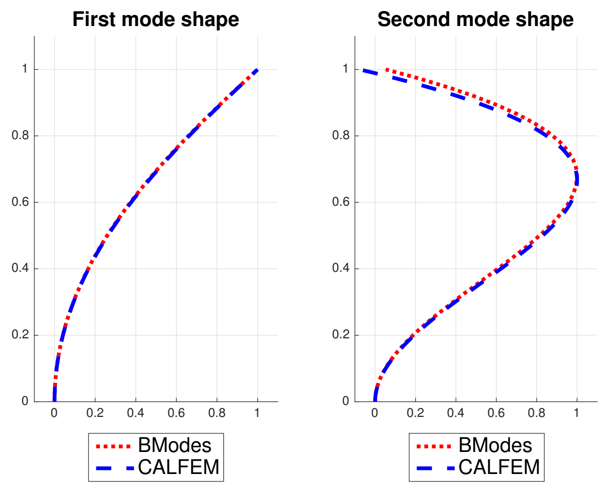

(a) Case 1: Clamped support

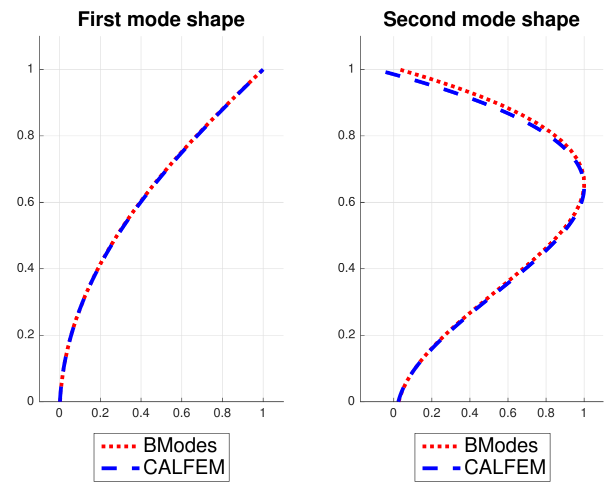

(b) Case 2: Stiff spring support

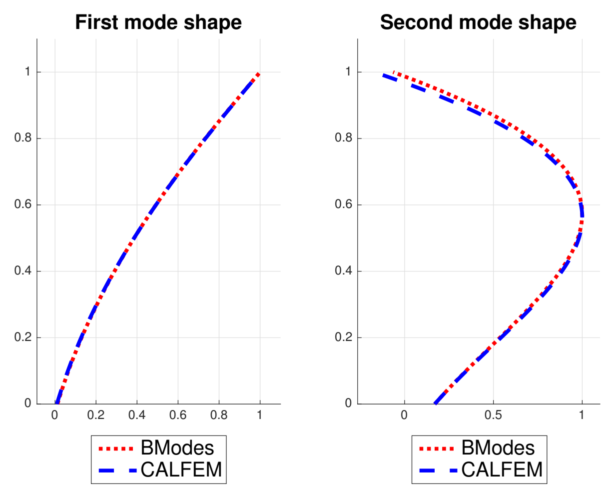

(c) Case 3: Soft spring support

Figure 4.12: Comparison of the first and second normalised mode shapes obtained from BModes and CALFEM.

The final comparison between FAST and CALFEM was performed on the free vibrating wind turbine. The FFT of the displacement in the top of the tower for all three cases are presented in Figure 4.13. The general trend is that the amplitude peaks are found at lower frequencies in FAST than in CALFEM. This coincides with the results from the natural frequency analysis where the results from BModes are slightly lower than the result from CALFEM. The discrepancy between the two models are increasing with decreased stiffness which is also in line with the result from the natural frequency calculations.

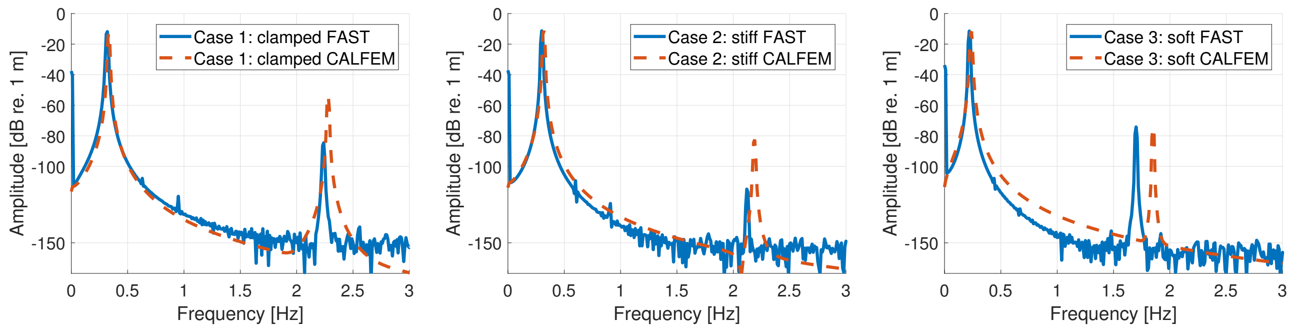

(a) Case 1: Clamped support **(b)** Case 2: Stiff support **(c)** Case 3: Soft support

Figure 4.13: Comparison of the displacement amplitudes obtained from FAST and CALFEM for the free vibrating wind turbine.

The behaviour of a clamped wind turbine modelled in FAST and CALFEM shows a close resemblance under static/quasi-static loading, in natural frequency and in free vibration. This indicate that the modelling is correct and the clamped model in FAST can be trusted. The results shows small discrepancies but these are considered to be not due to any faults in modelling but rather in different techniques of solving and the more holistic wind turbine model used in FAST.

Considering the results for the clamped wind turbine as correct the implementation of SSI, as a spring boundary conditions, also show a similar change in behaviour for FAST and CALFEM. The change of magnitude for both displacement and natural frequencies are very close in magnitude in the two models. The test where the wind turbine was vibrating freely also showed that the behaviour of the wind turbine are changing in the expected and same way for both the models.

Finally, the comparison of results between Case 1, Case 2 and Case 3 for both CALFEM and FAST shows that the implementation of SSI into FAST have been successful. FAST are from now onward the software used in the investigation of the behaviour of a wind turbine when considering the influence of SSI.

5 Study of the influence of SSI on the behaviour of the NREL 5 MW wind turbine

The FAST model and the three formulations for the boundary conditions presented in Section 4.3 were also used to investigate the behaviour of the wind turbine under normal operational conditions for a time period of 630 seconds. This time period is chosen to find equilibrium in the first 30 s, and the following 10 minutes simulation corresponds to a standard time defined in IEC-61400 (2014) for turbulent winds under normal wind conditions. The three cases defined in Section 4.3 were used to investigate the influence of SSI on the wind turbine. Furthermore, two additional simulations including damping added to case 3 were performed to further investigate the influence of SSI. The stiffness and damping properties are implemented in the HydroDyn module in FAST. The following results are presented and discussed: platform moment, rotation and displacement along with the tower top displacement. These result are all considered in the fore-aft direction except for the platform moments that are around the y-axis. For all the cases, a simulated wind was created using TurbSim with pseudorandom number 1000 and a mean wind speed of 12 m/s. This wind is shown in Figure 5.1.

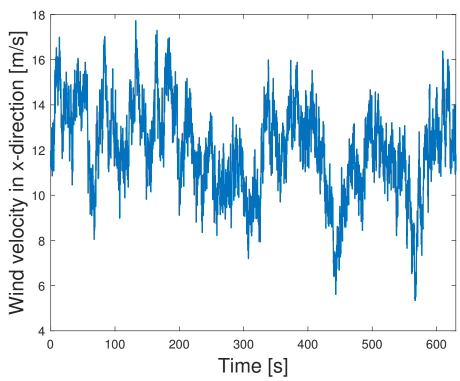

(a) Horizontal wind velocity in x-direction.

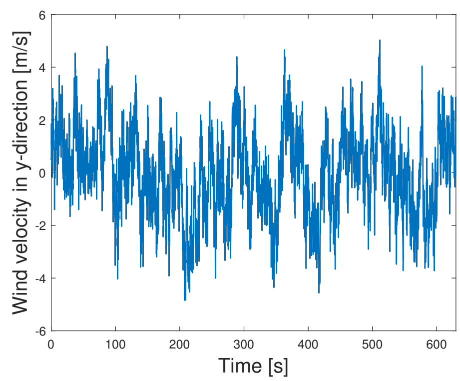

(b) Horizontal wind velocity in y-direction.

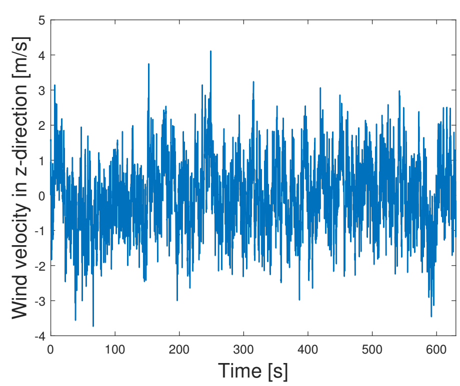

(c) Vertical wind velocity in z-direction

Figure 5.1: Turbulent wind scenario with a mean wind speed of 12 m/s used in the FAST simulation, created in TurbSim.

5.1 Initial study: Cases 1, 2 and 3

First the minimum and maximum values are presented in Table 5.1 for the three cases. Secondly plots of the moment, rotation and displacement for a time span of 20 seconds are shown in Figures 5.2 - 5.4. The maximum rotations and displacements increase for each case with a similar magnitude as shown in previous comparisons, see Table 4.8, which is an expected behaviour since a reduced stiffness is expected to result in larger displacements. The difference in moments and forces are relatively small. Case 3 stands out with slightly higher forces and moments and Case 2 has the lowest forces.

Table 5.1: Analysis of the wind turbine with turbulent wind in FAST for Case 1-3. The results are presented with the maximum and minimum values for each case.

		Case 1	Case 2	Case 3
Max M_y	[kNm]	78091	76769	79814
Min M_y	[kNm]	29180	30394	34000
Max M_x	[kNm]	12805	11862	11280
Min M_x	[kNm]	-1319	-1984	-1749
Max F_y	[kN]	94	118	120
Min F_y	[kN]	-121	-134	-117
Max F_x	[kN]	970	988	1029
Min F_x	[kN]	292	285	278
Max θ_y	[rad]	-	5.20e-04	54.01e-04
Min θ_y	[rad]	-	2.05e-04	22.98e-04
Max $u_{x,top}$	[m]	0.49	0.53	0.97
Min $u_{x,top}$	[m]	0.19	0.22	0.43

In the time interval of 20 seconds a variation between the 3 cases can be observed. The variations for the base moment occur with an oscillating behaviour within rather small time periods. The displacement and rotation of the platform are much larger for Case 3 compared to Case 1 and Case 2, which is expected since a smaller stiffness yields larger displacements when excited with an equal force. Case 3 shows a more oscillating behaviour compared to Case 2. The fore-aft movement shows the same trend as the previous results, a decreased stiffness leads to increased displacements. The trend for the displacement from previous figures can again be observed regarding the magnitude of displacement. The variations over time between the three cases are also similar.

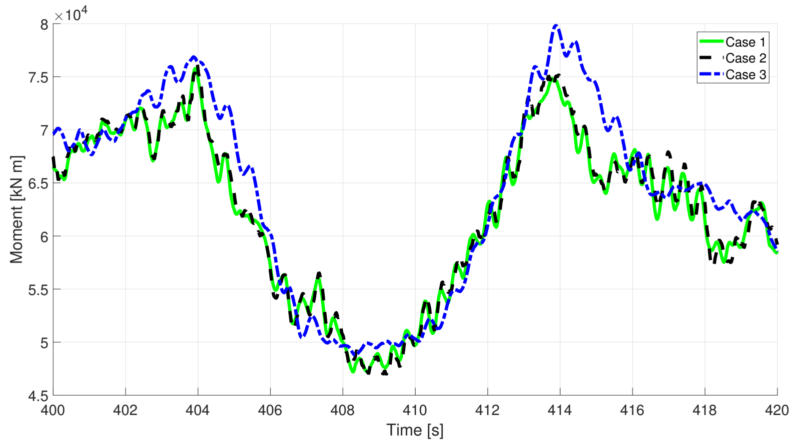

Figure 5.2: Bending moment M_y for case 1, 2 and 3, in a time span of 20 seconds.

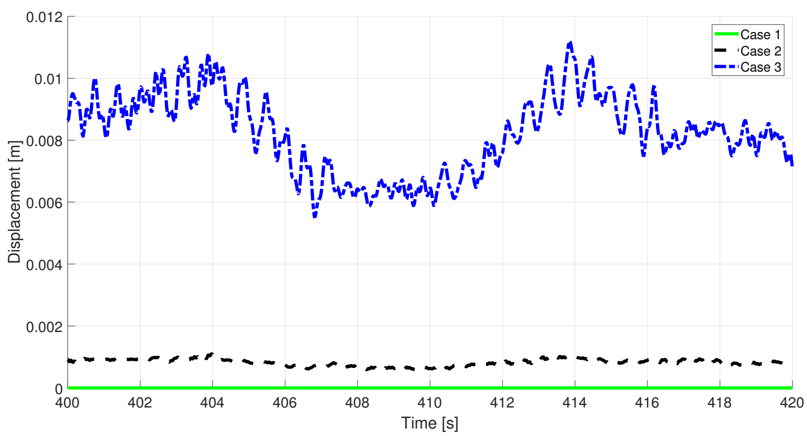

Figure 5.3: Displacement u_x in the tower base for case 1, 2 and 3, in a time span of 20 seconds.

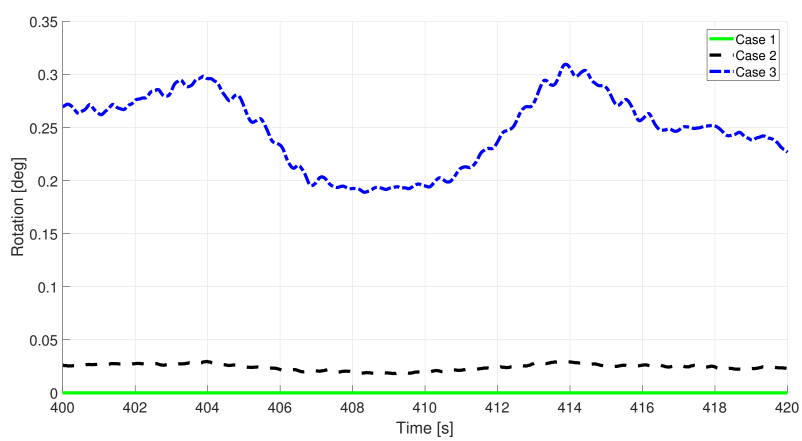

Figure 5.4: Rotation θ_y in the base of the tower for case 1, 2 and 3, in a time span of 20 seconds.

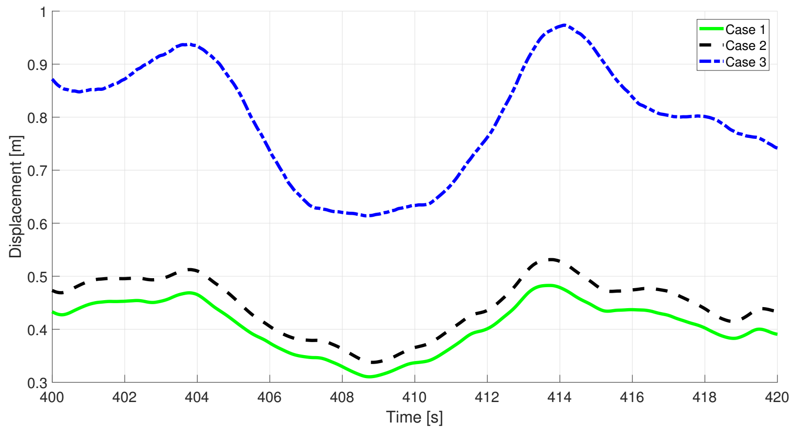

Figure 5.5: Displacement u_x at the tower top for case 1, 2 and 3, in a time span of 20 seconds.

From the figures above, it can be summarised that Case 3 shows large variations compared with Case 1 and 2 considering displacements and rotations. Regarding the moments, Case 1 and 2 resemble each other compared with Case 3 which could not be seen in Table 5.1. A behavioural difference which is seen in the figures is that the oscillations vary. This could indicate a variation in the design regarding parameters influenced by small amplitude oscillations, for instance fatigue. The relative differences are some percent when regarding the maximum moments and forces, see Table 5.1. This indicates that the maximum load cases will not be that influenced by including SSI.

5.2 Case 3 including damping

The damping was added to Case 3 to investigate the impact of including it in the FAST simulation. The first simulation was performed with a damping matrix calculated according to Equation 3.18 with a loading frequency of 0.3 Hz and a hysteretic damping ratio of 2 % calculated from Equation 3.8. The calculation of the hysteretic damping ratio was based on an approximate pressure from the wind turbine foundation of 56 kPa and the plasticity index was assumed to be 0. The radiation damping is not considered due to the low loading frequency as described in Section 4.3. To further investigate the influence of including damping in the analysis, the maximum possible hysteretic damping ratio of 20 % from Figure 3.5 was used.

In Figure 5.6 and Figure 5.7 it is shown that the included damping reduces the oscillations compared with the undamped case. This behaviour is more distinguished when looking at the increased damping case where the oscillations are very small in comparison with the other cases. This result is expected since an added damping parameter should show this behaviour. Figure 5.8 shows a variation in between the cases. The variations are not as clear as the previous figures but there is a difference. The reduced peak at approximately 414 seconds indicates that the increased damping could influence the maximum values.

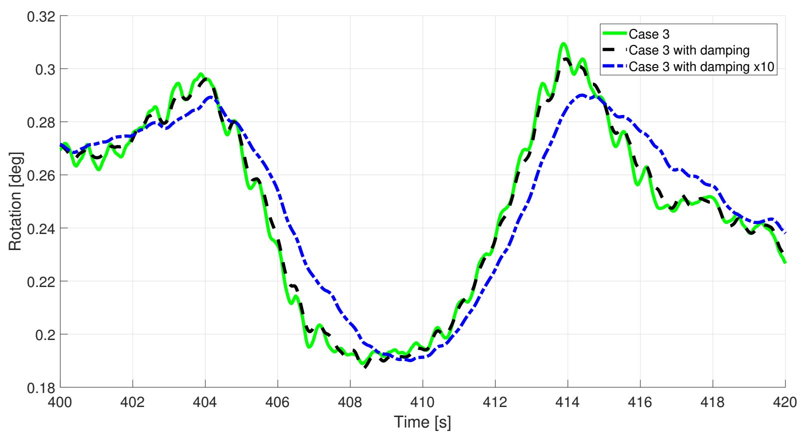

Figure 5.6: θ_y in the tower base for case 3 including damping, in a time span of 20 seconds.

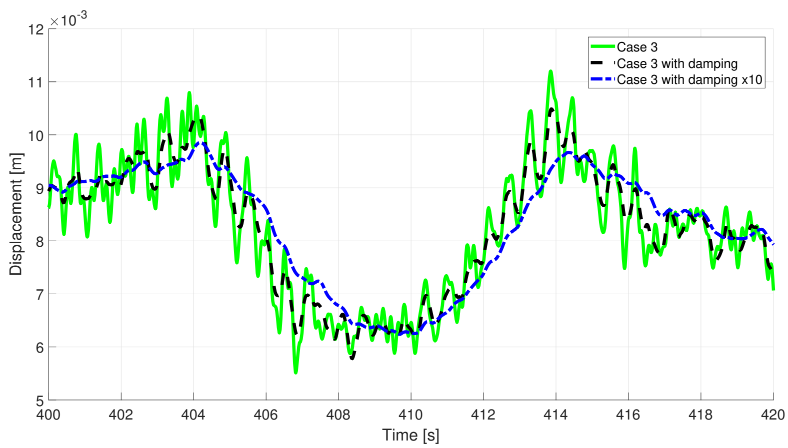

Figure 5.7: Displacement u_x in the tower base for case 3 including damping in a time span of 20 seconds.

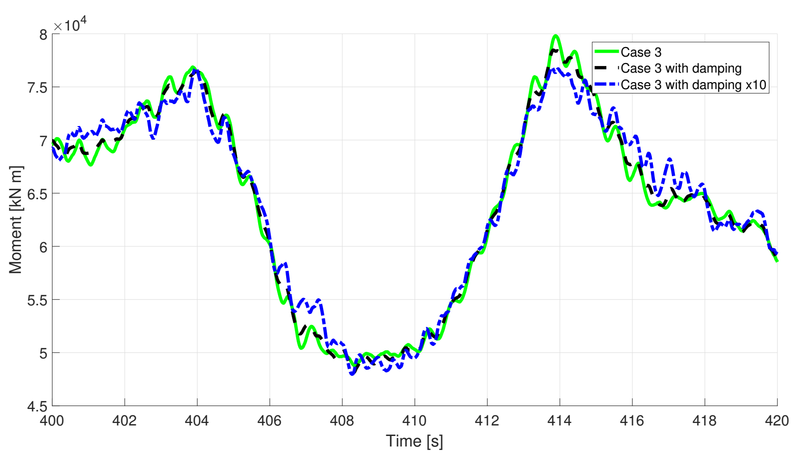

Figure 5.8: Bending moment M_y for case 3 including damping, in a time span of 20 seconds.

The results shows that including damping gives a smoother behaviour compared with an undamped case. The behaviour is noticeable even when including the smallest damping with regard to, loading frequency, strain and radiation, according to Equation 3.18.

5.3 Fatigue analysis of tower-foundation connection

A specified foundation-tower connection was needed to investigate the fatigue damage inflicted on a detail. A so-called bolt cage was used as foundation-tower connection for a wind turbine subjected to similar loads as the 5MW reference turbine. A bolt cage consists of a number of long bolts cast into the foundation that transfers the load from the bottom flange of the tower to the foundation, see Figure 5.9. A similar bolt cage was chosen to connect the tower to the foundation in the fatigue evaluation of the tower. The bolts are subjected to variable loading and was evaluated with respect to fatigue damage. The evaluated connection consists of 160 bolts with a diameter of 48 mm divided in two rows. The bottom flange of the tower has width of 500 mm. The MATLAB script fatigue.m, see Appendix H, was used to calculate the damage in the bolts. The stress in the connection induced by the variable moment in the tower base was calculated based on the assumption of a linear elastic stress distribution in the bottom flange. The stress in each bolt was calculated by multiplying the stress in the flange at the bolt location with the contributory area of the flange. A MATLAB rainflow counting function was applied on the moment-time data to obtain number of cycles and stress ranges. The detail category for a bolt subjected to normal stress is defined, according to EN1993-1-9 (2005), page 20, as 50 MPa.

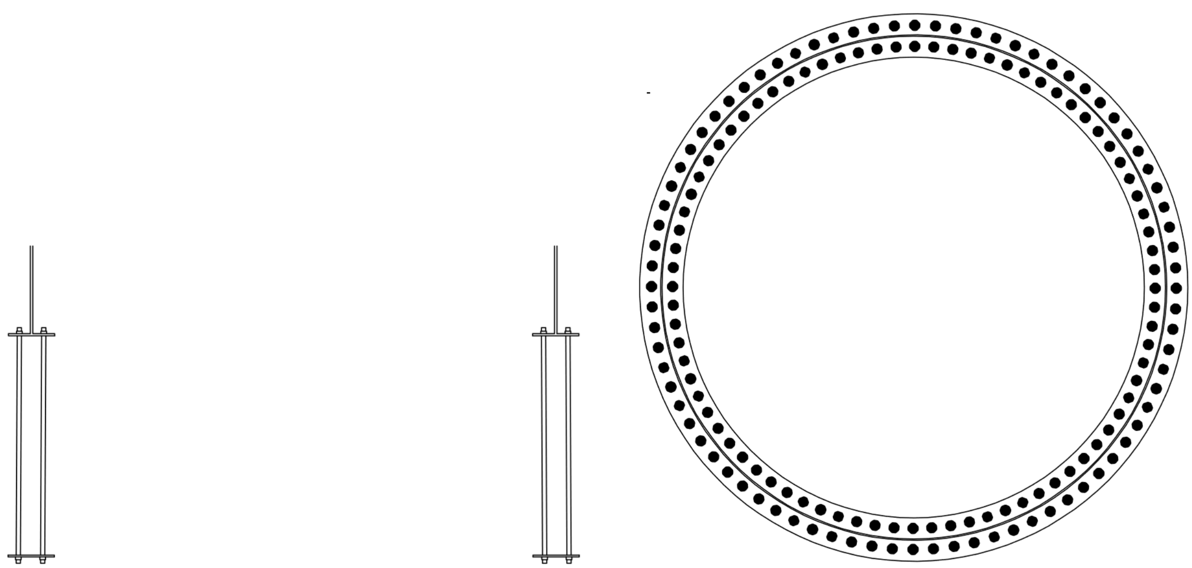

(a) Section. **(b)** Overview.

Figure 5.9: Illustration of the bolt cage connection.

According to DNV/Risø (2002) an accurate fatigue evaluation should be performed by analysing the wind turbine in different operational conditions such as at different wind speeds, start-up and shutdown.

The occurrence of the different scenarios will then be weighed differently based on expected time of occurrence before the fatigue loading is obtained. A simplified fatigue analysis was performed on the results from both constant and turbulent wind for Case 1, Case 2, Case 3 and the damped Case 3 defined in Section 4.3. The actual damage is not of interest since the connection is based on assumptions. The results were therefore normalised to focus on the change between the boundary conditions. The normalisation was performed with the results from Case 1 for the respective wind scenario, Table 5.2. For both wind scenarios the relation between the damage in Case 1 and the other cases are similar.

Table 5.2: Comparison of the fatigue related damage for Case 1-3 in the most stressed bolt in the bolt cage.

	Constant wind 12 [m/s]	Turbulent wind 12 [m/s]
Case 1	No damage	1
Case 2	No damage	0.98
Case 3	No damage	0.99
Case 3 damped	-	0.85

The results in Section 5.1 and Section 5.2 clearly show that the implementation of stiffness and damping parameters have an influence on the behaviour of a wind turbine. The included stiffness shows strong influence on the oscillations. These oscillations are shown to be reduced when including damping. Furthermore, it should be noted that only a time span of 20 s of the simulations are shown, but the same trends can be observed when studying the complete simulations.

5.4 Comprehensive study of the NREL 5 MW reference wind turbine supported on sand

As a final investigation on the effect of SSI on the behaviour of wind turbines a sand, used by Wichtmann (2005) in cyclic loading tests, was implemented as the supporting soil for the wind turbine. The investigation was conducted considering three different boundary conditions; a clamped wind turbine, a spring supported wind turbine and a spring supported damped wind turbine. The soil is a uniform medium coarse to course quartz sand with properties defined in Table 5.3. The choice of supporting soil was based on the fact that the behaviour of the small strain shear modulus of the sand is known.

Table 5.3: Soil properties, obtained from Wichtmann (2005).

G_{max} [MPa]	d_{50} [mm]	U [-]	C [-]	e_{max} [-]	e_{min} [-]	ϕ_c [deg]
120	0.55	1.8	1.2	0.874	0.577	31.2

The simulations in FAST were performed with different wind-speeds and wind scenarios created in TurbSim, see Section 4.1. The various speeds and scenarios were included to provide an indication of the stochastic influence from the turbulent winds. The random seed number and mean wind speed influence the generated wind scenarios. Using the same seed number with varying mean wind speed generates a random scenario, thus, a change of mean wind speed using the same seed number does not scale the wind scenario. The only turbulence considered was the normal Kaimal turbulence with turbulence characteristics B according to the IEC standard. Used wind scenarios are specified in Table 5.4.

Table 5.4: Random seed number and mean wind speed for TurbSim used to create wind scenarios for FAST simulations.

Wind mean [m/s]	6	9	12	15	18
Random seed number [-]	994	997	1000	1003	1006

5.4.1 Investigation of shear strain magnitude

The cyclic loading on the wind turbine leads to a varying shear strain of the supporting soil. The variation of shear strain could lead to a reduced shear stiffness, as discussed in Section 3.2. To investigate the range of stiffness a simplified calculation was performed of the magnitude of shear strain when the foundation was supported on with the maximum shear modulus.

The strain due to cyclic loading in the soil was assumed to depend only on the rotation of the foundation in the wind direction. Based on the assumption of a rigid foundation, the displacement in the edge of the foundation can be calculated from the base rotation, see Figure 5.10. The displacement was assumed to occur within the soil at a depth equal to the foundation radius based on Boussinesq theory of the influence of an applied load on the surface against depth for a quadratic foundation (Knappet & Craig, 2012). Simplifying the problem, excluding horizontal stress, the horizontal strain was calculated using the definition of Poisson's ratio. The shear strain was then calculated as the difference between the vertical and horizontal strain.

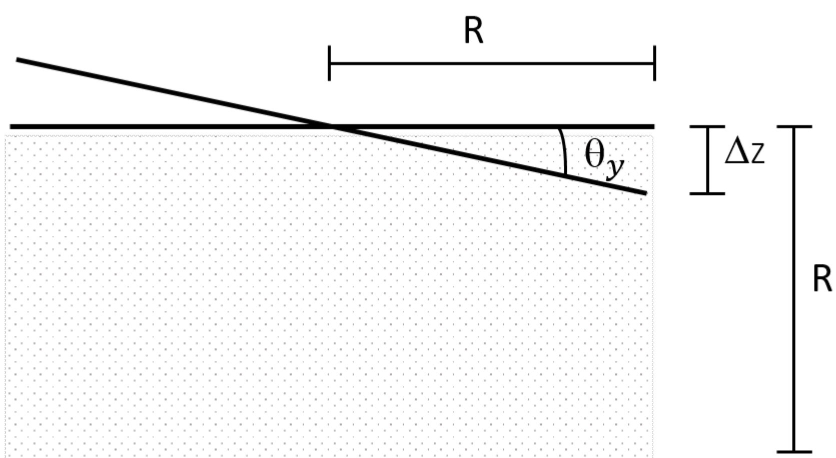

$$\varepsilon_z = \Delta z/R$$
$$\varepsilon_x = \nu\,\varepsilon_z$$
$$\gamma_{zx} = \varepsilon_z - \varepsilon_x$$

Figure 5.10: Illustration of geometry and equations used for calculation of the shear strain below the foundation.

The shear modulus as a function of shear strain for the supporting sand is shown in Figure 5.11, note the elastic strain threshold. The shear modulus is considered to be constant when strain is below this threshold, see Section 3.2.

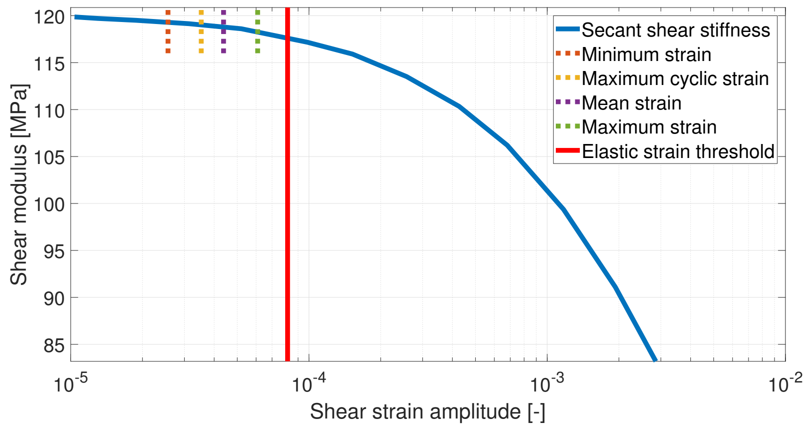

Figure 5.11: Shear modulus as a function of strain for the supporting sand. Obtained from Wichtmann (2005), sand number 3.

The vertical displacement Δz is calculated from the foundation pitch rotation. The maximum, minimum and mean shear strains are presented in Table 5.5 together with the highest amplitude strain cycle obtained in a rainflow analysis of the rotation-time series. All shear strains obtained in the soil are well below the elastic threshold strain of the sand, no reduction of shear modulus for this soil due to strain is therefore necessary.

Table 5.5: Rotations and calculated strains with implemented soil

ν	[-]	0.3
R	[m]	12.5
θ_{max}	[Rad]	$8.70 * 10^{-5}$
θ_{mean}	[Rad]	$6.25 * 10^{-5}$
θ_{min}	[Rad]	$3.65 * 10^{-5}$

5.4.2 Results

The natural frequency of the wind turbine system when implementing the quartz sand as a boundary condition is presented in Table 5.6. Figure 5.12 shows the relation between the maximum moment and fatigue damage inflicted on the bolt in the wind turbine for different wind speeds. The trend shows an increase in the maximum moment with an increased wind speed. The fatigue damage is also increasing with the wind speed if excluding the results from 6 m/s. An explanation was sought for the discrepancy in the trend. The number of cycles causing fatigue damage to the structure was noted and is presented in Table 5.7. The number of stress cycles do not change considerably in between the different wind scenarios, however the number of high amplitude cycles causing damage to the connection is different. The 6 m/s show more damage cycles than the 9 and 12 m/s scenarios. The trend with increasing number of damage cycles with increased wind speeds are in line with the increase in inflicted damage presented in Figure 5.12. When comparing the behaviour of the moment in the tower base in Figure 5.13 for the 6 and 12 m/s scenarios an oscillating behaviour can be spotted for the 6 m/s scenario which cannot be detected for other scenarios. A possible explanation could be that the mean rotational speed of the rotor for the 6 m/s is 8.0 rpm compared to the 11.9 rpm for the 12 m/s scenario. This causes the 3P excitation to be closer to the wind turbines first natural frequency and hence could explain the oscillation.

The number of cycles within a certain boundary condition for the different wind scenarios are fairly similar. However, the standard deviation is larger at higher wind speeds, for instance 1.98 for 12 m/s compared to 2.82 for 18 m/s, this corresponds with the larger fatigue damage presented in Figure 5.12. When comparing the number of cycles for the same wind scenario but different boundary conditions the number of counted cycles are different. The explanation can be seen in Figure 5.14 where the spring supported wind turbine show a large amount of low amplitude cycles compared to the other boundary conditions. A grouping of the different stress cycles, see Figure 5.15, show that the large majority of the stress cycles is in a range of a magnitude considerably lower than moment causing damage to the bolt.

Table 5.6: Natural frequencies for the wind turbine calculated in BModes for clamped and spring supported foundation

		Clamped	Spring support
$f_{n,1}$	[Hz]	0.332	0.319
$f_{n,2}$	[Hz]	2.241	2.205
$f_{n,1}/f_{n,1,Clamped}$	[-]	1	0.961
$f_{n,2}/f_{n,2,Clamped}$	[-]	1	0.984

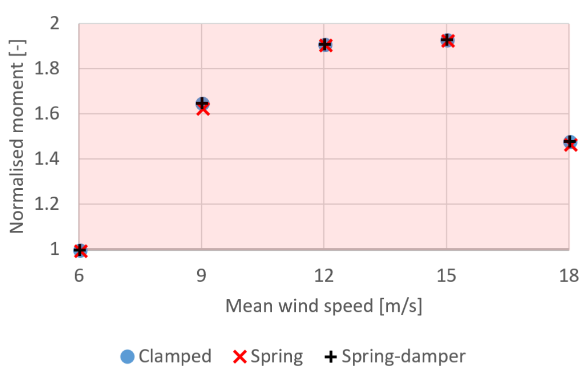

(a) Normalised maximum moment

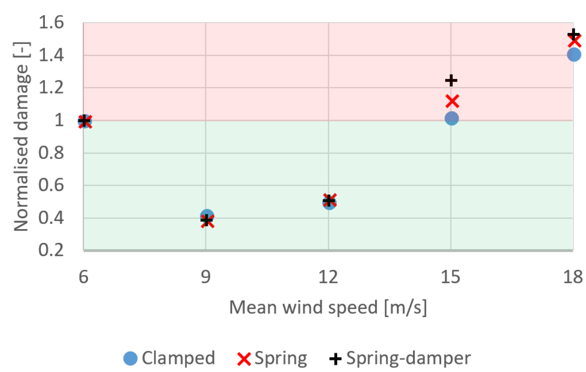

(b) Normalised fatigue damage

Figure 5.12: Maximum moment and accumulated damage normalised with results obtained for the analysis with a wind speed of 6 m/s. See Appendix A for numerical values.

Table 5.7: Number of cycles ($N_{TOT,cycle}$) obtained from rainflow count on the total cycles and number of cycles causing damage ($N_{D,cycle}$). The number of cycles are presented for different wind scenarios and boundary conditions.

Mean wind [m/s]	Clamped $N_{D,cycle}$ [-]	Clamped $N_{TOT,cycle}$ [-]	Spring $N_{D,cycle}$ [-]	Spring $N_{TOT,cycle}$ [-]	Damped $N_{D,cycle}$ [-]	Damped $N_{TOT,cycle}$ [-]
6	58	1592	56	8768	54	3068
9	27	1870	28	8027	27	2611
12	42	1829	44	6931	41	2351
15	59	1747	61	7206	60	2216
18	85	1762	86	7705	80	2236

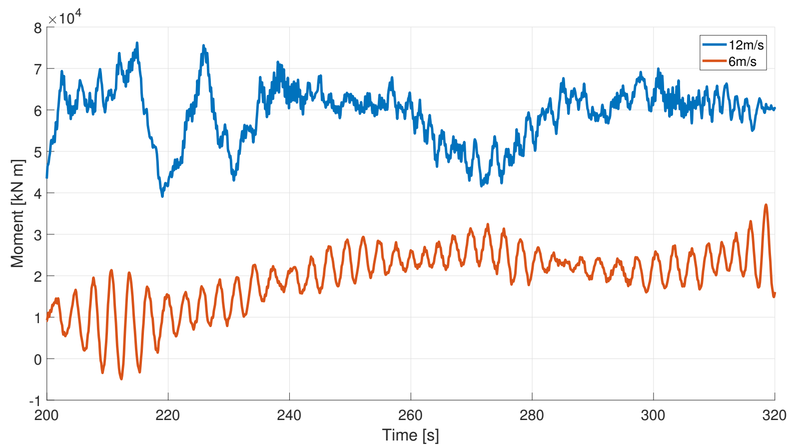

Figure 5.13: Bending moment M_y for a mean turbulent wind speed of 6 and 12 m/s.

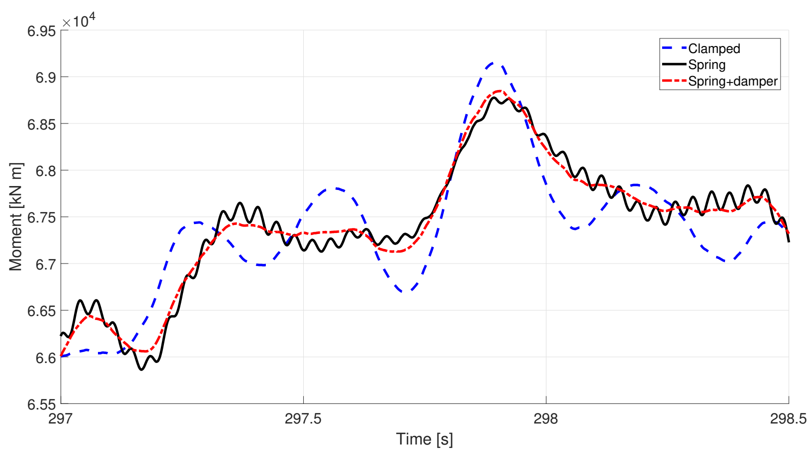

Figure 5.14: Bending moment M_y for different boundary conditions for a mean turbulent wind speed of 12 m/s.

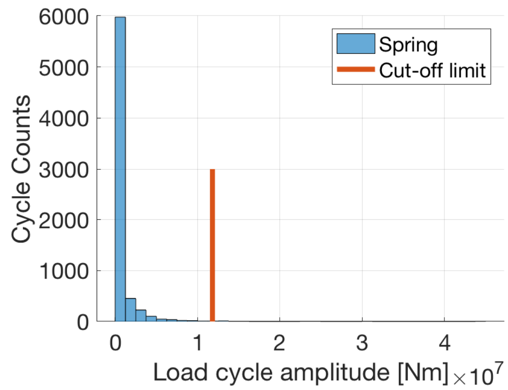

Figure 5.15: Histogram of stress cycles from the analysis of 12 m/s spring supported wind turbine. The cut-off limit is the minimum cyclic moment causing damage to the bolts.

In Figure 5.16 the results from the simulations using different boundary conditions are shown for each wind scenario normalised with the clamped support condition. The sum of all scenarios shows the highest damage for the spring supported followed by the spring and damped boundary condition. The general trend is that the spring supported turbine show higher fatigue damage than the clamped. The introduction of damping in the analysis gives less fatigue damage than when only implementing a spring. Comparing the clamped and damped tower the result indicates a lower fatigue damage for low wind speeds and a higher fatigue damage for higher wind speeds for the damped tower. The maximum moment in the base of the wind turbine show no indication to increase or decrease in any substantial magnitude.

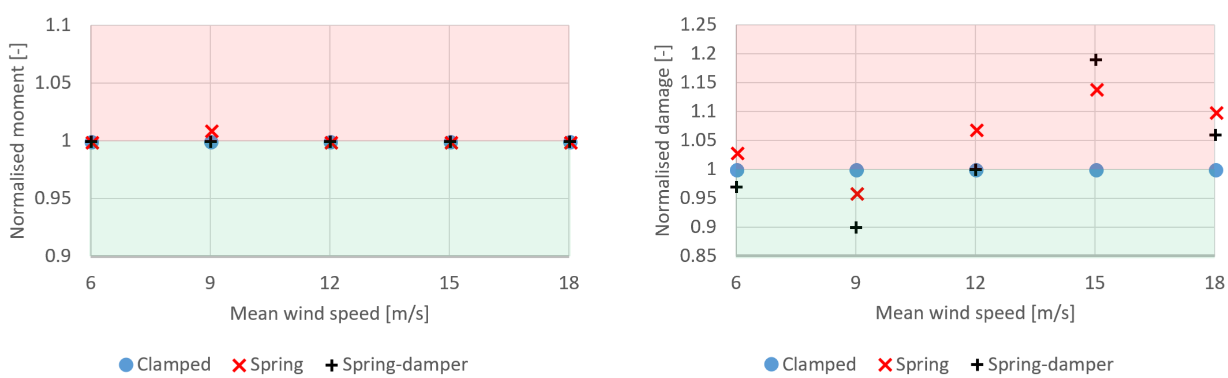

(a) Normalised maximum moment

(b) Normalised fatigue damage

Figure 5.16: The accumulated damage and maximum moment normalised with the results using a clamped boundary condition for each wind speed. See Appendix A for numerical values.

To investigate the impact of the randomised turbulence in the simulations two comparisons were conducted for different wind scenarios based on the same mean wind speed. The relative change in between the different boundary conditions for two different wind scenarios are presented in Table 5.8. The change between the different boundary conditions are similar for the two wind scenarios. There is a difference in the relation between the three different boundary conditions for the two wind scenarios. Scenario 999 shows a higher relative damage when including SSI than the original scenario.

Table 5.8: Results from two different turbulent wind scenarios based the clamped boundary condition for each scenario.

Mean wind	Clamped		Spring		Damped	
[m/s]	D_{PM} [-]	$M_{y.max}$ [-]	D_{PM} [-]	$M_{y.max}$ [-]	D_{PM} [-]	$M_{y.max}$ [-]
9	1	1	0.96	1.00	0.90	1.00
9_{999}	1	1	1.03	1.01	0.94	1.01

A second comparison of three simulations using different wind scenarios with the same mean speed of 12 m/s was performed. The results can be seen in Table 5.9 and indicate a large spread in the fatigue damage in different wind scenarios. The maximum moments are similar between the scenarios.

Table 5.9: Damage and maximum moment for three different turbulent wind scenarios based on a mean wind speed of 12 m/s.

Mean wind [m/s]	D_{PM} [-]	$M_{y.max}$ [-]
12	1	1
12_{3000}	1.37	1.00
12_{4000}	1.74	1.01

6 Conclusion and recommendations

6.1 Conclusion

The aim of the research presented in this Thesis was *to implement soil-structure interaction (SSI) in an existing open source code for wind turbine analyses (FAST). Furthermore, the impact of incorporating SSI on the analyses of an onshore wind turbine, supported by a gravity based concrete foundation has been studied*. The study shows that:

- SSI can be relatively easily be implemented in the wind turbine simulation software FAST by redefining the boundary conditions using a 6 DOF stiffness and damping formulations at the base of the wind turbine tower. The stiffness (spring) boundary conditions were formulated as a function of the shear modulus and Poisson's ratio of the soil below the foundation, combined with the foundation geometry. The damping boundary conditions were formulated as a function of the stiffness boundary conditions together with internal damping ratio of the subsoil.

- The inclusion of SSI, as opposed to a rigid foundation, in the analyses reduced the natural frequencies of the wind turbine. The rotations and displacements in the tower and foundation increased when including SSI in the analysis.

- Although the maximum moment in the tower base connection was not affected much by including SSI in the analyses, the time response of the moment does change significantly. The latter demonstrates that for these type of complex dynamic analyses both the amplitude and time needs to be incorporated in the data interpretation.

- A promising method to assess the impact of SSI on the wind turbine response, or indeed the changing spectral response of the dynamic loads, such as the moment-time response at foundation level, is to assess its impact as function of the fatigue damage sustained by the tower-foundation connection.

- The fatigue damage results indicate a significant influence of SSI, for which no general trend could be established. This inconsequential, case specific, response necessitates the incorporation of SSI in the holistic analyses of wind turbine response that includes the foundation response.

6.2 Recommendations for further studies

The analyses conducted show that the fatigue damage is influenced by SSI, however no clear general trend could be detected. To determine the impact of considering SSI, more wind scenarios and events should be simulated, decreasing the importance of the random seed of a single wind scenario or event, giving a more statistically certain result regarding the influence on fatigue damage. Furthermore, the influence of SSI for various soil, with possible reduction of shear modulus, and other site conditions should be analysed to investigate if a general trend can be detected.

A less stiff soil will be subjected to larger strains leading to a reduction in shear modulus. A non-linear soil stiffness is recommended to be implemented and compared to a linear stiffness to investigate the impact of considering the non-linear stiffness in soil. A full site-specific design process of a wind turbine and foundation is recommended to be performed considering the effect of SSI. A comparison with a clamped tower is recommended to be conducted to detect all possible changes in design.

Gazetas straightforward and comprehensive 6 DOF formulations of stiffness and damping used in this Thesis, are recommended to be validated against stiffness and damping measured at a real wind turbine foundation. The 6 DOF model is limited since it considers the shear modulus of the soil underneath the foundation as uniform. However, the loading on the foundation will create an uneven strain underneath the foundation which could lead to a nonuniform shear modulus. The analysis of SSI using a FE-formulation able to describe a more complex and diverse soil response is recommended to be compared to Gazetas formulation.

The accumulation of deformations in the soil below the foundation has not been considered in this Thesis. The accumulated deformations are affecting the settlements of the foundation regulated in the design codes. An investigation is recommended on how accumulation of settlements is affecting the behaviour of the wind turbine and if it need to be considered in the foundation design. The movement and accumulated deformations in the soil could lead to gaps in the soil-foundation interface leading to a change in the support stiffness.

References

Aasen, S., Page, A. M., Skau, K. S., & Nygaard, T. A. (2017). Effect of foundation modelling on the fatigue lifetime of a monopile-based offshore wind turbine. *Wind Energy Science*, *2*. (Cited on page 1).

Ackermann, T. (2005). *Wind power in power systems*. John Wiley & Sons, Incorporated, Hoboken. (Cited on pages 5, 6).

Bhattacharya, S., Nikitas, G., & Jalbi, S. (2018). On the use of scaled model tests for analysis and design of offshore wind turbines. *Developments in Geotechnical Engineering*, *6*. (Cited on page 6).

Bhattacharya, S. (2014). Challanges in design of foundations for offshore wind turbines. *Engineering & Technology Reference*, *112*. (Cited on page 6).

Bir, G. (2007). *User's guide to bmodes (software for computing rotating beam coupled modes*. National Renewable Energy Laboratory. (Cited on page 23).

Darendeli, M. B. (2001). *Development of a new family of normalized modulus reduction and material damping curves* (Doctoral dissertation, The University of Texas of Texas at Austin). (Cited on pages 13–16).

DNV/Risø. (2002). *Guidelines for design of wind turbines 2nd edition*. DNV/Risø. (Cited on pages 1, 7, 42).

Dobry, R. & Gazetas, G. (1986). Dynamic response of arbitrarily shaped foundations. *Journal of Geotechnical Engineering*, *112*. (Cited on pages 1, 16, 18, 20).

EN1993-1-9. (2005). *Eurocode - design of steel structures - fatigue*. EUROPEAN COMMITTEE FOR STANDARDIZATION. (Cited on pages 9, 42).

EN1997. (2005). *Eurocode 7: Geotechnical design – part 1: General rules*. EUROPEAN COMMITTEE FOR STANDARDIZATION. (Cited on page 8).

Gazetas, G. (1983). Analysis of machine foundation vibrations: State of the art. *Soil Dynamics and Earthquake Engineering*, *2*. (Cited on pages 1, 18).

Gazetas, G. (1991). Foundation vibrations. In H.-Y. Fang (Editor), *Foundation engineering handbook* (Pages 553–593). Springer, Boston, MA. (Cited on page 14).

GCR12-917-21. (2012). *Soil-structure interaction for building structures*. National Institute of Standards and Technology. US. (Cited on page 10).

Harte, M., Basu, B., & Nielsen, S. (2012). Dynamic analysis of wind turbines including soil-structure interaction. *Engineering structures*, *45*. (Cited on page 1).

IEC-61400. (2014). *Iec 61400-1 wind turbines – part 1: Design requirements*. The International Electrotechnical Commission. (Cited on pages 7, 23, 37).

Jonkman, B. & Kilcher, L. (2012). *Turbsim user's guide: Version 1.06.00*. National Renewable Energy Laboratory. (Cited on page 23).

Jonkman, J. (2015, January 23). Fast forum. Retrieved May 10, 2018, from https://wind.nrel.gov/forum/wind/viewtopic.php?f=3&t=1227&hilit=soil+structure+interaction. (Cited on page 24)

Jonkman, J. (2018, January 4). Fast. Retrieved April 16, 2018, from https://nwtc.nrel.gov/FAST. (Cited on page 22)

Jonkman, J. & Buhl, M. (2005). *Fast user's guide*. National Renewable Energy Laboratory. (Cited on page 23).

Jonkman, J., Butterfield, S., Musial, W., & Scott, G. (2009). *Definition of a 5-mw reference wind turbine for offshore system development*. National Renewable Energy Laboratory. (Cited on page 24).

Jonkman, J., Robertson, A., & Hayman, G. (2014). *Hydrodyn user's guide and theory manual*. National Renewable Energy Laboratory. (Cited on page 23).

Jung, S., Kim, S.-R., Patil, A., & Hung, L. C. (2015). Effect of monopile foundation modeling on the structural response of a 5-mw offshore wind turbine tower. *Ocean Engineering*, *109*. (Cited on page 1).

Knappet, J. & Craig, R. (2012). *Craig´s soil mechanics 8th edition*. Spon Press Abingdon. (Cited on pages 10, 26, 44).

Krathe, V. L. (2015). *Aero-hydro dynamic analysis of offshore wind turbine* (Master's thesis, CNorwegian University of Science and Technology, Department of Structural Engineering). (Cited on page 24).

Kropp, W. (2015). *Propagation and radiation of structure borne sound*. Division of Applied Acoustics Chalmers University of Technology. (Cited on page 11).

Manwell, J., McGowan, J. G., & Rogers, A. L. (2010). *Wind energy explained : Theory, design and application*. John Wiley & Sons, Incorporated, New York. (Cited on pages 4, 5).

Perry, M., McAlorum, J., Fusiek, G., Niewczas, P., McKeeman, L., & Rupert, T. (2017). Crack monitoring of operational wind turbine foundations. *Sensors*, *17*. (Cited on page 1).

Richart, F., Hall, J. G., & Woods, R. D. (1970). *Vibrations of soils and foundations*. Prentice Hall inc, Englewood Cliffs N.J. (Cited on page 14).

Swedish Energy Agency. (2016). *Vindkraftstatistik 2017*. Swedish Energy Agency. (Cited on page 1).

Taddei, F., Butenweg, C., & Klinkel, S. (2015). Parametric investigation of the soil–structure interaction effects on the dynamic behaviour of a shallow foundation supported wind turbine considering a layered soil. *Wind Energy*, *17*. (Cited on page 1).

UN Department of Economic and Social Affairs. (2015). Sustainable development goal 7. Retrieved January 30, 2018, from https://sustainabledevelopment.un.org/sdg7. (Cited on page 1)

Verruijt, A. (2010). *An introduction to soil dynamics*. Springer Dordrecht New York. (Cited on pages 11, 13, 14).

Warren-Codrington, C. J. (2013). *Geotechnical considerations for onshore wind turbines*. University of Cape Town Department of Civil Engineering. (Cited on pages 4, 7).

Wichtmann, T. (2005). *Explicit accumulation model for non-cohesive soils under cyclic loading* (Doctoral dissertation, Des institutes fürgrundbau und beodenmechanik der Ruhr-Universität Bochum). (Cited on pages 16, 43, 45).

World Energy Council. (2016). World energy resources wind 2016. Retrieved January 30, 2018, from https://www.worldenergy.org/wp-content/uploads/2017/03/WEResources_Wind_2016.pdf. (Cited on page 1)

A Tabulated results: Comprehensive analysis

Table A.1: Results for different wind scenarios and mean wind speeds. The accumulated damage and maximum moment from each analysis are presented normalised with results obtained for the analysis with a wind speed of 6 m/s. Presented in Figure 5.12 .

Mean wind [m/s]	Clamped D_{PM} [-]	Clamped $M_{y.max}$ [-]	Spring D_{PM} [-]	Spring $M_{y.max}$ [-]	Spring-Damper D_{PM} [-]	Spring-Damper $M_{y.max}$ [-]
6	1	1	1	1	1	1
9	0.42	1.65	0.39	1.63	0.39	1.65
12	0.50	1.91	0.52	1.91	0.51	1.91
15	1.02	1.93	1.13	1.93	1.25	1.93
18	1.41	1.48	1.50	1.47	1.53	1.48

Table A.2: The accumulated damage and maximum moment normalised with the results using a clamped boundary condition for each wind speed. Presented in Figure 5.16

Mean wind [m/s]		Clamped	Spring	Damped
6	D_{PM} [-]	1	1.03	0.97
	$M_{y.max}$ [-]	1	1.00	1.00
9	D_{PM} [-]	1	0.96	0.90
	$M_{y.max}$ [-]	1	1.01	1.00
12	D_{PM} [-]	1	1.07	1.00
	$M_{y.max}$ [-]	1	1.00	1.00
15	D_{PM} [-]	1	1.14	1.19
	$M_{y.max}$ [-]	1	1.00	1.00
18	D_{PM} [-]	1	1.10	1.06
	$M_{y.max}$ [-]	1	1.00	1.00
Sum of all wind scenarios	D_{PM} [-]	1	1.01	1.01

B BModes input file

```
=====================   BModes v3.00 Main Input File  =================
NREL 5MW Tower with fixed bottom

--------- General parameters
---------------------------------------------------------------------
true      Echo        Echo input file contents to *.echo file if true.
2         beam_type   1: blade, 2: tower (-)
0.        romg:       rotor speed, automatically set to zero for tower modal
analysis (rpm)
1.        romg_mult:  rotor speed muliplicative factor (-)
87.6      radius:     rotor tip radius measured along coned blade axis, OR tower
height above ground level [onshore] or MSL [offshore](m)
0.        hub_rad:    hub radius measured along coned blade axis OR tower
rigid-base height (m)
0.        precone:    built-in precone angle, automatically set to zero for a
tower (deg)
0.        bl_thp:     blade pitch setting, automatically set to zero for a tower
(deg)
1         hub_conn:   hub-to-blade or tower-base boundary condition [1:
cantilevered; 2: free-free; 3: only axial and torsion constraints] (-)
20        modepr:     number of modes to be printed (-)
t         TabDelim    (true: tab-delimited output tables; false: space-delimited
tables)
f         mid_node_tw  (true: output twist at mid-node of elements; false: no
mid-node outputs)

--------- Blade-tip or tower-top mass properties
----------------------------------------
3.500003109E+005   tip_mass    blade-tip or tower-top mass (kg)
-0.4137754432      cm_loc      tip-mass c.m. offset from the tower axis measured
along x-tower axis (m)
1.9669893542       cm_axial    tip-mass c.m. offset tower tip measures axially
along the z axis (m)
4.370E7            ixx_tip     blade lag mass moment of inertia about the
tip-section x reference axis (kg-m^2)
2.353E7            iyy_tip     blade flap mass moment of inertia about the
tip-section y reference axis (kg-m^2)
2.542E7            izz_tip     torsion mass moment of inertia about the
tip-section z reference axis (kg-m^2)
0.                 ixy_tip     cross product of inertia about x and y reference
axes(kg-m^2)
1.169E6            izx_tip     cross product of inertia about z and x reference
axes(kg-m^2)
0.                 iyz_tip     cross product of inertia about y and z reference
axes(kg-m^2)

--------- Distributed-property identifiers
--------------------------------------------------------
1         id_mat:     material_type [1: isotropic; non-isotropic composites
option not yet available]
'Frommanual.dat'   : sec_props_file   name of beam section properties file (-)

Property scaling factors............................
1.0       sec_mass_mult:   mass density multiplier (-)
```

```
1.0       flp_iner_mult:   blade flap or tower f-a inertia multiplier (-)
1.0       lag_iner_mult:   blade lag or tower s-s inertia multiplier (-)
1.0       flp_stff_mult:   blade flap or tower f-a bending stiffness multiplier
(-)
1.0       edge_stff_mult:  blade lag or tower s-s bending stiffness multiplier
(-)
1.0       tor_stff_mult:   torsion stiffness multiplier (-)
1.0       axial_stff_mult: axial stiffness multiplier (-)
1.0       cg_offst_mult:   cg offset multiplier (-)
1.0       sc_offst_mult:   shear center multiplier (-)
1.0       tc_offst_mult:   tension center multiplier (-)

--------- Finite element discretization
--------------------------------------------------
61        nselt:     no of blade or tower elements (-)
Distance of element boundary nodes from blade or flexible-tower root (normalized
wrt blade or tower length), el_loc()
0       0.003481894     0.010445682     0.017409471     0.024373259
0.031337047     0.038300836     0.045264624     0.052228412     0.059192201
0.066155989     0.073119777     0.080083565     0.087047354     0.094011142
0.10097493      0.107938719     0.114902507     0.121866295     0.128830084
0.135793872      0.13990        0.149721448     0.156685237     0.163649025
0.170612813     0.177576602     0.18454039      0.191504178     0.198467967
0.205431755     0.212395543     0.219359331     0.22632312      0.233286908
0.240250696     0.247214485     0.250696379     0.320334262      0.37971
0.424791072     0.45961 0.486635        0.51366 0.54068 0.5677  0.594715
0.62173 0.64875 0.67577 0.70279 0.72981 0.75683 0.78385 0.81087 0.83789 0.864905
0.89192 0.91894 0.94596 0.97298 1.0

--------- Properties of tower support subsystem (read only if beam_type is 2)
------------
1          tow_support: : aditional tower support [0: no additional support; 1:
floating-platform or monopile with or without tension wires] (-)
0.0       draft        : depth of tower base from the ground or the MSL (mean
sea level) (m)
0.0        cm_pform     : distance of platform c.m. below the MSL (m)
0.0        mass_pform   : platform mass (kg)
Platform mass inertia 3X3 matrix (i_matrix_pform):
0.   0.   0.
0.   0.   0.
0.   0.   0.
0.0       ref_msl    : distance of platform reference point below the MSL (m)
Platform-reference-point-referred hydrodynamic 6X6 matrix (hydro_M):
0.  0.  0.  0.  0.  0.
0.  0.  0.  0.  0.  0.
0.  0.  0.  0.  0.  0.
0.  0.  0.  0.  0.  0.
0.  0.  0.  0.  0.  0.
0.  0.  0.  0.  0.  0.
Platform-reference-point-referred hydrodynamic 6X6 stiffness matrix (hydro_K):
0.  0.  0.  0.  0.  0.
0.  0.  0.  0.  0.  0.
0.  0.  0.  0.  0.  0.
0.  0.  0.  0.  0.  0.
```

```
0.  0.  0.  0.  0.  0.
0.  0.  0.  0.  0.  0.
Mooring-system 6X6 stiffness matrix (mooring_K):
0.  0.  0.  0.  0.  0.
0.  0.  0.  0.  0.  0.
0.  0.  0.  0.  0.  0.
0.  0.  0.  0.  0.  0.
0.  0.  0.  0.  0.  0.
0.  0.  0.  0.  0.  0.

Distributed (hydrodynamic) added-mass per unit length along a flexible portion
of the tower length:
0           n_secs_m_distr: number of sections at which added mass per unit
length is specified (-)
0.  0.    : z_distr_m [row array of size n_added_m_pts; section locations wrt
the flexible tower base over which distributed mass is specified] (m)
0.  0.    : distr_m [row array of size n_added_m_pts; added distributed masses
per unit length] (kg/m)

Distributed elastic stiffness per unit length along a flexible portion of the
tower length:
0           n_secs_k_distr: number of points at which distributed stiffness per
unit length is specified (-)
0       1       2       3       4       5       6       7       8       9
10      11      12      13      14      15      16      17      18      19
20      21      22      23      24      25      26      27      28      29
30      31      32      33      34      35      36  : z_distr_k [row array of
size n_added_m_pts; section locations wrt the flexible tower base over which
distributed stiffness is specified] (m)
595318000.0     1165208000      1129400000      1095553000      1059931000
1024493000      989209000       953643000       918718000       883287000
847803000       812541000       777187000       741870000       706616000
671440000       636229000       600957000       565919000       530470000
495081000       459574000       385327000       305479000       280059000
254125000       227500000       200112000       171927000       143115000
114173000       80184000        52237000        35561000        20912000
9000000 1156000   : distr_k [row array of size n_added_m_pts; distributed
stiffness per unit length] (N/m^2)

Tension wires data
0         n_attachments: no of wire-attachment locations on tower [0: no tension
wires] (-)
3 3       n_wires:       no of wires attached at each location (must be 3 or
higher) (-)
6 9       node_attach:   node numbers of attacments location (node number must
be more than 1 and less than nselt+2) (-)
0.e0 0.e0 wire_stfness:  wire spring constant in each set (see users' manual)
(N/m)
0. 0.     th_wire:       angle of tension wires (wrt the horizontal ground
plane) at each attachment point (deg)

END of Main Input File Data
*********************************************************************
```

C FAST main input file

```
------- ELASTODYN v1.03.* INPUT FILE -------------------------------------------
NREL 5.0 MW Baseline Wind Turbine. Properties from Dutch Offshore Wind Energy
Converter (DOWEC) 6MW Pre-Design (10046_009.pdf) and REpower 5M 5MW (5m_uk.pdf)
---------------------- SIMULATION CONTROL --------------------------------------
False         Echo        - Echo input data to "<RootName>.ech" (flag)
          3   Method      - Integration method: {1: RK4, 2: AB4, or 3: ABM4} (-)
"DEFAULT"     DT          - Integration time step (s)
---------------------- ENVIRONMENTAL CONDITION ---------------------------------
    9.80665   Gravity     - Gravitational acceleration (m/s^2)
---------------------- DEGREES OF FREEDOM --------------------------------------
True          FlapDOF1    - First flapwise blade mode DOF (flag)
True          FlapDOF2    - Second flapwise blade mode DOF (flag)
True          EdgeDOF     - First edgewise blade mode DOF (flag)
True          TeetDOF     - Rotor-teeter DOF (flag) [unused for 3 blades]
True          DrTrDOF     - Drivetrain rotational-flexibility DOF (flag)
True          GenDOF      - Generator DOF (flag)
True          YawDOF      - Yaw DOF (flag)
True          TwFADOF1    - First fore-aft tower bending-mode DOF (flag)
True          TwFADOF2    - Second fore-aft tower bending-mode DOF (flag)
True          TwSSDOF1    - First side-to-side tower bending-mode DOF (flag)
True          TwSSDOF2    - Second side-to-side tower bending-mode DOF (flag)
True          PtfmSgDOF   - Platform horizontal surge translation DOF (flag)
True          PtfmSwDOF   - Platform horizontal sway translation DOF (flag)
True          PtfmHvDOF   - Platform vertical heave translation DOF (flag)
True          PtfmRDOF    - Platform roll tilt rotation DOF (flag)
True          PtfmPDOF    - Platform pitch tilt rotation DOF (flag)
True          PtfmYDOF    - Platform yaw rotation DOF (flag)
---------------------- INITIAL CONDITIONS --------------------------------------
          0   OoPDefl     - Initial out-of-plane blade-tip displacement (meters)
          0   IPDefl      - Initial in-plane blade-tip deflection (meters)
          0   BlPitch(1)  - Blade 1 initial pitch (degrees)
          0   BlPitch(2)  - Blade 2 initial pitch (degrees)
          0   BlPitch(3)  - Blade 3 initial pitch (degrees) [unused for 2
blades]
          0   TeetDefl    - Initial or fixed teeter angle (degrees) [unused for
3 blades]
          0   Azimuth     - Initial azimuth angle for blade 1 (degrees)
       12.1   RotSpeed    - Initial or fixed rotor speed (rpm)
          0   NacYaw      - Initial or fixed nacelle-yaw angle (degrees)
          0   TTDspFA     - Initial fore-aft tower-top displacement (meters)
          0   TTDspSS     - Initial side-to-side tower-top displacement (meters)
          0   PtfmSurge   - Initial or fixed horizontal surge translational
displacement of platform (meters)
          0   PtfmSway    - Initial or fixed horizontal sway translational
displacement of platform (meters)
          0   PtfmHeave   - Initial or fixed vertical heave translational
displacement of platform (meters)
          0   PtfmRoll    - Initial or fixed roll tilt rotational displacement
of platform (degrees)
          0   PtfmPitch   - Initial or fixed pitch tilt rotational displacement
of platform (degrees)
          0   PtfmYaw     - Initial or fixed yaw rotational displacement of
platform (degrees)
---------------------- TURBINE CONFIGURATION -----------------------------------
```

```
          3   NumBl       - Number of blades (-)
         63   TipRad      - The distance from the rotor apex to the blade tip
(meters)
        1.5   HubRad      - The distance from the rotor apex to the blade root
(meters)
       -2.5   PreCone(1)  - Blade 1 cone angle (degrees)
       -2.5   PreCone(2)  - Blade 2 cone angle (degrees)
       -2.5   PreCone(3)  - Blade 3 cone angle (degrees) [unused for 2 blades]
          0   HubCM       - Distance from rotor apex to hub mass [positive
downwind] (meters)
          0   UndSling    - Undersling length [distance from teeter pin to the
rotor apex] (meters) [unused for 3 blades]
          0   Delta3      - Delta-3 angle for teetering rotors (degrees) [unused
for 3 blades]
          0   AzimB1Up    - Azimuth value to use for I/O when blade 1 points up
(degrees)
    -5.0191   OverHang    - Distance from yaw axis to rotor apex [3 blades] or
teeter pin [2 blades] (meters)
      1.912   ShftGagL    - Distance from rotor apex [3 blades] or teeter pin [2
blades] to shaft strain gages [positive for upwind rotors] (meters)
         -5   ShftTilt    - Rotor shaft tilt angle (degrees)
        1.9   NacCMxn     - Downwind distance from the tower-top to the nacelle
CM (meters)
          0   NacCMyn     - Lateral  distance from the tower-top to the nacelle
CM (meters)
       1.75   NacCMzn     - Vertical distance from the tower-top to the nacelle
CM (meters)
   -3.09528   NcIMUxn     - Downwind distance from the tower-top to the nacelle
IMU (meters)
          0   NcIMUyn     - Lateral  distance from the tower-top to the nacelle
IMU (meters)
    2.23336   NcIMUzn     - Vertical distance from the tower-top to the nacelle
IMU (meters)
    1.96256   Twr2Shft    - Vertical distance from the tower-top to the rotor
shaft (meters)
       87.6   TowerHt     - Height of tower above ground level [onshore] or MSL
[offshore] (meters)
          0   TowerBsHt   - Height of tower base above ground level [onshore] or
MSL [offshore] (meters)
          0   PtfmCMxt    - Downwind distance from the ground level [onshore] or
MSL [offshore] to the platform CM (meters)
          0   PtfmCMyt    - Lateral distance from the ground level [onshore] or
MSL [offshore] to the platform CM (meters)
          0   PtfmCMzt    - Vertical distance from the ground level [onshore] or
MSL [offshore] to the platform CM (meters)
          0   PtfmRefzt   - Vertical distance from the ground level [onshore] or
MSL [offshore] to the platform reference point (meters)
---------------------- MASS AND INERTIA ----------------------------------------
          0   TipMass(1)  - Tip-brake mass, blade 1 (kg)
          0   TipMass(2)  - Tip-brake mass, blade 2 (kg)
          0   TipMass(3)  - Tip-brake mass, blade 3 (kg) [unused for 2 blades]
      56780   HubMass     - Hub mass (kg)
     115926   HubIner     - Hub inertia about rotor axis [3 blades] or teeter
axis [2 blades] (kg m^2)
```

```
    534.116   GenIner     - Generator inertia about HSS (kg m^2)
     240000   NacMass     - Nacelle mass (kg)
2.60789E+06   NacYIner    - Nacelle inertia about yaw axis (kg m^2)
          0   YawBrMass   - Yaw bearing mass (kg)
          0   PtfmMass    - Platform mass (kg)
          0   PtfmRIner   - Platform inertia for roll tilt rotation about the
platform CM (kg m^2)
          0   PtfmPIner   - Platform inertia for pitch tilt rotation about the
platform CM (kg m^2)
          0   PtfmYIner   - Platform inertia for yaw rotation about the platform
CM (kg m^2)
---------------------- BLADE ---------------------------------------------------
         17   BldNodes    - Number of blade nodes (per blade) used for analysis
(-)
"NRELOffshrBsline5MW_Blade.dat"    BldFile(1)  - Name of file containing
properties for blade 1 (quoted string)
"NRELOffshrBsline5MW_Blade.dat"    BldFile(2)  - Name of file containing
properties for blade 2 (quoted string)
"NRELOffshrBsline5MW_Blade.dat"    BldFile(3)  - Name of file containing
properties for blade 3 (quoted string) [unused for 2 blades]
---------------------- ROTOR-TEETER --------------------------------------------
          0   TeetMod     - Rotor-teeter spring/damper model {0: none, 1:
standard, 2: user-defined from routine UserTeet} (switch) [unused for 3 blades]
          0   TeetDmpP    - Rotor-teeter damper position (degrees) [used only
for 2 blades and when TeetMod=1]
          0   TeetDmp     - Rotor-teeter damping constant (N-m/(rad/s)) [used
only for 2 blades and when TeetMod=1]
          0   TeetCDmp    - Rotor-teeter rate-independent Coulomb-damping moment
(N-m) [used only for 2 blades and when TeetMod=1]
          0   TeetSStP    - Rotor-teeter soft-stop position (degrees) [used only
for 2 blades and when TeetMod=1]
          0   TeetHStP    - Rotor-teeter hard-stop position (degrees) [used only
for 2 blades and when TeetMod=1]
          0   TeetSSSp    - Rotor-teeter soft-stop linear-spring constant
(N-m/rad) [used only for 2 blades and when TeetMod=1]
          0   TeetHSSp    - Rotor-teeter hard-stop linear-spring constant
(N-m/rad) [used only for 2 blades and when TeetMod=1]
---------------------- DRIVETRAIN ----------------------------------------------
        100   GBoxEff     - Gearbox efficiency (%)
         97   GBRatio     - Gearbox ratio (-)
8.67637E+08   DTTorSpr    - Drivetrain torsional spring (N-m/rad)
  6.215E+06   DTTorDmp    - Drivetrain torsional damper (N-m/(rad/s))
---------------------- FURLING -------------------------------------------------
False         Furling     - Read in additional model properties for furling
turbine (flag) [must currently be FALSE)
"unused"      FurlFile    - Name of file containing furling properties (quoted
string) [unused when Furling=False]
---------------------- TOWER ---------------------------------------------------
         20   TwrNodes    - Number of tower nodes used for analysis (-)
"NRELOffshrBsline5MW_Onshore_ElastoDyn_Tower.dat"    TwrFile     - Name of file
containing tower properties (quoted string)
---------------------- OUTPUT --------------------------------------------------
True          SumPrint    - Print summary data to "<RootName>.sum" (flag)
          1   OutFile     - Switch to determine where output will be placed: {1:
```

```
in module output file only; 2: in glue code output file only; 3: both}
(currently unused)
True          TabDelim    - Use tab delimiters in text tabular output file?
(flag) (currently unused)
"ES10.3E2"    OutFmt      - Format used for text tabular output (except time).
Resulting field should be 10 characters. (quoted string) (currently unused)
          0   TStart      - Time to begin tabular output (s) (currently unused)
          1   DecFact     - Decimation factor for tabular output {1: output
every time step} (-) (currently unused)
          0   NTwGages    - Number of tower nodes that have strain gages for
output [0 to 9] (-)
         10,        19,         28    TwrGagNd    - List of tower nodes that
have strain gages [1 to TwrNodes] (-) [unused if NTwGages=0]
          3   NBlGages    - Number of blade nodes that have strain gages for
output [0 to 9] (-)
          5,         9,         13    BldGagNd    - List of blade nodes that
have strain gages [1 to BldNodes] (-) [unused if NBlGages=0]
              OutList     - The next line(s) contains a list of output
parameters.  See OutListParameters.xlsx for a listing of available output
channels, (-)
"BldPitch1"               - Blade 1 pitch angle
"Azimuth"                 - Blade 1 azimuth angle
"RotSpeed"                - Low-speed shaft and high-speed shaft speeds
"GenSpeed"                - Low-speed shaft and high-speed shaft speeds
"TTDspFA"                 - Tower-top / yaw bearing fore-aft (translational)
deflection (relative to the undeflected position)(m)
"TTDspSS"                 - Tower-top / yaw bearing side-to-side (translation)
deflection (relative to the undeflected position)(m)
"TTDspAx"                 - Tower-top / yaw bearing axial (translational)
deflection (relative to the undeflected position)(m)
"TTDspTwst"               - Tower fore-aft and side-to-side displacements and
top twist
"YawBrTAxp"               - Tower-top / yaw bearing fore-aft (translational)
acceleration (absolute)
"YawBrTAyp"               - Tower-top / yaw bearing side-to-side (translational)
acceleration (absolute)
"YawBrTAzp"               - Tower-top / yaw bearing axial (translational)
acceleration (absolute)
"YawBrFxn"                - Rotating (with nacelle) tower-top / yaw bearing
shear force (kN)
"YawBrFyn"                - Rotating (with nacelle) tower-top / yaw bearing
shear force (kN)
"YawBrFzn"                - Tower-top / yaw bearing axial force
(kN)
"TwrBsFxt"                - Fore-aft shear, side-to-side shear, and vertical
forces at the base of the tower (mudline)(kN)
"TwrBsFyt"                - Fore-aft shear, side-to-side shear, and vertical
forces at the base of the tower (mudline)(kN)
"TwrBsFzt"                - Fore-aft shear, side-to-side shear, and vertical
forces at the base of the tower (mudline)(kN)
"TwrBsMxt"                - Side-to-side bending, fore-aft bending, and yaw
moments at the base of the tower (mudline)(kNm)
"TwrBsMyt"                - Side-to-side bending, fore-aft bending, and yaw
moments at the base of the tower (mudline)(kNm)
```

```
"TwrBsMzt"                 - Side-to-side bending, fore-aft bending, and yaw
moments at the base of the tower (mudline)(kNm)
"PtfmHeave"                - Platform vertical heave (translational) displacement
(m)
"PtfmSurge"                - Platform horizontal surge (translational)
displacement    (m)
"PtfmSway"                 - Platform horizontal sway (translational)
displacement    (m)
"PtfmRoll"                 - Platform roll tilt angular (rotational) displacement
(deg)
"PtfmPitch"                - Platform pitch tilt angular (rotational)
displacement    (deg)
"PtfmYaw"                  - Platform yaw angular (rotational) displacement
(deg)
"YawBrTAzp"                - Acceleration in z at tower top
END of input file (the word "END" must appear in the first 3 columns of this
last OutList line)
--------------------------------------------------------------------------------
-------
```

D Elastodyn input file

```
------- ELASTODYN v1.03.* INPUT FILE -------------------------------------------
NREL 5.0 MW Baseline Wind Turbine. Properties from Dutch Offshore Wind Energy
Converter (DOWEC) 6MW Pre-Design (10046_009.pdf) and REpower 5M 5MW (5m_uk.pdf)
---------------------- SIMULATION CONTROL --------------------------------------
False         Echo        - Echo input data to "<RootName>.ech" (flag)
          3   Method      - Integration method: {1: RK4, 2: AB4, or 3: ABM4} (-)
"DEFAULT"     DT          - Integration time step (s)
---------------------- ENVIRONMENTAL CONDITION ---------------------------------
    9.80665   Gravity     - Gravitational acceleration (m/s^2)
---------------------- DEGREES OF FREEDOM --------------------------------------
True          FlapDOF1    - First flapwise blade mode DOF (flag)
True          FlapDOF2    - Second flapwise blade mode DOF (flag)
True          EdgeDOF     - First edgewise blade mode DOF (flag)
True          TeetDOF     - Rotor-teeter DOF (flag) [unused for 3 blades]
True          DrTrDOF     - Drivetrain rotational-flexibility DOF (flag)
True          GenDOF      - Generator DOF (flag)
True          YawDOF      - Yaw DOF (flag)
True          TwFADOF1    - First fore-aft tower bending-mode DOF (flag)
True          TwFADOF2    - Second fore-aft tower bending-mode DOF (flag)
True          TwSSDOF1    - First side-to-side tower bending-mode DOF (flag)
True          TwSSDOF2    - Second side-to-side tower bending-mode DOF (flag)
True          PtfmSgDOF   - Platform horizontal surge translation DOF (flag)
True          PtfmSwDOF   - Platform horizontal sway translation DOF (flag)
True          PtfmHvDOF   - Platform vertical heave translation DOF (flag)
True          PtfmRDOF    - Platform roll tilt rotation DOF (flag)
True          PtfmPDOF    - Platform pitch tilt rotation DOF (flag)
True          PtfmYDOF    - Platform yaw rotation DOF (flag)
---------------------- INITIAL CONDITIONS --------------------------------------
          0   OoPDefl     - Initial out-of-plane blade-tip displacement (meters)
          0   IPDefl      - Initial in-plane blade-tip deflection (meters)
          0   BlPitch(1)  - Blade 1 initial pitch (degrees)
          0   BlPitch(2)  - Blade 2 initial pitch (degrees)
          0   BlPitch(3)  - Blade 3 initial pitch (degrees) [unused for 2
blades]
          0   TeetDefl    - Initial or fixed teeter angle (degrees) [unused for
3 blades]
          0   Azimuth     - Initial azimuth angle for blade 1 (degrees)
       12.1   RotSpeed    - Initial or fixed rotor speed (rpm)
          0   NacYaw      - Initial or fixed nacelle-yaw angle (degrees)
          0   TTDspFA     - Initial fore-aft tower-top displacement (meters)
          0   TTDspSS     - Initial side-to-side tower-top displacement (meters)
          0   PtfmSurge   - Initial or fixed horizontal surge translational
displacement of platform (meters)
          0   PtfmSway    - Initial or fixed horizontal sway translational
displacement of platform (meters)
          0   PtfmHeave   - Initial or fixed vertical heave translational
displacement of platform (meters)
          0   PtfmRoll    - Initial or fixed roll tilt rotational displacement
of platform (degrees)
          0   PtfmPitch   - Initial or fixed pitch tilt rotational displacement
of platform (degrees)
          0   PtfmYaw     - Initial or fixed yaw rotational displacement of
platform (degrees)
---------------------- TURBINE CONFIGURATION -----------------------------------
```

```
          3   NumBl       - Number of blades (-)
         63   TipRad      - The distance from the rotor apex to the blade tip
(meters)
        1.5   HubRad      - The distance from the rotor apex to the blade root
(meters)
       -2.5   PreCone(1)  - Blade 1 cone angle (degrees)
       -2.5   PreCone(2)  - Blade 2 cone angle (degrees)
       -2.5   PreCone(3)  - Blade 3 cone angle (degrees) [unused for 2 blades]
          0   HubCM       - Distance from rotor apex to hub mass [positive
downwind] (meters)
          0   UndSling    - Undersling length [distance from teeter pin to the
rotor apex] (meters) [unused for 3 blades]
          0   Delta3      - Delta-3 angle for teetering rotors (degrees) [unused
for 3 blades]
          0   AzimB1Up    - Azimuth value to use for I/O when blade 1 points up
(degrees)
    -5.0191   OverHang    - Distance from yaw axis to rotor apex [3 blades] or
teeter pin [2 blades] (meters)
      1.912   ShftGagL    - Distance from rotor apex [3 blades] or teeter pin [2
blades] to shaft strain gages [positive for upwind rotors] (meters)
         -5   ShftTilt    - Rotor shaft tilt angle (degrees)
        1.9   NacCMxn     - Downwind distance from the tower-top to the nacelle
CM (meters)
          0   NacCMyn     - Lateral  distance from the tower-top to the nacelle
CM (meters)
       1.75   NacCMzn     - Vertical distance from the tower-top to the nacelle
CM (meters)
   -3.09528   NcIMUxn     - Downwind distance from the tower-top to the nacelle
IMU (meters)
          0   NcIMUyn     - Lateral  distance from the tower-top to the nacelle
IMU (meters)
    2.23336   NcIMUzn     - Vertical distance from the tower-top to the nacelle
IMU (meters)
    1.96256   Twr2Shft    - Vertical distance from the tower-top to the rotor
shaft (meters)
       87.6   TowerHt     - Height of tower above ground level [onshore] or MSL
[offshore] (meters)
          0   TowerBsHt   - Height of tower base above ground level [onshore] or
MSL [offshore] (meters)
          0   PtfmCMxt    - Downwind distance from the ground level [onshore] or
MSL [offshore] to the platform CM (meters)
          0   PtfmCMyt    - Lateral distance from the ground level [onshore] or
MSL [offshore] to the platform CM (meters)
          0   PtfmCMzt    - Vertical distance from the ground level [onshore] or
MSL [offshore] to the platform CM (meters)
          0   PtfmRefzt   - Vertical distance from the ground level [onshore] or
MSL [offshore] to the platform reference point (meters)
---------------------- MASS AND INERTIA ----------------------------------------
          0   TipMass(1)  - Tip-brake mass, blade 1 (kg)
          0   TipMass(2)  - Tip-brake mass, blade 2 (kg)
          0   TipMass(3)  - Tip-brake mass, blade 3 (kg) [unused for 2 blades]
      56780   HubMass     - Hub mass (kg)
     115926   HubIner     - Hub inertia about rotor axis [3 blades] or teeter
axis [2 blades] (kg m^2)
```

```
    534.116   GenIner     - Generator inertia about HSS (kg m^2)
     240000   NacMass     - Nacelle mass (kg)
2.60789E+06   NacYIner    - Nacelle inertia about yaw axis (kg m^2)
          0   YawBrMass   - Yaw bearing mass (kg)
          0   PtfmMass    - Platform mass (kg)
          0   PtfmRIner   - Platform inertia for roll tilt rotation about the
platform CM (kg m^2)
          0   PtfmPIner   - Platform inertia for pitch tilt rotation about the
platform CM (kg m^2)
          0   PtfmYIner   - Platform inertia for yaw rotation about the platform
CM (kg m^2)
---------------------- BLADE ---------------------------------------------------
         17   BldNodes    - Number of blade nodes (per blade) used for analysis
(-)
"NRELOffshrBsline5MW_Blade.dat"    BldFile(1)  - Name of file containing
properties for blade 1 (quoted string)
"NRELOffshrBsline5MW_Blade.dat"    BldFile(2)  - Name of file containing
properties for blade 2 (quoted string)
"NRELOffshrBsline5MW_Blade.dat"    BldFile(3)  - Name of file containing
properties for blade 3 (quoted string) [unused for 2 blades]
---------------------- ROTOR-TEETER --------------------------------------------
          0   TeetMod     - Rotor-teeter spring/damper model {0: none, 1:
standard, 2: user-defined from routine UserTeet} (switch) [unused for 3 blades]
          0   TeetDmpP    - Rotor-teeter damper position (degrees) [used only
for 2 blades and when TeetMod=1]
          0   TeetDmp     - Rotor-teeter damping constant (N-m/(rad/s)) [used
only for 2 blades and when TeetMod=1]
          0   TeetCDmp    - Rotor-teeter rate-independent Coulomb-damping moment
(N-m) [used only for 2 blades and when TeetMod=1]
          0   TeetSStP    - Rotor-teeter soft-stop position (degrees) [used only
for 2 blades and when TeetMod=1]
          0   TeetHStP    - Rotor-teeter hard-stop position (degrees) [used only
for 2 blades and when TeetMod=1]
          0   TeetSSSp    - Rotor-teeter soft-stop linear-spring constant
(N-m/rad) [used only for 2 blades and when TeetMod=1]
          0   TeetHSSp    - Rotor-teeter hard-stop linear-spring constant
(N-m/rad) [used only for 2 blades and when TeetMod=1]
---------------------- DRIVETRAIN ----------------------------------------------
        100   GBoxEff     - Gearbox efficiency (%)
         97   GBRatio     - Gearbox ratio (-)
8.67637E+08   DTTorSpr    - Drivetrain torsional spring (N-m/rad)
  6.215E+06   DTTorDmp    - Drivetrain torsional damper (N-m/(rad/s))
---------------------- FURLING -------------------------------------------------
False         Furling     - Read in additional model properties for furling
turbine (flag) [must currently be FALSE)
"unused"      FurlFile    - Name of file containing furling properties (quoted
string) [unused when Furling=False]
---------------------- TOWER ---------------------------------------------------
         20   TwrNodes    - Number of tower nodes used for analysis (-)
"NRELOffshrBsline5MW_Onshore_ElastoDyn_Tower.dat"    TwrFile     - Name of file
containing tower properties (quoted string)
---------------------- OUTPUT --------------------------------------------------
True          SumPrint    - Print summary data to "<RootName>.sum" (flag)
          1   OutFile     - Switch to determine where output will be placed: {1:
```

```
in module output file only; 2: in glue code output file only; 3: both}
(currently unused)
True          TabDelim    - Use tab delimiters in text tabular output file?
(flag) (currently unused)
"ES10.3E2"    OutFmt      - Format used for text tabular output (except time).
Resulting field should be 10 characters. (quoted string) (currently unused)
          0   TStart      - Time to begin tabular output (s) (currently unused)
          1   DecFact     - Decimation factor for tabular output {1: output
every time step} (-) (currently unused)
          0   NTwGages    - Number of tower nodes that have strain gages for
output [0 to 9] (-)
         10,        19,        28    TwrGagNd    - List of tower nodes that
have strain gages [1 to TwrNodes] (-) [unused if NTwGages=0]
          3   NBlGages    - Number of blade nodes that have strain gages for
output [0 to 9] (-)
          5,         9,        13    BldGagNd    - List of blade nodes that
have strain gages [1 to BldNodes] (-) [unused if NBlGages=0]
              OutList     - The next line(s) contains a list of output
parameters.  See OutListParameters.xlsx for a listing of available output
channels, (-)
"BldPitch1"               - Blade 1 pitch angle
"Azimuth"                 - Blade 1 azimuth angle
"RotSpeed"                - Low-speed shaft and high-speed shaft speeds
"GenSpeed"                - Low-speed shaft and high-speed shaft speeds
"TTDspFA"                 - Tower-top / yaw bearing fore-aft (translational)
deflection (relative to the undeflected position)(m)
"TTDspSS"                 - Tower-top / yaw bearing side-to-side (translation)
deflection (relative to the undeflected position)(m)
"TTDspAx"                 - Tower-top / yaw bearing axial (translational)
deflection (relative to the undeflected position)(m)
"TTDspTwst"               - Tower fore-aft and side-to-side displacements and
top twist
"YawBrTAxp"               - Tower-top / yaw bearing fore-aft (translational)
acceleration (absolute)
"YawBrTAyp"               - Tower-top / yaw bearing side-to-side (translational)
acceleration (absolute)
"YawBrTAzp"               - Tower-top / yaw bearing axial (translational)
acceleration (absolute)
"YawBrFxn"                - Rotating (with nacelle) tower-top / yaw bearing
shear force (kN)
"YawBrFyn"                - Rotating (with nacelle) tower-top / yaw bearing
shear force (kN)
"YawBrFzn"                - Tower-top / yaw bearing axial force
(kN)
"TwrBsFxt"                - Fore-aft shear, side-to-side shear, and vertical
forces at the base of the tower (mudline)(kN)
"TwrBsFyt"                - Fore-aft shear, side-to-side shear, and vertical
forces at the base of the tower (mudline)(kN)
"TwrBsFzt"                - Fore-aft shear, side-to-side shear, and vertical
forces at the base of the tower (mudline)(kN)
"TwrBsMxt"                - Side-to-side bending, fore-aft bending, and yaw
moments at the base of the tower (mudline)(kNm)
"TwrBsMyt"                - Side-to-side bending, fore-aft bending, and yaw
moments at the base of the tower (mudline)(kNm)
```

```
"TwrBsMzt"                - Side-to-side bending, fore-aft bending, and yaw
moments at the base of the tower (mudline)(kNm)
"PtfmHeave"               - Platform vertical heave (translational) displacement
(m)
"PtfmSurge"               - Platform horizontal surge (translational)
displacement    (m)
"PtfmSway"                - Platform horizontal sway (translational)
displacement    (m)
"PtfmRoll"                - Platform roll tilt angular (rotational) displacement
(deg)
"PtfmPitch"               - Platform pitch tilt angular (rotational)
displacement    (deg)
"PtfmYaw"                 - Platform yaw angular (rotational) displacement
(deg)
"YawBrTAzp"               - Acceleration in z at tower top
END of input file (the word "END" must appear in the first 3 columns of this
last OutList line)
--------------------------------------------------------------------------------
-------
```

E Hydrodyn input file

```
------- HydroDyn v2.03.* Input File ----------------------------------------
NREL 5.0 MW Onshore wind turbine
False            Echo           - Echo the input file data (flag)
---------------------- ENVIRONMENTAL CONDITIONS ----------------------------
          1025   WtrDens        - Water density (kg/m^3)
           150   WtrDpth        - Water depth (meters)
             0   MSL2SWL        - Offset between still-water level and mean sea
level (meters) [positive upward; unused when WaveMod = 6; must be zero if
PotMod=1 or 2]
---------------------- WAVES -----------------------------------------------
             0   WaveMod        - Incident wave kinematics model {0: none=still
water, 1: regular (periodic), 1P#: regular with user-specified phase, 2:
JONSWAP/Pierson-Moskowitz spectrum (irregular), 3: White noise spectrum
(irregular), 4: user-defined spectrum from routine UserWaveSpctrm (irregular),
5: Externally generated wave-elevation time series, 6: Externally generated full
wave-kinematics time series [option 6 is invalid for PotMod/=0]} (switch)
             0   WaveStMod      - Model for stretching incident wave kinematics
to instantaneous free surface {0: none=no stretching, 1: vertical stretching, 2:
extrapolation stretching, 3: Wheeler stretching} (switch) [unused when WaveMod=0
or when PotMod/=0]
          3630   WaveTMax       - Analysis time for incident wave calculations
(sec) [unused when WaveMod=0; determines WaveDOmega=2Pi/WaveTMax in the IFFT]
          0.25   WaveDT         - Time step for incident wave calculations
(sec) [unused when WaveMod=0; 0.1<=WaveDT<=1.0 recommended; determines
WaveOmegaMax=Pi/WaveDT in the IFFT]
             5   WaveHs         - Significant wave height of incident waves
(meters) [used only when WaveMod=1, 2, or 3]
          12.4   WaveTp         - Peak-spectral period of incident waves
(sec) [used only when WaveMod=1 or 2]
"DEFAULT"        WavePkShp      - Peak-shape parameter of incident wave spectrum
(-) or DEFAULT (string) [used only when WaveMod=2; use 1.0 for
Pierson-Moskowitz]
             0   WvLowCOff      - Low  cut-off frequency or lower frequency
limit of the wave spectrum beyond which the wave spectrum is zeroed (rad/s)
[unused when WaveMod=0, 1, or 6]
           500   WvHiCOff       - High cut-off frequency or upper frequency
limit of the wave spectrum beyond which the wave spectrum is zeroed (rad/s)
[unused when WaveMod=0, 1, or 6]
             0   WaveDir        - Incident wave propagation heading direction
                     (degrees) [unused when WaveMod=0 or 6]
             0   WaveDirMod     - Directional spreading function {0: none, 1:
COS2S}                  (-)       [only used when WaveMod=2,3, or 4]
             1   WaveDirSpread  - Wave direction spreading coefficient ( > 0 )
                     (-)       [only used when WaveMod=2,3, or 4 and
WaveDirMod=1]
             1   WaveNDir       - Number of wave directions
                     (-)       [only used when WaveMod=2,3, or 4 and
WaveDirMod=1; odd number only]
            90   WaveDirRange   - Range of wave directions (full range: WaveDir
+/- 1/2*WaveDirRange) (degrees) [only used when WaveMod=2,3,or 4 and
WaveDirMod=1]
     123456789   WaveSeed(1)    - First  random seed of incident waves
[-2147483648 to 2147483647]    (-)       [unused when WaveMod=0, 5, or 6]
    1011121314   WaveSeed(2)    - Second random seed of incident waves
```

```
[-2147483648 to 2147483647]    (-)       [unused when WaveMod=0, 5, or 6]
TRUE             WaveNDAmp      - Flag for normally distributed amplitudes
                    (flag)    [only used when WaveMod=2, 3, or 4]
""               WvKinFile      - Root name of externally generated wave data
file(s)        (quoted string)    [used only when WaveMod=5 or 6]
             1   NWaveElev      - Number of points where the incident wave
elevations can be computed (-)       [maximum of 9 output locations]
             0   WaveElevxi     - List of xi-coordinates for points where the
incident wave elevations can be output (meters) [NWaveElev points, separated by
commas or white space; usused if NWaveElev = 0]
             0   WaveElevyi     - List of yi-coordinates for points where the
incident wave elevations can be output (meters) [NWaveElev points, separated by
commas or white space; usused if NWaveElev = 0]
---------------------- 2ND-ORDER WAVES ----------------------------------------
[unused with WaveMod=0 or 6]
False            WvDiffQTF      - Full difference-frequency 2nd-order wave
kinematics (flag)
False            WvSumQTF       - Full summation-frequency  2nd-order wave
kinematics (flag)
             0   WvLowCOffD     - Low  frequency cutoff used in the
difference-frequencies (rad/s) [Only used with a difference-frequency method]
           3.5   WvHiCOffD      - High frequency cutoff used in the
difference-frequencies (rad/s) [Only used with a difference-frequency method]
           0.1   WvLowCOffS     - Low  frequency cutoff used in the
summation-frequencies  (rad/s) [Only used with a summation-frequency  method]
           3.5   WvHiCOffS      - High frequency cutoff used in the
summation-frequencies  (rad/s) [Only used with a summation-frequency  method]
---------------------- CURRENT ------------------------------------------------
[unused with WaveMod=6]
             0   CurrMod        - Current profile model {0: none=no current, 1:
standard, 2: user-defined from routine UserCurrent} (switch)
             0   CurrSSV0       - Sub-surface current velocity at still water
level  (m/s) [used only when CurrMod=1]
"DEFAULT"        CurrSSDir      - Sub-surface current heading direction
(degrees) or DEFAULT (string) [used only when CurrMod=1]
            20   CurrNSRef      - Near-surface current reference depth
 (meters) [used only when CurrMod=1]
             0   CurrNSV0       - Near-surface current velocity at still water
level (m/s) [used only when CurrMod=1]
             0   CurrNSDir      - Near-surface current heading direction
(degrees) [used only when CurrMod=1]
             0   CurrDIV        - Depth-independent current velocity
    (m/s) [used only when CurrMod=1]
             0   CurrDIDir      - Depth-independent current heading direction
(degrees) [used only when CurrMod=1]
---------------------- FLOATING PLATFORM --------------------------------------
[unused with WaveMod=6]
             0   PotMod         - Potential-flow model {0: none=no potential
flow, 1: frequency-to-time-domain transforms based on WAMIT output, 2:
fluid-impulse theory (FIT)} (switch)
"HydroData/Barge"    PotFile        - Root name of potential-flow model data;
WAMIT output files containing the linear, nondimensionalized, hydrostatic
restoring matrix (.hst), frequency-dependent hydrodynamic added mass matrix and
damping matrix (.1), and frequency- and direction-dependent wave excitation
```

```
force vector per unit wave amplitude (.3) (quoted string) [MAKE SURE THE
FREQUENCIES INHERENT IN THESE WAMIT FILES SPAN THE PHYSICALLY-SIGNIFICANT RANGE
OF FREQUENCIES FOR THE GIVEN PLATFORM; THEY MUST CONTAIN THE ZERO- AND
INFINITE-FREQUENCY LIMITS!]
             1   WAMITULEN      - Characteristic body length scale used to
redimensionalize WAMIT output (meters) [only used when PotMod=1]
          6000   PtfmVol0       - Displaced volume of water when the platform is
in its undisplaced position (m^3) [only used when PotMod=1; USE THE SAME VALUE
COMPUTED BY WAMIT AS OUTPUT IN THE .OUT FILE!]
             0   PtfmCOBxt      - The xt offset of the center of buoyancy (COB)
from the platform reference point (meters)  [only used when PotMod=1]
             0   PtfmCOByt      - The yt offset of the center of buoyancy (COB)
from the platform reference point (meters)  [only used when PotMod=1]
             2   RdtnMod        - Radiation memory-effect model {0: no
memory-effect calculation, 1: convolution, 2: state-space} (switch) [only used
when PotMod=1; STATE-SPACE REQUIRES *.ss INPUT FILE]
            60   RdtnTMax       - Analysis time for wave radiation kernel
calculations (sec) [only used when PotMod=1; determines RdtnDOmega=Pi/RdtnTMax
in the cosine transform; MAKE SURE THIS IS LONG ENOUGH FOR THE RADIATION IMPULSE
RESPONSE FUNCTIONS TO DECAY TO NEAR-ZERO FOR THE GIVEN PLATFORM!]
         0.005   RdtnDT         - Time step for wave radiation kernel
calculations (sec) [only used when PotMod=1; DT<=RdtnDT<=0.1 recommended;
determines RdtnOmegaMax=Pi/RdtnDT in the cosine transform]
---------------------- 2ND-ORDER FLOATING PLATFORM FORCES ----------------------
[unused with WaveMod=0 or 6, or PotMod=0 or 2]
             0   MnDrift        - Mean-drift 2nd-order forces computed
                            {0: None; [7, 8, 9, 10, 11, or 12]: WAMIT file to
use} [Only one of MnDrift, NewmanApp, or DiffQTF can be non-zero]
             0   NewmanApp      - Mean- and slow-drift 2nd-order forces computed
with Newman's approximation {0: None; [7, 8, 9, 10, 11, or 12]: WAMIT file to
use} [Only one of MnDrift, NewmanApp, or DiffQTF can be non-zero. Used only when
WaveDirMod=0]
             0   DiffQTF        - Full difference-frequency 2nd-order forces
computed with full QTF          {0: None; [10, 11, or 12]: WAMIT file to use}
      [Only one of MnDrift, NewmanApp, or DiffQTF can be non-zero]
             0   SumQTF         - Full summation -frequency 2nd-order forces
computed with full QTF          {0: None; [10, 11, or 12]: WAMIT file to use}
---------------------- FLOATING PLATFORM FORCE FLAGS  --------------------------
[unused with WaveMod=6]
True             PtfmSgF        - Platform horizontal surge translation force
(flag) or DEFAULT
True             PtfmSwF        - Platform horizontal sway translation force
(flag) or DEFAULT
True             PtfmHvF        - Platform vertical heave translation force
(flag) or DEFAULT
True             PtfmRF         - Platform roll tilt rotation force (flag) or
DEFAULT
True             PtfmPF         - Platform pitch tilt rotation force (flag) or
DEFAULT
True             PtfmYF         - Platform yaw rotation force (flag) or DEFAULT
---------------------- PLATFORM ADDITIONAL STIFFNESS AND DAMPING  --------------
             0             0             0             0             0
  0   AddF0    - Additional preload (N, N-m)
             7058823529 0       0       0       -4235294118     0   AddCLin  -
```

```
Additional linear stiffness (N/m, N/rad, N-m/m, N-m/rad)
             0  7058823529      0       4235294118      0       0
             0  0       8571428571      0       0       0
             0  4235294118      0       895398319328    0       0
             -4235294118        0       0       0       895398319328    0
             0  0       0       0       0       1250000000000
             0             0             0             0             0
  0   AddBLin  - Additional linear damping(N/(m/s), N/(rad/s), N-m/(m/s),
N-m/(rad/s))
             0             0             0             0             0
  0
             0             0             0             0             0
  0
             0             0             0             0             0
  0
             0             0             0             0             0
  0
             0             0             0             0             0
  0
             0             0             0             0             0
  0   AddBQuad - Additional quadratic drag(N/(m/s)^2, N/(rad/s)^2, N-m(m/s)^2,
N-m/(rad/s)^2)
             0             0             0             0             0
  0
             0             0             0             0             0
  0
             0             0             0             0             0
  0
             0             0             0             0             0
  0
             0             0             0             0             0
  0
---------------------- AXIAL COEFFICIENTS --------------------------------------
             1   NAxCoef        - Number of axial coefficients (-)
AxCoefID  AxCd     AxCa     AxCp
   (-)    (-)      (-)      (-)
    1     0.00     0.00     1.00
---------------------- MEMBER JOINTS -------------------------------------------
             2   NJoints        - Number of joints (-)   [must be exactly 0 or
at least 2]
JointID   Jointxi     Jointyi     Jointzi  JointAxID   JointOvrlp   [JointOvrlp=
0: do nothing at joint, 1: eliminate overlaps by calculating super member]
   (-)     (m)         (m)         (m)        (-)       (switch)
    1     0.00000     0.00000    -4.00000      1           0
    2     0.00000     0.00000     0.00000      1           0
---------------------- MEMBER CROSS-SECTION PROPERTIES -------------------------
             1   NPropSets      - Number of member property sets (-)
PropSetID    PropD         PropThck
   (-)        (m)           (m)
    1       45.13520       0.00010
---------------------- SIMPLE HYDRODYNAMIC COEFFICIENTS (model 1) --------------
     SimplCd    SimplCdMG    SimplCa    SimplCaMG    SimplCp    SimplCpMG
SimplAxCa  SimplAxCaMG  SimplAxCp   SimplAxCpMG
       (-)         (-)         (-)         (-)         (-)         (-)
```

```
(-)         (-)         (-)         (-)
       0.00        0.00        0.00        0.00        0.00        0.00
0.00        0.00        0.00        0.00
---------------------- DEPTH-BASED HYDRODYNAMIC COEFFICIENTS (model 2) ---------
            0   NCoefDpth       - Number of depth-dependent coefficients (-)
Dpth      DpthCd   DpthCdMG   DpthCa   DpthCaMG       DpthCp   DpthCpMG
DpthAxCa   DpthAxCaMG       DpthAxCp   DpthAxCpMG
(m)       (-)      (-)        (-)      (-)            (-)      (-)          (-)
      (-)              (-)         (-)
---------------------- MEMBER-BASED HYDRODYNAMIC COEFFICIENTS (model 3) --------
            0   NCoefMembers       - Number of member-based coefficients (-)
MemberID    MemberCd1     MemberCd2    MemberCdMG1   MemberCdMG2    MemberCa1
 MemberCa2    MemberCaMG1   MemberCaMG2    MemberCp1     MemberCp2
MemberCpMG1   MemberCpMG2   MemberAxCa1   MemberAxCa2  MemberAxCaMG1
MemberAxCaMG2  MemberAxCp1  MemberAxCp2   MemberAxCpMG1   MemberAxCpMG2
   (-)        (-)           (-)           (-)           (-)           (-)
    (-)           (-)           (-)           (-)           (-)           (-)
       (-)           (-)           (-)           (-)           (-)           (-)
          (-)           (-)           (-)
-------------------- MEMBERS -------------------------------------------------
            1   NMembers       - Number of members (-)
MemberID  MJointID1  MJointID2  MPropSetID1  MPropSetID2  MDivSize   MCoefMod
PropPot   [MCoefMod=1: use simple coeff table, 2: use depth-based coeff table,
3: use member-based coeff table] [ PropPot/=0 if member is modeled with
potential-flow theory]
  (-)        (-)        (-)         (-)          (-)        (m)      (switch)
(flag)
    1         1          2           1            1        0.5000      1
False
---------------------- FILLED MEMBERS ------------------------------------------
            0   NFillGroups     - Number of filled member groups (-) [If
FillDens = DEFAULT, then FillDens = WtrDens; FillFSLoc is related to MSL2SWL]
FillNumM FillMList             FillFSLoc     FillDens
(-)      (-)                   (m)           (kg/m^3)
---------------------- MARINE GROWTH -------------------------------------------
            0   NMGDepths      - Number of marine-growth depths specified (-)
MGDpth     MGThck       MGDens
(m)        (m)         (kg/m^3)
---------------------- MEMBER OUTPUT LIST --------------------------------------
            0   NMOutputs      - Number of member outputs (-) [must be < 10]
MemberID   NOutLoc    NodeLocs [NOutLoc < 10; node locations are normalized
distance from the start of the member, and must be >=0 and <= 1] [unused if
NMOutputs=0]
  (-)        (-)        (-)
---------------------- JOINT OUTPUT LIST ---------------------------------------
            0   NJOutputs      - Number of joint outputs [Must be < 10]
   0           JOutLst        - List of JointIDs which are to be output
(-)[unused if NJOutputs=0]
---------------------- OUTPUT --------------------------------------------------
True             HDSum          - Output a summary file [flag]
False            OutAll         - Output all user-specified member and joint
loads (only at each member end, not interior locations) [flag]
            2   OutSwtch       - Output requested channels to: [1=Hydrodyn.out,
2=GlueCode.out, 3=both files]
```

```
"ES11.4e2"       OutFmt         - Output format for numerical results (quoted
string) [not checked for validity!]
"A11"            OutSFmt        - Output format for header strings (quoted
string) [not checked for validity!]
---------------------- OUTPUT CHANNELS -----------------------------------------
END of output channels and end of file. (the word "END" must appear in the first
3 columns of this line)
```

F TurbSim input file

```
TurbSim Input File. Valid for TurbSim v1.06.00, 2018-05-18

---------Runtime Options-----------------------------------
1000 RandSeed1 - First random seed (-2147483648 to 2147483647)
RANLUX RandSeed2 - Second random seed (-2147483648 to 2147483647) for intrinsic
pRNG, or an alternative pRNG: "RanLux" or "RNSNLW"
False WrBHHTP - Output hub-height turbulence parameters in binary form?
(Generates RootName.bin)
False WrFHHTP - Output hub-height turbulence parameters in formatted form?
(Generates RootName.dat)
False WrADHH - Output hub-height time-series data in AeroDyn form? (Generates
RootName.hh)
True WrADFF - Output full-field time-series data in TurbSim/AeroDyn form?
(Generates Rootname.bts)
True WrBLFF - Output full-field time-series data in BLADED/AeroDyn form?
(Generates RootName.wnd)
False WrADTWR - Output tower time-series data? (Generates RootName.twr)
False WrFMTFF - Output full-field time-series data in formatted (readable) form?
(Generates RootName.u, RootName.v, RootName.w)
False WrACT - Output coherent turbulence time steps in AeroDyn form? (Generates
RootName.cts)
True Clockwise - Clockwise rotation looking downwind? (used only for full-field
binary files - not necessary for AeroDyn)
0 ScaleIEC - Scale IEC turbulence models to exact target standard deviation?
[0=no additional scaling; 1=use hub scale uniformly; 2=use individual scales]

--------Turbine/Model Specifications-----------------------
31 NumGrid_Z - Vertical grid-point matrix dimension
31 NumGrid_Y - Horizontal grid-point matrix dimension
0.05 TimeStep - Time step [seconds]
630.0 AnalysisTime - Length of analysis time series [seconds] (program will add
time if necessary: AnalysisTime = MAX(AnalysisTime,
UsableTime+GridWidth/MeanHHWS) )
630.0 UsableTime - Usable length of output time series [seconds] (program will
add GridWidth/MeanHHWS seconds)
90.0 HubHt - Hub height [m] (should be > 0.5*GridHeight)
177.50 GridHeight - Grid height [m]
177.50 GridWidth - Grid width [m] (should be >= 2*(RotorRadius+ShaftLength))
0 VFlowAng - Vertical mean flow (uptilt) angle [degrees]
0 HFlowAng - Horizontal mean flow (skew) angle [degrees]

--------Meteorological Boundary Conditions-------------------
"IECKAI" TurbModel - Turbulence model ("IECKAI"=Kaimal, "IECVKM"=von Karman,
"GP_LLJ", "NWTCUP", "SMOOTH", "WF_UPW", "WF_07D", "WF_14D", "TIDAL", or "NONE")
"1-ED3" IECstandard - Number of IEC 61400-x standard (x=1,2, or 3 with optional
61400-1 edition number (i.e. "1-Ed2") )
"B" IECturbc - IEC turbulence characteristic ("A", "B", "C" or the turbulence
intensity in percent) ("KHTEST" option with NWTCUP model, not used for other
models)
"NTM" IEC_WindType - IEC turbulence type ("NTM"=normal, "xETM"=extreme
turbulence, "xEWM1"=extreme 1-year wind, "xEWM50"=extreme 50-year wind, where
x=wind turbine class 1, 2, or 3)
default ETMc - IEC Extreme Turbulence Model "c" parameter [m/s]
PL WindProfileType - Wind profile type ("JET";"LOG"=logarithmic;"PL"=power
```

```
law;"H2L"=Log law for TIDAL spectral model;"IEC"=PL on rotor disk, LOG
elsewhere; or "default")
90 RefHt - Height of the reference wind speed [m]
12 URef - Mean (total) wind speed at the reference height [m/s] (or "default"
for JET wind profile)
default ZJetMax - Jet height [m] (used only for JET wind profile, valid 70-490
m)
0.2 PLExp - Power law exponent [-] (or "default")
default Z0 - Surface roughness length [m] (or "default")

--------Non-IEC Meteorological Boundary Conditions------------
default Latitude - Site latitude [degrees] (or "default")
0.05 RICH_NO - Gradient Richardson number
default UStar - Friction or shear velocity [m/s] (or "default")
default ZI - Mixing layer depth [m] (or "default")
default PC_UW - Hub mean u'w' Reynolds stress (or "default")
default PC_UV - Hub mean u'v' Reynolds stress (or "default")
default PC_VW - Hub mean v'w' Reynolds stress (or "default")
default IncDec1 - u-component coherence parameters (e.g. "10.0 0.3e-3" in
quotes) (or "default")
default IncDec2 - v-component coherence parameters (e.g. "10.0 0.3e-3" in
quotes) (or "default")
default IncDec3 - w-component coherence parameters (e.g. "10.0 0.3e-3" in
quotes) (or "default")
default CohExp - Coherence exponent (or "default")

--------Coherent Turbulence Scaling Parameters-------------------
"C:\DesignCodes\TurbSim\Test\EventData" CTEventPath - Name of the path where
event data files are located
"Random" CTEventFile - Type of event files ("LES", "DNS", or "RANDOM")
true Randomize - Randomize the disturbance scale and locations? (true/false)
1.0 DistScl - Disturbance scale (ratio of wave height to rotor disk). (Ignored
when Randomize = true.)
0.5 CTLy - Fractional location of tower centerline from right (looking downwind)
to left side of the dataset. (Ignored when Randomize = true.)
0.5 CTLz - Fractional location of hub height from the bottom of the dataset.
(Ignored when Randomize = true.)
10.0 CTStartTime - Minimum start time for coherent structures in RootName.cts
[seconds]

==================================================
NOTE: Do not add or remove any lines in this file!
==================================================
```

G Windturbine.m - MATLAB script for numerical evaluation of structural behaviour using the function package CALFEM

Table of Contents

Windturbine.m

```
%%%%%%%%%%%%%%%%%%%%%%%%%%%%%%%%%%%%%%%%%%%%%%%%%%%%%%%%%%%%%%
% Master Thesis: Soil-structure interactions effect on behaviour of
 wind
% turbine
% Simplified 2-d beam model
% Natural frequency and displacement analysis of wind turbine using
 the
% function package CALFEM
% Created by: Jonatan Isaksson and David Tenenbaum
% Date: 2018-02-22
%
%%%%%%%%%%%%%%%%%%%%%%%%%%%%%%%%%%%%%%%%%%%%%%%%%%%%%%%%%%%%%%

clear all                           % Clear variables and command
 window
close all                           % Closes ev. open figures
clc
format shortG                       % Choose to view numbers this way

%%%%%%%%%%%%%%%%%%%%%%%%%%%%%%%%%%%%%%%%%%%%%%%%%%%%%%%%%%%%%%%%%%%%%%%%%%%%%
```

Input data

```
nonodes=100;        % Number of element divisions.
% Material properties
E=210*10^9;     % E-modulus of steel [Pa]
rho=8500;       % Steel density [kg/m^3]

%Dimensions
h=87.6 ;         % Height of tower [m]
Dtop=3.87;      % Top diamater of tower [m]
Dbottom=6;      % Bottom diameter of tower [m]
ttop=0.019*1.3;     % Thickness top of tower [m]
tbottom=0.027*1.3;  % Thickness bottom of tower [m]
dtop=Dtop-2*ttop;   % Internal diameter top [m]
dbottom=Dbottom-2*tbottom; % Internal diamaeter bottom [m]
```

```
%Calculations of cross sectional constants
l=zeros(nonodes,1);
A=zeros(nonodes,1);
I=zeros(nonodes,1);
D=zeros(nonodes,1);
d=zeros(nonodes,1);
for i=1:nonodes
    D(i)=Dbottom-(Dbottom-Dtop)/(nonodes-1)*(i-1);
    d(i)=dbottom-(dbottom-dtop)/(nonodes-1)*(i-1);
    A(i)=((D(i))^2-(d(i))^2)*pi/4;
    I(i)=pi*(D(i)^4-d(i)^4)/64;

end
    m=A*rho;
```

Element properties vector for wind turbine tower

```
Ev=ones(nonodes,1)*E;
NodeEP=[Ev A I m];          % Plane-frame elements (road and towers)
ep1=zeros(nonodes-1,4);
for i=1:(nonodes-1)
    ep1(i,:)=[(Ev(i)+Ev(i+1))/2 (A(i)+A(i+1))/2 (I(i)+I(i+1))/2
 (m(i)+m(i+1))/2];
end


Edof=zeros(nonodes-1,7);
for i=1:nonodes-1
Edof(i,:)=[i i*3-2 i*3-1 i*3 i*3+1 i*3+2 i*3+3];
end
% Coordinates for the elements
Ex=zeros(nonodes-1,2);
Ey=zeros(nonodes-1,2);
for i=1:nonodes-1
    Ey(i,:)=[i-1 i]*h/(nonodes-1);
end
```

Assembly of Stiffness and Mass matrices

```
ndof=nonodes*3;
K=zeros(ndof);          % Pre-locating space
M=zeros(ndof);          % Pre-locating space
C=zeros(ndof);          % Pre-locating space

% Plane-frame elements (road and towers) (element 1-8)
for i=1:nonodes-1

    % Element mass and stiffness matrices
    [Kebeam,Mebeam]=beam2d(Ex(i,:),Ey(i,:),ep1(i,:));
```

```
    % Assemble into K and M
   K(Edof(i,2:7),Edof(i,2:7))=...
                               K(Edof(i,2:7),Edof(i,2:7))+Kebeam;
    M(Edof(i,2:7),Edof(i,2:7))=...
                              M(Edof(i,2:7),Edof(i,2:7))+Mebeam;
end
```

2 Calculation of Eigenfrequencies for the wind turbine

```
bc=[1 0     % Boundary conditions clamped
    2 0
    3 0];
[lambda,U]=eigen(K,M,bc(:,1));     % Calculates the eigenvalues for K-
w^2M
w=sqrt(lambda);
fn=w/(2*pi);

% extracting x-values from eigenvector
xdisp1nomass=zeros(nonodes,1);
xdisp2nomass=zeros(nonodes,1);
for i=1:nonodes
xdisp1nomass(i)=U(1+(i-1)*3,1);
xdisp2nomass(i)=U(1+(i-1)*3,2);
end
xdisp1nomass=xdisp1nomass/norm(xdisp1nomass);
xdisp2nomass=xdisp2nomass/norm(xdisp2nomass);
% Definition of top mass and inertia and assigning it to the right
 place in
% stiffness and mass matrices.
topmass=3.500003109E+5;
% ixx_tip     blade lag mass moment of inertia about the tip-section x
% reference axis (kg-m^2)
topinertiaxx=4.370E7;
% iyy_tip     blade flap mass moment of inertia about the tip-section
 y
% reference axis (kg-m^2)
topinertiayy=2.353E7;

Mfa=M;
Mss=M;

Mfa(3*nonodes-2,3*nonodes-2)=M(3*nonodes-2,3*nonodes-2)+topmass;
Mfa(3*nonodes-1,3*nonodes-1)=M(3*nonodes-1,3*nonodes-1)+topmass;
Mfa(3*nonodes,3*nonodes)=M(3*nonodes,3*nonodes)+topinertiayy;

Mss(3*nonodes-2,3*nonodes-2)=M(3*nonodes-2,3*nonodes-2)+topmass;
Mss(3*nonodes-1,3*nonodes-1)=M(3*nonodes-1,3*nonodes-1)+topmass;
Mss(3*nonodes,3*nonodes)=M(3*nonodes,3*nonodes)+topinertiaxx;

[lambda,U]=eigen(K,Mfa,bc(:,1));     % Calculates the eigenvalues for
 K-w^2M
```

```
w1=sqrt(lambda);
fnfa=w1/(2*pi);
xdisp1fa=zeros(nonodes,1);
xdisp2fa=zeros(nonodes,1);
xdisp3fa=zeros(nonodes,1);
xdisp4fa=zeros(nonodes,1);
for i=1:nonodes
xdisp1fa(i)=U(1+(i-1)*3,1);
xdisp2fa(i)=U(1+(i-1)*3,2);
xdisp3fa(i)=U(1+(i-1)*3,3);
xdisp4fa(i)=U(1+(i-1)*3,4);
end

% Calculates the eigenvalues for K-w^2M and corresponding eigen
 vectors U
[lambda,U]=eigen(K,Mss,bc(:,1));



w2=sqrt(lambda);
fnss=w2/(2*pi);
xdisp1ss=zeros(nonodes,1);
xdisp2ss=zeros(nonodes,1);
% Extracting the x-value of the eogen vector
for i=1:nonodes
xdisp1ss(i)=U(1+(i-1)*3,1);
xdisp2ss(i)=U(1+(i-1)*3,2);
end
% 3 Displacement due to horizontal force in top of tower
f=zeros(nonodes*3,1);
a=zeros(nonodes*3,1);
fxtop=631*10^3;          % 12mps steady state (Value from fast)
f(nonodes*3-2)=fxtop;


% Solving system displacements a and forces Q
[a,Q]=solveq(K,f,bc);
```

Stiffness in bottom of wind turbine

Stiffness is calculateed in accordance with Gazetas theory. Calculation of stiffness is performed in excel file Stiffnesscoefficient.xlsx

```
Kboundary=[1176470588.2 0.0 0.0 0.0 -705882352.9 0.0
           0.0 1176470588.2 0.0 705882352.9 0.0 0.0
           0.0 0.0 1428571428.6 0.0 0.0 0.0
           0.0 705882352.9 0.0 149233053221.3 0.0 0.0
           -705882352.9 0.0 0.0 0.0 149233053221.3 0.0
           0.0 0.0 0.0 0.0 0.0 208333333333.3];
```

Solving for spring

Assigning spring stiffness to element stiffness matrix

```
Kspring=[Kboundary(1,1) 0 0
        0 Kboundary(3,3) 0
        0 0 Kboundary(4,4)]/1;
% Boundary condition spring supported

bcspring=[2 0];
Ksprings=K;
% Assigning sppring stiffness to global stiffness matrix
Ksprings(1:3,1:3)=Kspring+K(1:3,1:3);

% Calculates the eigenvalues (FA) for K-w^2M and corresponding eigen
 vectors U
[lambda,UFAspring]=eigen(Ksprings,Mfa,bcspring(:,1));
w1SPRING=sqrt(lambda);
fnfaspring=w1SPRING/(2*pi);
xdisp1springFA=zeros(nonodes,1);
xdisp2springFA=zeros(nonodes,1);
for i=1:nonodes
xdisp1springFA(i)=UFAspring(1+(i-1)*3,1);
xdisp2springFA(i)=UFAspring(1+(i-1)*3,2);
end
```

SOlving for soft spring

Assigning spring stiffness to element stiffness matrix

```
Kspringsoft=[Kboundary(1,1) 0 0
        0 Kboundary(3,3) 0
        0 0 Kboundary(4,4)]/10;
% Boundary condition spring supported
bcspringsoft=[2 0];
Ksoft=K;
% Assigning sppring stiffness to global stiffness matrix
Ksoft(1:3,1:3)=Kspringsoft+K(1:3,1:3);
% Calculates the eigenvalues (FA) for K-w^2M and corresponding eigen
 vectors U
[lambda,UFAsoftspring]=eigen(Ksoft,Mfa,bcspringsoft(:,1));
w1SPRING=sqrt(lambda);
fnfaspring=w1SPRING/(2*pi);


xdisp1springsoftFA=zeros(nonodes,1);
xdisp2springsoftFA=zeros(nonodes,1);
for i=1:nonodes
xdisp1springsoftFA(i)=UFAsoftspring(1+(i-1)*3,1);
xdisp2springsoftFA(i)=UFAsoftspring(1+(i-1)*3,2);
end
% Calculates the eigenvalues (SS) for K-w^2M and corresponding eigen
 vectors U
[lambda,U]=eigen(K,Mss);
w2SPRING=sqrt(lambda);
fnsspring=w2SPRING/(2*pi);
[as,Qs]=solveq(K,f,bcspring);
```

```
as(length(as)-2)
```

Published with MATLAB® R2015b

H fatigue.m - MATLAB script for rainflow counting and fatigue accumulation in a bolt in the tower-base connection of wind turbine tower

fatigue.m

Master Thesis: Soil-structure interactions effect on behaviour of wind turbine

```
%Fatigue calculations written for bolts in a so called bolt cage in a
 wind
%turbine. Input values need to be specified. Moment around the central
 axis
%of base are the force considered.


% Created by: Jonatan Isaksson and David Tenenbaum
% Date: 2018-05-02
%


clc
clear all
close all
% Input files with vectors as [time Moment] i*2
filenames =
 {'Case1Uniform.mat','Case2Uniform.mat','Case3Uniform.mat','Case1Turbulent.mat','C
results=cell(length(filenames),1);
% Definition of geometry.
D=6; % [m] Tower base outer diamater
d=0.027; % [m] Tower base steel thickness.
bf=0.5; % [m] Flange width for tower including diameter of tower.
NObolts=160; % [-]
boltrows=2; % [-]
t=48 % [mm] Thickness of bolt.
SAb=1473*(10^-3)^2 % [m^2] Stress area for bolt
% Starting time for fatigue counting to give FAST ttime to adjust.
startt=70; % [s]
% Size of intervals for grouping of cycles.
binsize=50; %[kNM]
% Fatigue classification
sigmaC=50*10^6 % Pa
% Reduction due to size effect of bolt.
kc=(30/t)^0.25
sigmaC=sigmaC*kc
% CAFL and Cut-off limit calculated from fatigue class according to
 EC3
sigmaD=0.737*sigmaC % Pa
sigmaL=0.549*sigmaD % Pa
% Script for calculation of fatigue loads.
% Total damage for case defined by input file j
Totaldamage=zeros(length(filenames),1);

% [count (max stress in bin) (Damage from stress range)] unknown:3
cycleranges=cell(length(filenames),3);

for j=1:length(filenames)
```

```
dtm=importdata(filenames{(j)});
% [n,edgesigma,Damage] = fatiguefunction(D,d,bf,NObolts,...
% boltrows,dtm,startt ,binsize,sigmaD,sigmaL,SAb);

% Rainflow counting
[c]=rainflow(dtm(startt:end,2)*1000,dtm(startt:end,1));
% Binning of cycles in stress range group defined as binsize

[n,edges] = histcounts(c(:,2),'BinWidth',binsize);
Ncafl=5*10^6;
R=(D-d/2)/2 % Distance to center of towerbaseflange from centre of
 tower
z=R+bf/2; % Distance to bolt assuming it is in middle of outer partof
 flange
I=pi*((R+bf/2)^4-(R-bf/2)^4)/4; % Second moment of inertia bottom part
 of tower

% Area of the flange contributing to the stress in bolt.
cAf=((R+bf/2)^2-(R-bf/2)^2)*pi/NObolts/boltrows;


edgesigma=zeros(length(n),1);
Damage=zeros(length(n),1);
for i=1:length(n)
sigmaflange=edges(i+1)/I*z;
Fb=sigmaflange*cAf;
sigmabolt=Fb/SAb;
edgesigma(i)=sigmabolt;

% Deciding in what damage range the load cycles are in.
    if sigmabolt>=sigmaD
    Ni=Ncafl*(sigmaD/sigmabolt)^3;
    end
    if sigmabolt>=sigmaL && sigmabolt<sigmaD
    Ni=Ncafl*(sigmaL/sigmabolt)^5;
    end
    if sigmabolt <sigmaL
    Ni=inf;
    end

Damage(i)=n(i)/Ni;
end

% Storing results.
Totaldamage(j,1)=sum(Damage);
cycleranges{j,1}=n;
cycleranges{j,2}=edgesigma;
cycleranges{j,3}=Damage;

end
```

Published with MATLAB® R2017b

I FFT.m - MATLAB script to compute the fast fourier transform

```
%**********************************************************************
%   Master thesis: Script to convert time domain signals into the frequency
%   domain using the fast fourier transform. The signals are divided into
%   arbitary block lengths, windowed with a hanning window and transformed.
%
%   Created by: David Tenenbaum and Jonatan Isaksson
%   Date: 2018-04-25
%**********************************************************************

%% Reset Matlab
clc
clf
close all
clear
%% Indata
N = 50000;
ref_value = 1;                          % 1m

%% Load files
CHOICE=4;  %1Original sound, 2David data, 3Jonatan data, 4
if CHOICE==1        %Original Data
    load signaldata.mat
elseif CHOICE==2    %Davids Data
load FA_LOAD.mat
load t_LOAD.mat
x=FA;
y=FA;
fs=length(t)/t(length(t));
clear t;
elseif CHOICE==3    %Jonatans Data
load Davidsvector.mat
x=Davidsvector(:,2);
y=Davidsvector(:,2);
t=Davidsvector(:,1);
fs=length(t)/t(length(t));
elseif CHOICE==4
    load Davidsloosespring.mat
    t=Davidsloosespring(:,1);
    x=Davidsloosespring(:,2);
    y=Davidsloosespring(:,2);
    fs=length(t)/t(length(t));
end
%% Divide the signals into blocks of arbitrary length

Nxy = length(x);                                  % Number of samples/frequency
components in total for signal x and y

Nb = floor(Nxy/N);                                % Number of blocks

mat_x = vec2mat(x,N);
mat_y = vec2mat(y,N);
mat_x(Nb+1,:) = [];
mat_y(Nb+1,:) = [];
dt = 1/fs;                                       % time step [s]
t = (0:N-1)*dt;                                  % time vector [s]
df = fs/N;                                       % frequency step [Hz]
f = (0:N-1)*df;                                  % frequency vector
```

```
%% Average over eack block

for nb = 1:Nb

    % Windowing

    hw = hanning(N);
    hw_scale = sqrt(sum(hw.^2)/length(hw));

    xhw = (mat_x(nb,:)'.*hw)/hw_scale;
    yhw = (mat_y(nb,:)'.*hw)/hw_scale;

    %% Calculate the instantenous doublesided spectrum and scale to get amplitude ↙
spectrum

    X = fft(xhw)/N;
    Y = fft(yhw)/N;

    %% Calculate the instantaneous and averaged doublesided autospectrum

    Sxx = conj(X).*X;
    Syy = conj(Y).*Y;

    if nb==1

        ASxx = Sxx;
        ASyy = Syy;

    else

        ASxx = ASxx - (ASxx - Sxx)/nb;
        ASyy = ASyy - (ASyy - Syy)/nb;

    end

    %% Calculate the singlesided autospectrum

    AGxx(1) = ASxx(1);
    AGxx(2:N/2-1) = 2*ASxx(2:N/2-1);
    AGxx(N/2)=ASxx(N/2);
    AGyy(1) = ASyy(1);
    AGyy(2:N/2-1) = 2*ASyy(2:N/2-1);
    AGyy(N/2)=ASyy(N/2);
end
```

J Dynamicbeammodel.m - MATLAB script for dynamic numerical evaluation of wind turbine in the time domain.

Table of Contents

Dynamicbeammodel.m

Master Thesis: Soil-structure interactions effect on behaviour of wind turbine Dynamic analysis of wind turbine tower in the time domain using the function package CALFEM. Tower are given a prescribed displacement and then allowed to vibrate freely. Displacement in the top of the tower are stored.

```
% Created by: Jonatan Isaksson and David Tenenbaum
% Date: 2018-05-02
%

clear all
close all
clc
```

Input data

```
nonodes=100;        % Number of element divisions.
% Materil properties
E=210*10^9;     % E-modulus of steel [Pa]
rho=8500;       % Steel density [kg/m^3]

%Dimensions
h=87.6 ;         % Height of tower [m]
Dtop=3.87;      % Top diamater of tower [m]
Dbottom=6;      % Bottom diameter of tower [m]
ttop=0.019*1.3;     % Thickness top of tower [m]
tbottom=0.027*1.3;  % Thickness bottom of tower [m]
dtop=Dtop-2*ttop;   % Internal diameter top [m]
dbottom=Dbottom-2*tbottom; % Internal diamaeter bottom [m]
%Further dimensions and stiffness (FROM FAST)
%prop=[[fraction[-] massdensity[kg/m] TWFastiff[Nm^2] TWSSstiff[Nm^2]]
% Used only to see if calculated constants are the same as properties
 given
% in FAST.
propfast=[0.0000000E+00  5.5908700E+03  6.1434300E+11  6.1434300E+11
1.0000000E-01  5.2324300E+03  5.3482100E+11  5.3482100E+11
2.0000000E-01  4.8857600E+03  4.6326700E+11  4.6326700E+11
3.0000000E-01  4.5508700E+03  3.9913100E+11  3.9913100E+11
4.0000000E-01  4.2277500E+03  3.4188300E+11  3.4188300E+11
5.0000000E-01  3.9164100E+03  2.9101100E+11  2.9101100E+11
```

```
6.0000000E-01  3.6168300E+03  2.4602700E+11  2.4602700E+11
7.0000000E-01  3.3290300E+03  2.0645700E+11  2.0645700E+11
8.0000000E-01  3.0530100E+03  1.7185100E+11  1.7185100E+11
9.0000000E-01  2.7887500E+03  1.4177600E+11  1.4177600E+11
1.0000000E+00  2.5362700E+03  1.1582000E+11  1.1582000E+11] ;
%Calculations of cross sectional constants
l=zeros(nonodes,1);
A=zeros(nonodes,1);
I=zeros(nonodes,1);
D=zeros(nonodes,1);
d=zeros(nonodes,1);
for i=1:nonodes
    D(i)=Dbottom-(Dbottom-Dtop)/(nonodes-1)*(i-1);
    d(i)=dbottom-(dbottom-dtop)/(nonodes-1)*(i-1);
    A(i)=((D(i))^2-(d(i))^2)*pi/4;
    I(i)=pi*(D(i)^4-d(i)^4)/64;

end
    m=A*rho;
```

Element properties

```
Ev=ones(nonodes,1)*E;
NodeEP=[Ev A I m];
ep1=zeros(nonodes-1,4);
for i=1:(nonodes-1)
    ep1(i,:)=[(Ev(i)+Ev(i+1))/2 (A(i)+A(i+1))/2 (I(i)+I(i+1))/2 ...
        (m(i)+m(i+1))/2];
end
Edof=zeros(nonodes-1,7);
for i=1:nonodes-1
Edof(i,:)=[i i*3-2 i*3-1 i*3 i*3+1 i*3+2 i*3+3];
end
% Coordinates for the elements
Ex=zeros(nonodes-1,2);
Ey=zeros(nonodes-1,2);
for i=1:nonodes-1
    Ey(i,:)=[i-1 i]*h/(nonodes-1);
end
```

1 Stiffness and Mass matrices

```
ndof=nonodes*3;
K=zeros(ndof);          % Pre-locating space
M=zeros(ndof);          % Pre-locating space
C=zeros(ndof);
% Assembly of K and M
for i=1:nonodes-1

    % Element mass and stiffness matrices
    [Kebeam,Mebeam]=beam2d(Ex(i,:),Ey(i,:),ep1(i,:));
    % Assemble into K and M
   K(Edof(i,2:7),Edof(i,2:7))=...
```

```
                                                   K(Edof(i,2:7),Edof(i,2:7))+Kebeam;
    M(Edof(i,2:7),Edof(i,2:7))=...
                                                  M(Edof(i,2:7),Edof(i,2:7))+Mebeam;
    % tf = issymmetric(K)   % Check that K is symmetric
    % tf = issymmetric(M)   % Check that M is symmetric
end
% Assigning inertia and mass to top of tower.
topmass=3.500003109E+5;
topinertiaxx=4.370E7;
topinertiayy=2.353E7;
Mfa=M;
Mss=M;
Mfa(3*nonodes-2,3*nonodes-2)=M(3*nonodes-2,3*nonodes-2)+topmass;
Mfa(3*nonodes-1,3*nonodes-1)=M(3*nonodes-1,3*nonodes-1)+topmass;
Mfa(3*nonodes,3*nonodes)=M(3*nonodes,3*nonodes)+topinertiayy;
Mss(3*nonodes-2,3*nonodes-2)=M(3*nonodes-2,3*nonodes-2)+topmass;
Mss(3*nonodes-1,3*nonodes-1)=M(3*nonodes-1,3*nonodes-1)+topmass;
Mss(3*nonodes,3*nonodes)=M(3*nonodes,3*nonodes)+topinertiaxx;
```

SOlving dynamic system clamped support

```
d0=zeros(ndof,1);        % Prescribed displacement for the system t=0.
d0(ndof-2)=0.5;          % Prescribed displacement for the system t=0.
f=zeros(ndof,1);         % Prescribed force on the system t=0.
v0=zeros(ndof,1);        % Prescribed velocity for the system t=0.
pdisp=[1 0               % Boundary conditions for clamped turbine
        2 0
        3 0];
dt=0.002;                % Time step
time=100;                 % Length of time.
% Store displacement for node. This case the x-displacement in the top
 of
% the tower.
storenode=ndof-2;
ip=[dt time 0.25 0.5 [10 2500 [1 2 3 4 5 6 7 8 9 9.9] storenode]];
xt=linspace(0,time,time/dt+1);
[Dsnap,Dclamped,V,A]=step2(K,C,Mfa,d0,v0,ip,f,pdisp);
```

Solving dynamic system spring support

Assigning spring stiffness to system.

```
Kboundary=[1176470588.2 0.0 0.0 0.0 -705882352.9 0.0
           0.0 1176470588.2 0.0 705882352.9 0.0 0.0
           0.0 0.0 1428571428.6 0.0 0.0 0.0
           0.0 705882352.9 0.0 149233053221.3 0.0 0.0
           -705882352.9 0.0 0.0 0.0 149233053221.3 0.0
           0.0 0.0 0.0 0.0 0.0 208333333333.3];
% Boundary conditions used for the spring and soft spring. (Scaling ca
 be
% performed on the Kspring matrix)
Kspring=[Kboundary(1,1) 0 0
        0 Kboundary(3,3) 0
```

```
        0 0 Kboundary(4,4)]/10;
K(1:3,1:3)=+Kspring+K(1:3,1:3);
bcspring=[1 0
    2 0
    nonodes*3-2 0.5];
[as,Qs]=solveq(K,f,bcspring);
as(length(as)-2)
d0=zeros(ndof,1);
d0=as;
f=zeros(ndof,1);
v0=zeros(ndof,1);
% Boundary conditions
pdispspring=[1 0
        2 0];
ip=[dt time 0.25 0.5 [1 1 2 [3 storenode]]];
xt=linspace(0,time,time/dt+1);
[Dsnap,Dspring,V,A]=step2(K,C,Mfa,d0,v0,ip,f,pdispspring);
```

Plot of displacements over time for clamped and spring supported cantilevered beam.

```
figure(7)
hold on
% plot(xt(1),Dclamped)
plot(xt,Dspring(2,:),'r')
plot(xt,Dclamped)
legend('Clamped','Spring')
```

Published with MATLAB® R2017b